

MISSION ORIENTED
ADVANCED NUCLEAR SYSTEM
PARAMETERS STUDY

DECEMBER 1966
PHASE IV FINAL REPORT

VOLUME II
O1977-6006-R000

**DETAILED
TECHNICAL REPORT**

FOR
GEORGE C. MARSHALL SPACE FLIGHT CENTER
BY

N67-34792

TRW SYSTEM
AN OPERATING GROUP OF TRW I

FACILITY FORM 602

(ACCESSION NUMBER)

142

(PAGES)

CR-87488

(NASA CR OR TMX OR AD NUMBER)

(THRU)

(CODE)

(CATEGORY)

01977-6005-R000

MISSION ORIENTED STUDY
OF
ADVANCED NUCLEAR SYSTEM PARAMETERS

Phase IV Final Report

Volume II
Detailed Technical Report

for

George C. Marshall Space Flight Center
National Aeronautics and Space Administration


by

TRW Systems
Redondo Beach, California

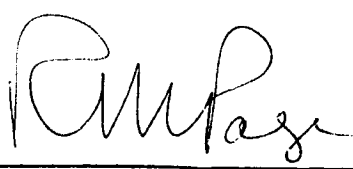
Volume II Detailed Technical Report

Prepared by: A. R. Chovit, Analytical Research Operations
 L. D. Simmons, Mission Design Department

Approved:



A. R. Chovit, Project Manager
Mission Oriented Study of Advanced
Nuclear System Parameters



R. M. Page, Manager
Analytical Research Operations

FOREWORD

This volume, which is one of a set of three volumes, describes the study tasks, analyses, and results that were accomplished under Contract NAS8-5371, Mission Oriented Study of Advanced Nuclear System Parameters, for George C. Marshall Space Flight Center, Huntsville, Alabama. This work was performed during the period from May 1965 to December 1966 and covers Phase IV of the subject contract.

The final report has been organized into a set of three separate volumes on the basis of contractual requirements. The volumes in this set are:

Volume I	Summary Technical Report
Volume II	Detailed Technical Report
Volume III	Research and Technology Implications Report

Volumes I and II include a summary and the details, respectively, of the basic study guidelines and assumption, the analysis approach, the analytic techniques developed, the analyses performed, the results obtained, and an evaluation of these results together with specific conclusions and recommendations. Volume III delineates those areas of research and technology in which further efforts would be desirable based on the results of the study.

The principal contributors to this study were Messrs. A. R. Chovit, R. D. Fiscus, and L. D. Simmons. In addition, Dr. C. D. Kylstra, in a consulting capacity, provided technical support on on computer program revisions.

Also the assistance given by the following persons is gratefully acknowledged: Dr. R. K. Plebuch and Messrs. W. H. Bayless, G. W. Cannon, H. W. Hawthorne, G. Rosler, and R. L. Sohn, TRW Systems; Mr. C. D. McKereghan, Lockheed Missile and Space Division; Mr. P. G. Johnson, SNPO-W; and R. J. Harris, W. Y. Jordon, and D. R. Saxton, MSFC.

ABSTRACT

The details of the study approach and basic guidelines and assumptions which were used in a series of analyses of manned Mars stopover missions are given. Analyses were performed for five separate study tasks, viz, (1) an analysis and comparison of swingby, opposition, and conjunction class missions, (2) a detailed parametric analysis of the conjunction class mission, (3) an investigation of the effects of providing launch windows at Earth and Mars for various missions, (4) an evaluation of the vehicle's abort capabilities for various missions, and (5) an analysis to determine the effects of Earth launch azimuth and constraints for various missions and launch opportunities. The results obtained for each of these study tasks are presented as well as an evaluation of and recommendations based on the results.

CONTENTS

Section		Page
I	INTRODUCTION	I-1
	STUDY OBJECTIVES	I-1
	STUDY TASKS	I-1
	REVIEW OF PREVIOUS STUDY PHASES	I-3
	SWOP DESCRIPTION	I-4
	REPORT ORGANIZATION	I-6
II	SWINGBY MISSION ANALYSIS	II-1
	TASK DESCRIPTION	II-1
	ASSUMPTIONS AND CONSTRAINTS	II-1
	GRAVITY TURN SWINGBY MISSIONS	II-20
	POWERED TURN SWINGBY MISSIONS	II-61
III	CONJUNCTION CLASS MISSION ANALYSIS	III-1
	TASK DESCRIPTION	III-1
	ASSUMPTIONS AND CONTRAINTS	III-1
	RESULTS AND DISCUSSION	III-8
IV	MISSION ABORT ANALYSIS	IV-1
	TASK DESCRIPTION	IV-1
	ASSUMPTIONS AND CONSTRAINTS	IV-1
	ANALYSIS APPROACH	IV-2
	CONTOUR MAPS	IV-4
	RESULTS AND DISCUSSION	IV-7
V	LAUNCH AZIMUTH CONSTRAINT ANALYSIS	V-1
	TASK DESCRIPTION	V-1
	ASSUMPTIONS AND CONSTRAINTS	V-1
	ANALYSIS APPROACH	V-3
	RESULTS AND DISCUSSIONS	V-7
VI	SUMMARY	VI-1
	SWINGBY MISSION ANALYSIS	VI-1
	CONJUNCTION CLASS MISSION ANALYSIS	VI-1
	LAUNCH WINDOW ANALYSIS	VI-2
	MISSION ABORT ANALYSIS	VI-2
	LAUNCH AZIMUTH CONSTRAINT ANALYSIS	VI-2
VII	REFERENCES	VII-1

ILLUSTRATIONS

Number		Page
II-1	Manned Mars Mission Sequence	II-3
II-2	Connecting Mode Vehicle Configuration	II-7
II-3	Typical Possible Gravity Turn Swingby Trajectories	II-22
II-4	Typical Matching of Gravity Turn Swingby Trajectory Legs	II-23
II-5	Typical Matched Gravity Turn Swingby Trajectory	II-24
II-6	Velocity Data for 1980 Inbound Gravity Turn Swingby Trajectory	II-26
II-7	Velocity Data for 1982 Inbound Gravity Turn Swingby Trajectory	II-27
II-8	Gravity Turn Swingby Mission Analysis Results	II-39
II-9	Launch Opportunity Comparison for Gravity Turn Swingby Missions	II-53
II-10	Mission Mode Comparison, NNNA Vehicle Configuration	II-56
II-11	Mission Mode Comparison, CCCA Vehicle Configuration	II-57
II-12	Mission Mode Comparison, NASA Vehicle Configuration	II-59
II-13	Mission Mode Comparison, CASA Vehicle Configuration	II-60
II-14	Surface of Powered Swingby Velocities	II-63
II-15	Characteristics of Powered Swingby Velocity Surface	II-64
II-16	Typical Powered Swingby Velocity Data	II-66
II-17	Powered Swingby Velocity Data Along Valley Line	II-67
II-18	1980 Inbound Swingby Mission Weight Comparison	II-71
II-19	1982 Inbound Swingby Mission Weight Comparison	II-72
II-20	1980 Inbound Swingby Mission Velocity Comparison	II-73
II-21	1982 Inbound Swingby Mission Velocity Comparison	II-74
III-1	Velocity Contour Map	III-2
III-2	Conjunction Mission Trajectory Type Comparison	III-11
III-3	Conjunction Mission Mass Fraction No. 2 Payload Comparison	III-12
III-4	Conjunction Mission Mass Fraction No. 3 Payload Comparison	III-13
IV-1	Typical Abort Velocity Contour Map	IV-6
IV-2a	1982 Opposition Mission Vehicle Abort Capability	IV-8a
IV-2b	1982 Opposition Mission Abort Velocity Contour Map	IV-8b
IV-3a	1983 Conjunction Mission Vehicle Abort Capability	IV-9a
IV-3b	1983 Conjunction Mission Abort Velocity Contour Map	IV-9b
IV-4a	1982 Inbound Swingby Mission Vehicle Abort Capability	IV-10a
IV-4b	1982 Inbound Swingby Mission Abort Velocity Contour Map	IV-10b

ILLUSTRATIONS (Continued)

Number		Page
IV-5a	1986 Outbound Swingby Mission Vehicle Abort Capability	IV-11a
IV-5b	1986 Outbound Swingby Mission Abort Velocity Contour Map	IV-11b
V-1	Allowable Firing Sector for ETR	V-4
V-2	Launch Azimuth and Declination Limits for ETR	V-5
V-3	1975 Earth Departure Declination Limits	V-9
V-4	1978 Earth Departure Declination Limits	V-10
V-5	1980 Earth Departure Declination Limits	V-11
V-6	1982 Earth Departure Declination Limits	V-12
V-7	1984 Earth Departure Declination Limits	V-13
V-8	1986 Earth Departure Declination Limits	V-14
V-9	1988 Earth Departure Declination Limits	V-15
V-10	1990 Earth Departure Declination Limits	V-16
V-11	1980 Earth Departure Declination Limits	V-17
V-12	1986 Earth Departure Declination Limits	V-18

TABLES

Number		Page
II-1	Comparative Mission Matrix	II-4
II-2	Mass Fraction Case No. 2	II-8
II-3	Mass Fraction Case No. 3	II-9
II-4	Connecting Mode Scaling Laws	II-10
II-5	Payload and Expendable Weights	II-14
II-6	Propellant Vaporized in Earth Orbit	II-18
II-7	Propellant Vaporization Rates	II-18
II-8	Vehicle Mode Matrix	II-19
II-9	Available Swingby Trajectory Data	II-28
II-10	Gravity Turn Swingby Mission Analysis Results	II-30
II-11	Minimum Weight Swingby Trajectories	II-52
II-12	Mission Mode Comparison	II-61
III-1	Mass Fraction Case No. 3	III-4
III-2	Conjunction Mission Payloads	III-5
III-3	Vehicle Mode Matrix	III-7
III-4	1983 Conjunction Class Mission Initial Vehicle Weights	III-9
III-5	1983 Type IA Conjunction Class Mission Initial	III-10
IV-1	Abort Analysis Vehicles	IV-1
V-1	Launch Azimuth Constraint Mission Matrix	V-2
V-2	Effects of Earth Departure Declination Limits	V-8

I. INTRODUCTION

This final report presents the details of the mission, trajectory, and vehicle analyses conducted during Phase IV of the Mission Oriented Study of Advanced Nuclear System Parameters performed by TRW Systems for the George C. Marshall Space Flight Center.

Included in this volume are the basic guidelines and assumptions, the analysis approach, the analytic techniques developed, the analyses performed, the results obtained, and an evaluation of these results together with specific conclusions and recommendations.

STUDY OBJECTIVES

The basic objectives of this study were to expand the mission evaluations performed in the earlier study phases to include trade-offs, mission mode comparisons, and sensitivity investigations of the Venus swingby mode for manned Mars stopover missions; to perform vehicle and engine sizing computations for evaluating launch and abort operations and constraints; and to revise and modify existing computer programs to incorporate additional mission concepts and parameters that would render the programs more effective. To this end, five separate analysis tasks were established.

STUDY TASKS

A brief description of each of the five study tasks is given below. A more detailed description of each task is included at the beginning of each task section in this report.

Swingby Mission Analysis

This task involved the mission analysis of Mars stopover missions employing both gravity and powered turn Venus swingby trajectories for the 1980 to 1986 opportunities. These investigations included variations in trajectory types, vehicle weights, vehicle propulsive systems, nuclear engine performance parameters, and structural scaling laws. The results for the swingby missions were compared with analogous results for opposition and conjunction class missions.

Conjunction Class Mission Analysis

An analysis was made of the 1983 conjunction class mission which included the determination of the initial vehicle weight requirements for parametric variations in trajectory types, vehicle and propulsive modes, structural scaling laws, stopover times, and payload weights.

Launch Window Analysis

An investigation was conducted to determine the effect on initial vehicle weight for Mars stopover missions when launch windows are provided both at Earth and Mars. Fixed module hardware and reasonable vehicle configurations were assumed. The effects of the nodal regression of the parking orbits were taken into account and the modular propellant tanks were sized so as to provide the minimum initial weight vehicle necessary for permitting a launch on any day during the launch window. Opposition, swingby, and conjunction class missions were investigated for various window widths and launch opportunities.

(Due to a discrepancy in a computer program utilized in this task, many of the final results obtained were invalid. The computer program has been corrected and the launch window analysis is in the process of being revised. The results of the revised analysis will be presented in a supplemental report at a later date.)

Mission Abort Analysis

The mission abort task involved an investigation of opposition, swingby, and conjunction class missions to determine the abort capability of the vehicle from various points along the outbound trajectory using the available vehicle propulsive systems. Various combinations of the vehicle propulsive systems were considered for providing the abort velocity increment and the Earth deceleration requirements.

Launch Azimuth Constraint Analysis

An analysis was made to determine the effects on Mars stopover mission launches due to the constraints imposed on allowable launch azimuths by range safety restrictions and the physical limits on the departure declination achievable for launches from the ETR. Mission opportunities from 1975 to 1990 were investigated as well as several types of missions, interplanetary trajectories, and vehicle configurations.

REVIEW OF PREVIOUS STUDY PHASES

Phase IV of the study utilized the mission optimization and vehicle sizing computer program developed during the earlier phases of the study as well as some of the parametric data and analysis techniques developed during Phase III. Therefore, a brief review of Phase I, II, and III is given here in order to present the study continuity and background applicable to Phase IV.

The first major task of the previous phases was to develop a computer program that would permit the rapid determination of the optimum (minimum weight) trajectory for a variety of mission modes, propulsive systems, vehicle configurations, system and payload weights and scaling laws, and performance parameters. This computer program was given the acronym, SWOP (SWingby Optimization Program). The development of this computer program required detailed analyses of interplanetary trajectories, nuclear engines, and the spacecraft in order to determine the required scaling laws, data, and correlations which would relate all of the pertinent variables.

The SWOP program was then utilized to analyze opposition class and flyby missions for various trajectory types, launch opportunities, vehicle configurations, and performance parameters in order to determine the best compromise engine thrust level for these missions in the 1975 to 1990 time period. Following the determination of this compromise thrust, a detailed analysis was made to determine the vehicle and stage weight sensitivity to variations in performance, vehicle, and mission parameters. Concurrently, a nuclear optimization computer program (NOP) also developed in the study, was used for analyzing the detailed engine design parameters in terms of their effect on the engine weight, thrust, and specific impulse.

In this manner, it was possible to determine within a narrow range, the mission, vehicle, and engine requirements for these future manned interplanetary missions. Within this narrow range a more detailed analysis was then performed which related the vehicle and mission requirements to variations in specific engine design parameters. The information obtained from the detailed evaluations then permitted the identification of the optimum engine design requirements and the major vehicle and mission criteria. A point engine and point vehicle design analysis or check was then performed for the selected engine and vehicle.

Finally, all of the parametric data that were generated in the course of this study were compiled in an extensive parametric data book, to support future analyses

of interplanetary missions, vehicles, and propulsion systems. (The detailed technical report of the mission and vehicle analysis portion of Phases I, II, and III is given in Reference 1. Reference 2 is the parametric data book mentioned above.)

SWOP DESCRIPTION

The SWOP program was the primary tool utilized in optimizing and analyzing the various missions in this study as well as sizing the vehicle component systems and computing the initial vehicle weights. Therefore, a more or less detailed description of the program is included here to indicate the manner in which the program was utilized and to present the level of detail to which the vehicles were configured.

The SWOP program uses a unique employment of analytic and mathematical techniques, specified curve fit routines, and precomputational processing, selection, and storage of trajectory and performance data to minimize the initial vehicle weight in Earth orbit with respect to all the velocity changes (propulsive and aerodynamic braking), the perihelion distance (solar flare shielding), the trip times (life support expendables, and micrometeoroid protection), the propellant boiloff requirements, and the planet passage distance constraints (for swingby missions). The vehicle is configured by the program by means of parameter options and payload specifications. In addition to the variable propulsive or aerodynamic stage weights which make up the vehicle, the program computes or provides for various weight provisions including attitude control, midcourse corrections, planet lander, and Earth lander (after retro or aerodynamic braking). The program also considers the addition or deletion of fixed weights at various points along the mission trajectory on option.

All variable weights are sized using general scaling laws whose coefficients are input. The trajectory data used by the program are preprocessed free flight data and powered flight information. The program has the capability of optimizing a mission for one or more constrained trajectory or velocity parameters. These include the launch or arrival dates at Earth, the target, or the swingby planet; the individual leg or total trip times; one or more of the velocity increments; the perihelion distance; the periapsis distance; and the propulsion systems' thrust, thrust-to-weight ratio, or percentage gravity loss. When one or more of the independent parameters are constrained, the program optimizes those that are unconstrained; if all are constrained, the vehicle is sized for the fixed trajectory.

The flexible constraint option was very useful for the launch window, the abort, and for vehicle sizing analyses.

The program can optimize the trajectory and size the vehicle for three general mission classes: stopover missions, stopover missions with a third planet gravity swingby during either the inbound or outbound leg, and stopover missions with a third planet powered swingby during either the inbound or outbound leg. The vehicle propulsion stages can be selected to be nuclear (aftercooled and non-aftercooled), chemical cryogenic, or storable chemical. The planet braking maneuvers can be propulsive, aerodynamic, or a combination of propulsive and aerodynamic braking.

When the program is employed in its mission optimization mode, the computed vehicle weight is the minimum gross spacecraft weight that is required to perform the mission for the specified vehicle, payload, trajectory, and performance constraints. This weight corresponds to the overall vehicle weight at the point just prior to boost out of Earth parking orbit. The vehicle weight in all cases is computed using trajectory characteristics that are optimum for the selected constraints, i.e., the particular launch dates and trip times used (with the corresponding characteristic velocities and perihelion distance) produce the minimum overall vehicle weight. In addition, the program computes and outputs the vehicle weight before and after every powered phase of the mission as well as all propellant, insulation, and tank weights. The vehicle weights, performance parameters, and trajectory parameters, are obtained on a three or four page printout.

The initial vehicle weight data are based on calculations for the propellant weight in which the velocity losses due to operation in a gravity field are taken into account in an exact manner. The gravity losses can be determined by either specifying a) a fixed engine thrust, b) a fixed percentage increase of the impulsive velocity, or c) a fixed vehicle thrust-to-weight ratio.

For vehicles employing nuclear propulsion stages, these losses are based on the required velocity change, the engine specific impulse, and the vehicle thrust-to-weight ratio obtained from the computed vehicle weight and the specified engine thrust.

For vehicles employing chemical propulsion systems, the characteristic velocity is obtained by increasing the required impulsive velocity change by a fixed percentage. The percentage values used are shown in the following schedule.

<u>Propulsive Phase</u>	<u>Propulsion Mode</u>	<u>Percentage Increase</u>
Depart Earth	Cryogenic (LO_2/LH_2)	2.3%
Arrive Planet	Cryogenic (LO_2/LH_2)	0%
Depart Planet	Cryogenic (LO_2/LH_2)	1%
Depart Planet	Storable	1%
Arrive Earth Retro	Storable	0%

The impulsive velocities used by the program are based on the assumption that the spacecraft injects into an interplanetary orbit from a 500 km circular orbit at Earth and a 600 km circular orbit at Mars; for the braking maneuver at Mars, the vehicle is decelerated into a 600 km circular orbit.

Running time for the SWOP program is typically two seconds per case.

REPORT ORGANIZATION

Each of the following five sections of the report describes the analyses and results for one of the study tasks. Each section essentially is complete within itself presenting the analysis approach, assumptions and constraints, mission and vehicle mode matrices, performance parameters, and results that are applicable to the specific task. For those cases in which specific task data are identical to those of a previously described task, repetition has been avoided by referencing back to the section where the data was first presented.

A final section presents a summary of only the more salient results for each task.

II. SWINGBY MISSION ANALYSIS

TASK DESCRIPTION

The Swingby Optimization Program (SWOP) was utilized to determine the initial weight requirements in Earth orbit for manned Mars stopover missions employing the Venus swingby mission profile. The necessary free flight trajectory data for the gravity turn swingby legs were supplied to TRW Systems by NASA. The mission analyses included both gravity turns and powered turns at Venus for mission opportunities from 1980 to 1986. Both outbound and inbound Venus swingby trajectories were analyzed together with both long and short trajectories for the direct leg of the round trip mission.

These investigations included variations in the vehicle propulsive and deceleration systems both at Mars and at Earth, in nuclear engine performance parameters, and vehicle structural scaling laws.

Opposition class round trip missions to Mars were reanalyzed for those vehicle weight and performance parameters which were not investigated in Phase III. The results of these mission evaluations were incorporated with existing data from Phase III, the swingby mission results, and the conjunction class mission results (Section III) to illustrate the effect on initial vehicle weight of the variations in launch opportunities, mission and trajectory types, performance parameters, and vehicle systems and scaling laws.

ASSUMPTIONS AND CONSTRAINTS

A set of assumptions and constraints were postulated for this task in order to circumscribe the mission types and modes, the vehicle system weights and performance parameters, the mission and vehicle operational criteria, and the scope of analysis.

Missions

The basic set of missions analyzed and compared in this task consists of the following:

- o Manned Mars stopover mission with a Venus gravity turn swingby during one leg
- o Manned Mars stopover mission (opposition class)
- o Manned Mars stopover mission (conjunction class)
- o Manned Mars stopover mission with a Venus powered turn swingby during one leg

Mission Description - A typical opposition class stopover mission is shown in Figure II-1 which depicts the major operational phases that occur during the mission and the points along the trajectory at which major velocity and vehicle weight changes occur. Additional vehicle weight requirements are considered for life support expendables, propellant boiloff, and attitude control. If an aerodynamic braking mode is employed at the target planet (Mars), a propulsive velocity change is used for circularizing or adjusting the resulting orbit. The earth braking propulsive retro can be eliminated by option and an all aerodynamic earth braking mode employed.

A swingby mission is essentially the same as the Mars stopover mission depicted in Figure II-1 except the trajectory is constrained to pass in the vicinity of the planet Venus either during the outbound or inbound leg. The vehicle, therefore, performs a hyperbolic turn about Venus. For a given approach V_{∞} the degree of turn is governed by the choice of the periapsis radius. For the swingby mission, a third midcourse correction propulsion maneuver is assumed.

For the Venus powered turn swingby, a desired departure hyperbola is attained by initiating a propulsive impulse at the optimum (minimum ΔV) point on the incoming swingby hyperbola. For a given approach V_{∞} the magnitude and direction of this departure asymptote is a function of the radius of closest approach and the magnitude of the impulse. A discrete closest approach distance exists that minimizes the propulsive impulse required to attain the desired outgoing asymptote. If this approach distance is less than the specified minimum, the approach distance is constrained to the minimum and the corresponding (non-minimum) propulsive impulse is computed.

The conjunction class stopover mission is essentially similar to the opposition class mission except a stopover time at Mars is selected so that the return trip to Earth occurs during the next Earth-Mars opposition following the opposition that occurs during the outbound leg. The spacecraft, therefore, dwells at Mars during the Earth-Mars conjunction which occurs between the two oppositions. This dwell time is characteristically about 400 days.

Trajectory Types - Two types of trajectories were considered for the direct leg of the swingby missions, types I or B and types II or A. Types I and II refer to the outbound leg; types A and B refer to the inbound leg. The I or B denotes a trajectory leg where the heliocentric angle traversed, θ , is greater than 180° and

less than 360° ; the II or A designates a trajectory leg where $0^{\circ} < \theta < 180^{\circ}$.

Three types of trajectories were considered for the swingby leg of a swingby mission, types 1, 3, and 5. A detailed discussion of swingby trajectory characteristics is presented later in this section and in Ref 3.

Only the IIB round trip trajectory was considered for the opposition class mission comparisons. It was previously shown in Phase III (Ref 1) that the IIB trajectory generally produces the minimum initial vehicle weight for all opportunities. For a few opportunities in the Earth-Mars synodic cycle and for certain vehicle mode and performance combinations, the IB trajectory can result in a slightly lower weight vehicle (approximately two percent) but with an attendant increase in total trip time of approximately 13 percent.

A IA conjunction class mission trajectory was selected for comparing the conjunction class mission with the opposition and swingby class missions in this task. The IA conjunction class trajectory yields a lower weight vehicle than the other three possible trajectories (types IB, IIA, and IIB). The total trip time for the type IA trajectory is within approximately three percent of the minimum trip time obtained for the other types. (A full discussion of conjunction class missions is presented in Section III.)

Mission Matrix - Table II-1 presents the matrix of opportunity years and mission and trajectory types analyzed for this task in order to provide comparisons among opposition, swingby, and conjunction class missions.

Table II-1 Comparative Mission Matrix

<u>Mission Type</u>	<u>Year</u>	<u>Trajectory Type</u>	
		<u>Outbound</u>	<u>Inbound</u>
Swingby (Gravity Turn)	1980	I and II	1
		3	A and B
	1982	I and II	3
		1	A and B
	1984	I and II	5
		5	A and B
	1986	I and II	1
		3	A and B

<u>Mission Type</u>	<u>Year</u>	<u>Trajectory Type</u>	
		<u>Outbound</u>	<u>Inbound</u>
Swingby (Powered Turn)	1980	I	1
	1982	I	3
Opposition Class	1980, 1982, 1984 and 1986	II	B
Conjunction Class	1983	I	A

Vehicle Configuration and System Weights

A number of assumptions, constraints, and scaling laws were used concerning the mission payloads, propellant tanks, propulsion systems, secondary spacecraft systems, and operational modes.

Propulsion System Weight Scaling Laws - Two inherently different types of vehicle configurations were used for this study task, a tanking mode and a connecting mode.

The tanking mode tends to make full use of the Earth launch vehicle payload volume capacity, which may be restricted by overall vehicle length limitations, by orbiting empty or partially filled modules. The modules are then filled via propellant transfer from tanker vehicles or from an orbital propellant storage facility. In this configuration approach all tanks clustered in any given stage were assumed to be the same capacity; the maximum capacity of each tank set by the limitations of the Earth launch vehicle. In order to increase the gross effective thrust for vehicles employing nuclear engines, thereby reducing the velocity gravity losses, engine clustering or the simultaneous use of two or more nuclear engines were investigated for the leave Earth stage. The optimum number of engines, i.e., the configuration producing the minimum weight vehicle was then selected as the optimum configuration.

In the connecting mode, the modules are orbited fully loaded with propellant, hence, their propellant capacity is limited by the Earth launch vehicle payload weight capacity. The use of the connecting mode gives rise to a specific vehicle design configuration or method of adding tanks to each stage as the propellant requirements increase. For the leave Earth stage, a cluster of three propulsion modules is first assumed, each propulsion module containing a nuclear engine. This set of three modules is designated tier 1. If these three modules have insufficient capacity to contain the required propellant a single propellant module, designated tier 2A is attached above tier 1. If the total propellant capacity of

tier 1 and tier 2A is still insufficient, two additional propellant modules are clustered to the single propellant module. The resultant three propellant modules are designated tier 2B. Should the total propellant capacity still be insufficient another single propellant module, designated tier 3, is attached above tier 2B.

The configurations for the arrive Mars and leave Mars stages are similar to the leave Earth stage except single propulsion modules or propellant modules are used at each level or tier. A schematic depiction of the connecting mode configuration is shown in Figure II-2.

In addition to the tank and engine weights associated with each stage of the connecting mode configuration, a block weight is assigned to each stage to account for the docking and interstage structure, the attachment members, and the separating mechanism. This weight is designated the stage constant and takes the form of a fixed weight assigned to each stage.

Each of the two modes, the tanking mode and the connecting mode, has its own set of structural scaling laws. Two sets of scaling laws were investigated for the tanking mode. These sets of scaling laws were taken from Phase III and are designated mass fraction case No. 2 and No. 3 (Ref 1). These two sets of scaling laws are given in Tables II-2 and II-3. Included in these tables are the scaling laws used for the midcourse correction stages, the Mars orbit circularizing stage (used with aerodynamic braking at Mars), and the arrive Earth retro stage.

Vehicle configurations employing either chemical or nuclear propulsion systems for main stages were analyzed for mass fraction case No. 2. Mass fraction case No. 3 was used only for the vehicle configurations employing chemical main stage propulsion systems.

The scaling laws for the connecting mode configuration were based on preliminary results from the LMSC Modular Nuclear Vehicle Study, Phase II. These scaling laws are listed in Table II-4 and include the additional laws used for the secondary propulsion systems. Subsequent LMSC design analyses have shown that these mass fraction values can be considerably improved. The connecting mode configuration was used only for vehicle configurations employing nuclear propulsion stages-

For the conjunction class mission, an additional weight was added to the planet depart stage to account for the increased micrometeoroid protection required due to the longer planet stopover period. This weight was added to the tank weight for all

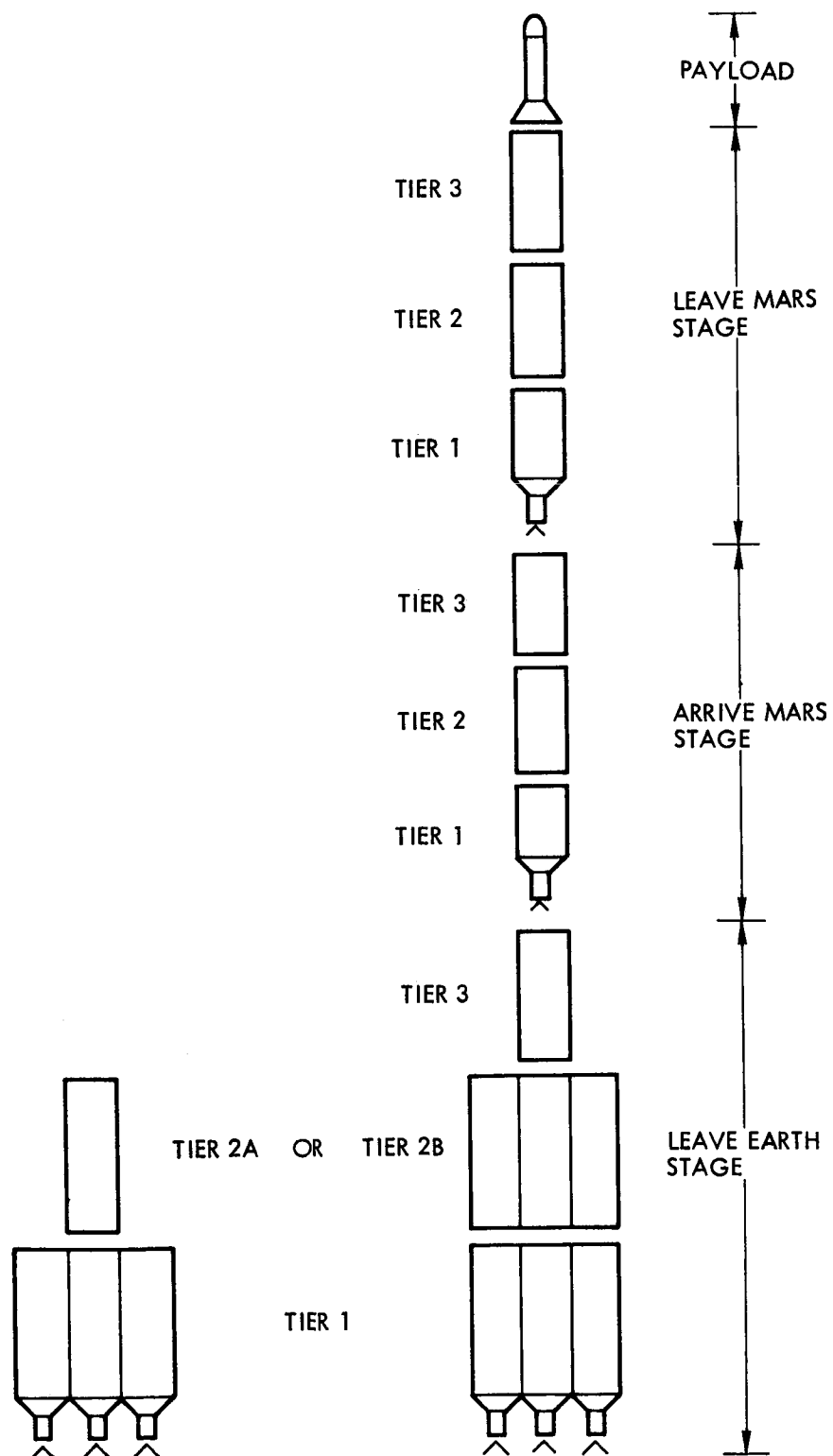


Figure II-2. Connecting Mode Vehicle Configuration

Table II-2 Mass Fraction Case No. 2

<u>Mode</u>	<u>Equation (lbs)</u>	<u>Single Tank Max Propellant Capacity (lbs)</u>
Earth Depart		
Nuclear Propulsion	$W_j = .16520 W_p + 6,357$	342,540
Cryogenic Propulsion	$W_j = .09622 W_p + 18,184$	1,540,000
Midcourse Correction Outbound		
Storable Propulsion	$W_j = .09193 W_p + 1,541$	
Planet Braking		
Nuclear Propulsion	$W_j = .19088 W_p + 3,198$	342,540
Cryogenic Propulsion	$W_j = .13154 W_p + 11,013$	700,000
Aero Capture Orbit Circularizing		
Storable Propulsion	$W_j = .09193 W_p + 1,541$	
Planet Depart		
Nuclear Propulsion	$W_j = .19088 W_p + 3,198$	342,540
Cryogenic Propulsion	$W_j = .13154 W_p + 11,013$	700,000
Storable Propulsion	$W_j = .07554 W_p + 16,561$	800,000
Midcourse Correction Inbound		
Storable Propulsion	$W_j = .06596 W_p + 951$	
Earth Braking		
Storable Propulsion	$W_j = .09931 W_p + 3,828$	

Notes:

1. Includes micrometeoroid protection
2. Includes insulation for Earth depart stages
3. Does not include insulation for all other stages
4. Includes engine weight for all non-nuclear stages
5. Does not include engine weight for all nuclear stages

Table II-3 Mass Fraction Case No. 3

<u>Mode</u>	<u>Equation (lbs)</u>	<u>Single Tank Max Propellant Capacity (lbs)</u>
Earth Depart		
Cryogenic Propulsion	$W_j = .14692 W_p + 19,921$	1,540,000
Midcourse Correction Outbound		
Storable Propulsion	$W_j = .12888 W_p + 1652$	
Planet Braking		
Cryogenic Propulsion	$W_j = .19937 W_p + 12,404$	700,000
Aero Capture Orbit Circularizing		
Storable Propulsion	$W_j = .12888 W_p + 1652$	
Planet Depart		
Cryogenic Propulsion	$W_j = .19937 W_p + 12,404$	700,000
Storable Propulsion	$W_j = .12385 W_p + 18,131$	800,000
Midcourse Correction Inbound		
Storable Propulsion	$W_j = .10094 W_p + 1021$	
Earth Braking		
Storable Propulsion	$W_j = .14973 W_p + 4215$	

Notes:

1. Includes micrometeoroid protection
2. Includes insulation for Earth depart stages
3. Does not include insulation for all other stages
4. Includes engine weight for all stages

Table II-4 Connecting Mode Scaling Laws

<u>Mode</u>	<u>Equation (lbs)</u>	<u>Max Capacity (lbs)</u>
Earth Depart		
Nuclear Propulsion		
Tier 1	$W_j = .2106 W_p + 30,804$	657,540
Tier 2A	$W_j = .2106 W_p + 15,090$	244,122
Tier 2B	$W_j = .2106 W_p + 44,409$	736,449
Tier 3	$W_j = .2106 W_p + 14,621$	
Stage Constant	17,550	
Midcourse Correction Outbound		
Storable Propulsion	$W_j = .1100 W_p + 1600$	
Planet Braking		
Nuclear Propulsion		
Tier 1	$W_j = .2106 W_p + 9,105$	224,700
Tier 2	$W_j = .2106 W_p + 14,621$	246,349
Tier 3	$W_j = .2106 W_p + 14,621$	
Stage Constant	16,240	
Aero Capture Orbit Circularizing		
Storable Propulsion	$W_j = .12888 W_p + 1652$	
Planet Depart		
Nuclear Propulsion		
Tier 1	$W_j = .2106 W_p + 9,105$	224,700
Tier 2	$W_j = .2106 W_p + 14,621$	246,349
Tier 3	$W_j = .2106 W_p + 14,621$	
Stage Constant	6,875	
Storable Propulsion	$W_j = .12385 W_p + 18,131$	800,000
Powered Turn for Venus Swingby		
Cryogenic Propulsion	$W_j = .19937 W_p + 12404$	
Midcourse Correction Inbound		
Storable Propulsion	$W_j = .06596 W_p + 951$	
Earth Braking		
Storable Propulsion	$W_j = .09931 + 3828$	

Table II-4 Connecting Mode Scaling Laws (Continued)

Notes:

1. Includes micrometeoroid protection
2. Includes insulation for all cryogenic stages
3. Includes engine weight for all non-nuclear stages
4. Does not include engine weight(s) for all nuclear stages
5. Scaling equations and max propellant capacities for Earth depart, Tiers 1 and 2B are for three clustered modules.

sets of scaling laws, i.e., mass fraction case No. 2 and No. 3 and connecting mode. The additional weight is equal to 38,000 pounds plus 40 times the stopover time in days and is jettisoned prior to Mars departure.

A single nuclear engine weight of 38,000 pounds was used and each engine was assumed to have 230,000 pounds thrust. The engine weight and thrust for clusters of two or more nuclear engines were taken as direct multiples of these values.

Payload and Expendable Weights - The payloads and expendable weights assigned to the various missions were selected jointly by MSFC and TRW. They represent reasonable values and obtained from the many interplanetary mission studies performed by NASA, TRW and industry in the past years.

The Earth recovered payload lands the crew on the Earth's surface after aerodynamic braking has been accomplished. It consists of the crew and the required structure, landing and recovery aids, power supply, communications, guidance, and navigation equipment, reaction jets, life support systems, and any space or planetary payloads that may be returned to earth.

The mission module contains all systems, equipment, and living quarters required during the full duration of the mission. This module is jettisoned just prior to retrobraking at Earth or aerodynamic braking if a retro is not employed. It consists of structure, crew quarters, life support systems, medical supplies and recreation equipment, communication, guidance, and navigation systems, power supplies, maintenance facilities and spare parts, and air locks. The solar flare shield is not included in the mission module weight. The shield weight is computed as a function of the assumed solar activity and perihelion distance. This weight is added to the mission module weight to determine the total weight to be jettisoned prior to Earth arrival.

The crew exposure to solar flare radiation is limited by a solar flare shield. The amount of shielding, or the shield weight, depends on the solar activity, the trip time, the total dose permitted, the distance from the sun, and the volume of space to be protected by the shield. Since the shield weight depends on trajectory parameters, its effect is included in the optimization equations.

The solar flare activity varies in an approximate 11-year cycle from a quiet sun to an active sun and back again. This yearly variation was accounted for by developing three solar flare shield weight scaling laws, for a quiet, intermediate, and active sun. These laws were developed in Phase III (Ref 1) and are represented by the equations below which relate the weight of the solar flare shield, W_S , to the minimum perihelion distance, r_p , encountered during the mission. W_S is in lbs and r_p is in astronomical units.

Active Solar Flare Activity

$$W_S = 12,672 + \frac{2615}{r_p - 0.27165}$$

Intermediate Solar Flare Activity

$$W_S = 14,463 + \frac{1315}{r_p - 0.27085}$$

Quiet Solar Flare Activity

$$W_S = 16,266 + \frac{0.01}{r_p - 0.3}$$

The scaling law for the quiet sun was used for the opportunity year of 1986. The intermediate sun scaling law was used for the 1984 opportunity year. For 1980 and 1982, the active sun solar flare radiation shield weight scaling law was used. Due to the absence of perihelion distances in the available swingby trajectory data, a perihelion distance of 0.72 was used to compute the solar flare shield weight for all swingby missions. A perihelion distance of 1.0 AU was used for conjunction class mission.

The Mars excursion module for the stopover mission is jettisoned from the spacecraft out of the Mars circular orbit. It contains the required systems and equipment for landing the module on the planet surface and subsequently performing scientific and engineering experiments. In addition, the Mars excursion module contains the ascent or orbit return module which returns the crew and payload to the orbiting spacecraft. The specified weight for the orbit return module includes only that portion of the module which is taken onboard the orbiting spacecraft and subsequently boosted out of planetary orbit.

The life support expendables include all of the crew's environmental and biological requirements which are expended at an average daily rate for the duration of the mission.

A list of the payload and expendable weight data used in this task are given in Table II-5. It should be noted that the weights for the conjunction class mission are approximately 50 percent greater than the weights for the opposition and swingby class missions to account for an increased crew size and crew and system requirements dictated by the long stay time at Mars. The weights for the conjunction class mission correspond to the payload set No. 3 given in Section III of this report in which the payloads were varied parametrically for the conjunction class mission.

Table II-5 Payload and Expendable Weights

<u>Payload</u>	<u>Mission Mode</u>	
	<u>Opposition and Swingby</u>	<u>Conjunction</u>
Earth Return Module	10,000 lb	15,000 lb
Mission Module (not including Solar Flare Shield)	68,734 lb	100,000 lb
Mars Excursion Module	80,000	135,000 lb
Orbit Return Weight	1,500 lb	3,100 lb
Life Support Expendables	50 lb/day	75 lb/day

Aerodynamic Braking Scaling Laws - As part of the mission analyses, it was necessary to express the weight of the aerodynamic heat shield as a function of the entry velocity for the operational modes employing aerodynamic braking for the Earth entry module and for arriving at Mars. The analysis and derivation of the scaling laws were accomplished during Phase III and this work is fully described in Ref 1.

The scaling laws for aerodynamically braking the Earth return module are given below for the two module weights used in this task.

$$W_R = 10,000$$

$$W_{ERM} = 46.71 V_{AE}^2 - 1042.3 V_{AE} + 20,122$$

$$W_R = 15,000$$

$$W_{ERM} = 55.82 V_{AE}^2 - 1237.7 V_{AE} + 27,384$$

where

W_R - Recovered or useable payload weight after Earth entry (lbs)

W_{ERM} - Gross vehicle weight or Earth entry module weight (lbs)

V_{AE} = Entry velocity relative to a non-rotating Earth at an altitude of 100 km (km/sec)

The weight scaling law for aerodynamic braking at Mars is:

$$\frac{W_S}{W_{AM}} = 0.001385 V_{AP}^2 + 0.183$$

where W_S - Heat shield weight including all jettisonable ablative material, structure, and insulation (lbs)

W_{AM} - Gross vehicle weight arriving at Mars (lbs)

V_{AP} - Arrival velocity relative to Mars at an altitude of 167 km (km/sec)

Secondary Spacecraft Systems - Additional weight expenditures were allowed for secondary spacecraft systems including midcourse corrections, attitude control, and orbit adjustment for modes employing aerodynamic braking at Mars.

It was assumed in all mission calculations, that the midcourse corrections were performed with a liquid storable propellant system having a specific impulse of 330 sec. Separate jettisonable stages were used for the outbound and inbound leg velocity corrections and for a third leg correction for swingby missions. The scaling laws for the jettisonable stages were given previously under Propulsion System Weight Scaling Laws. A midcourse correction of 100 m/sec was used for each outbound and inbound leg as well as for the additional leg of a swingby mission.

The attitude control functions include orientation for midcourse corrections, spinning of the spacecraft or mission module for artificial gravity or thermal control, orientation of communication antennas, sensors, radiators, or solar panels or collectors, and orientation for planetary rendezvous and aerodynamic braking or propulsive maneuvers. One percent of the vehicle weight was used for attitude control during each leg of the mission including the third swingby leg.

The attitude control provisions during the planetary stopover period were computed on the basis of 0.2 percent of the vehicle weight in planetary orbit.

A separate propulsion system is included in the spacecraft for all modes employing aerodynamic braking at Mars for circularizing and adjusting the orbit after braking at Mars. This jettisonable propulsion stage utilizes liquid storable propellants at a specific impulse of 330 sec and is sized for a characteristic velocity of 130 m/sec. The stage weight scaling laws were given previously under Propulsion System Weight Scaling Laws.

Cryogenic Propellant Vaporization - Due to the basically different design, launch, and assembly philosophies inherent in the two configuration modes, viz, the tanking mode and the connecting mode, two separate computational techniques were employed for determining the propellant vaporized during the interplanetary trip.

For the tanking mode the analysis determines the optimum trade-off between the thickness or weight of insulation and the weight of vaporized propellant such that a minimum weight vehicle results. The insulation requirements for each stage are determined separately resulting in different insulation thicknesses for each stage. The connecting mode assumes that the insulation thickness is the same for all of the stages and is preselected to form the best compromise for all of the mission phases during which propellant is vaporized.

The cryogenic propellant storage analysis for the tanking mode permits the sizing of the required tankage insulation and calculation of the weight of propellant boiled off during the mission to yield a minimum overall vehicle weight. The analysis and derivation of the necessary equations was performed during Phase III and is detailed in Ref 1. The equations form the basis of the insulation/boiloff optimization subroutine in the SWOP program. The assumption of vented tanks was made and insulation requirements were considered and sized only for the conditions and storage durations commencing with the point just prior to boost out of Earth orbit. At this initial point, it was assumed that all tanks were full.

The optimum selection of the insulation requirements for subsequent cryogenic propellant stages is dependent not only on the insulation and thermal parameters (density, conductivity, temperatures, etc.) but also considers the duration of storage and the size, number, and time of vehicle propulsive velocity changes.

For a multistage vehicle, the relationships between these latter factors has a major influence in the trade-off between insulation and propellant boiloff.

The optimization analysis applies for either cryogenic monopropellants, or bipropellants. For bipropellants, the equations are employed for the fuel and oxidizer separately, obtaining separate insulation and boiloff weights for each propellant component. Appropriate tank areas, heats of vaporization, and temperature differences are used in each case.

The following assumptions and values were used for specifying the various insulation and thermal constants in the optimization analysis for the tanking mode.

The insulation was assumed to be National Research Corporation's NRC-2, which consists of layers of crinkled aluminized mylar 0.25 mil thick. The nominal values of the insulation thermal conductivity and density are 7×10^{-5} Btu/hr. ft. $^{\circ}\text{R}$ and 3 lb/ft^3 , respectively. In determining the temperature differences across the insulation, a nonspinning tank was assumed and an average temperature difference over the entire tank surface was calculated. No planetary influence or heat sources other than the sun were assumed and an average distance to the sun of 1.2 AU was used. A solar absorptivity of 0.20 and an emissivity equal to 0.80 were used for the tank surface conditions. The average temperature differences across the insulation computed for liquid hydrogen tanks is 160°R and for liquid oxygen tanks, 34°R . The heats of vaporization for hydrogen and oxygen are 192.7 and 91.6 Btu/lb, respectively.

The cryogenic propellant storage analysis for the connecting mode determines the weight of propellant vaporized during the various phases of the mission based on specified rates of propellant boiloff, i.e., fixed insulation thickness. The weight of this insulation per tank is, therefore, a fixed quantity and is included in the scaling laws previously listed for the connecting mode.

Since the propellant tanks for this mode are not filled or topped off in Earth orbit, the quantity of propellant vaporized from the tanks during assembly and checkout prior to injection into the interplanetary orbit must be considered. The amount of hydrogen vaporized in Earth orbit was computed and the scaling laws and tank capacities were adjusted for the additional tankage and reduction in available tank capacity required to contain this vaporized propellant. The weights of propellant vaporized in Earth orbit for the various modules of the connecting mode are given in Table II-6.

Table II-6 Propellant Vaporized in Earth Orbit

<u>Module</u>	<u>Propellant Vaporized</u>
Depart Earth	
Tier 1 (3 modules)	23,760 lbs
Tier 2A	4,701
Tier 2B (3 modules)	10,020
Tier 3	2,474
Arrive and Depart Mars	
Tier 1	2,400
Tier 2	2,474
Tier 3	2,474

The propellant vaporized for the arrive and depart Mars stages during the interplanetary trajectory was based on the actual mission durations and propellant tank requirements and subsequently computed for each mission case investigated. The propellant boiloff rates used for these computations are listed in Table II-7. This table also includes the rates used for determining the propellant vaporized in Earth orbit.

Table II-7 Propellant Vaporization Rates

<u>Mission</u> <u>Phase</u>	<u>Propellant Vaporization Rates</u>	
	<u>Structural</u>	<u>Tank Wall</u>
Earth Orbit	75.24 lb/day per tank	5.43×10^{-3} lb/day ft ² of tank area
Outbound leg	24	2.388×10^{-3}
Mars Orbit	58.32	4.674×10^{-3}

Vehicle Mode Matrix

Each of the mission cases represented in the Comparative Mission Matrix, Table II-1, pg II-4 was analyzed for a variety of vehicle modes, propulsion types, engine performance parameters, and stage scaling laws.

Table II-8 shows the combination of sets of scaling laws and propulsion and aerodynamic braking systems analyzed for each of the opposition, conjunction, and gravity turn swingby class missions of the Comparative Mission Matrix.

Table II-8 Vehicle Mode Matrix

<div>Earth Depart</div> <div>Mars Arrival</div> <div>Mars Depart</div> <div>Earth Arrival</div>				
	NNN	NAS	CCC	CAS
A	MF #2 Connecting Mode	MF #2 Connecting Mode	MF #2 MF #3	MF #2 MF #3
S(P)	MF #2 Connecting Mode		MF #2 MF #3	

N - Nuclear Propulsion (800 and 850 sec)

C - Chemical Cryogenic Propulsion, H_2/O_2 (440 sec)

S - Liquid Storable Propulsion (330 sec)

A - Aerodynamic braking

S(P) - Liquid storable propulsion (330 sec) to parabolic entry velocity followed by aerodynamic braking

The vehicle modes employing nuclear stages were analyzed for both 800 and 850 sec specific impulse. In addition the use of one, two, three and four clustered nuclear engines were investigated for mass fraction case No. 2 for the depart Earth stage in order to determine the optimum engine configuration, i.e., the number of engines which produce the optimum thrust-to-weight ratios for the depart Earth stage. As mentioned previously, three clustered nuclear engines were used for all connecting mode configurations. A specific impulse of 440 sec was used for the chemical cryogenic (H_2/O_2) stages and 330 sec for the liquid storable stages.

The powered turn swingby mode was analyzed primarily to obtain a comparison with the gravity turn swingby. For this purpose only the NNNA connecting mode configuration was investigated. A specific impulse of 850 sec was used for the nuclear engines and a chemical cryogenic propulsion system with a specific impulse of 440 sec was assumed for providing the propulsive kick during the Venus swingby.

GRAVITY TURN SWINGBY MISSIONS

The major objectives for this task were 1) to determine the initial vehicle weight requirements for Mars stopover missions employing gravity turn swingbys at Venus for the years 1980 through 1986, and 2) to compare these results with the analogous results for opposition and conjunction class missions for the same time period. Variations in vehicle propulsion and deceleration systems both at Mars and Earth, in nuclear engine performance parameters, and in vehicle structural scaling laws were investigated in order to obtain a set of broad comparative data for assisting future manned interplanetary mission planning activities. The complete set of mission modes and vehicle modes investigated were previously listed in Tables II-1 and II-8 on pages II-4 and II-19, respectively. A succeeding portion of this section extends the swingby mission comparison to powered turn swingbys.

In order to illustrate some of the basic characteristics of gravity swingby trajectories, this portion of the Swingby Mission Analysis section first presents a discussion of the methods of trajectory data generation and data processing to obtain the free flight trajectory data used in the mission optimization program (SWOP). Following this discussion are the results of the mission and vehicle mode analyses together with a comparative evaluation of these data.

Generation and Processing of Trajectory Data

The generation of the gravity turn swingby trajectory data was accomplished at the NASA/Office of Manned Space Flight (Washington) and transmitted to TRW. The method of trajectory data generation is reviewed in this section for the purposes of completeness. Only the generation of the inbound gravity turn swingby will be discussed since analogous procedures would be carried out for the outbound gravity turn swingby.

Possible Venus swingby missions were found by matching one-way, Mars-Venus and Venus-Earth trajectories at Venus. In order for Venus to perturb the vehicle sufficiently to alter its heliocentric trajectory, it is necessary for the vehicle to pass well within the sphere of influence of Venus. The approach used is the restricted two-body (so-called "patched conic") approximation of the vehicle's trajectory. While the vehicle is within the sphere of influence of Venus, it is assumed to be on a free-flight conic section (hyperbolic) trajectory about Venus and gravitational effects of all other bodies are neglected. There is no change of energy of the vehicle with respect to Venus. Therefore, conservation of energy requires that the magnitude of the vehicle's velocity at infinity (V_∞) leaving Venus must equal its arrival velocity at infinity. It is possible, then, to match Mars-Venus trajectories and Venus-Earth trajectories at Venus (for a given date at Venus) to form the Mars-Venus-Earth gravity turn swingby trajectories simply by matching the arrival and departure V_∞ magnitudes. The magnitudes and directions of the arrival V_∞ and the departure V_∞ together define a unique hyperbolic trajectory about Venus, i.e., the planet passage distance (periapsis) is uniquely determined.

Figure II-3 illustrates the V_∞ matching procedure for a given Venus encounter date. The graph on the left represents the Mars-Venus trip and that on the right the Venus-Earth trip. Gravity turn swingbys are possible for a given Venus encounter date (TEV) wherever the arrival and departure V_∞ 's match. It is evident that the V_∞ 's of branch 1 of the left graph can be matched with the V_∞ 's of branch A, branch B, branch C or branch D of the right graph. There are actually sixteen possible matching combinations yielding sixteen combinations of first leg time and second leg time (TI_1 and TI_2) for a given TEV. If Venus is assumed to be a dimensionless point mass and if we ignore what happens to the velocities leaving Mars and arriving at Earth, all of the sixteen combinations are theoretically possible. However, practical restrictions eliminate some of these possible

matching combinations. Since Venus is an approximate sphere of finite size with an atmosphere, it is necessary to eliminate any combinations yielding a planet passage distance less than some minimum value (1.05 Venus radii was assumed to allow some margin above the atmosphere). Also combinations yielding impractically high speeds leaving Mars or arriving at Earth can be eliminated. After these practical restrictions are applied, typically two to four combinations remain.

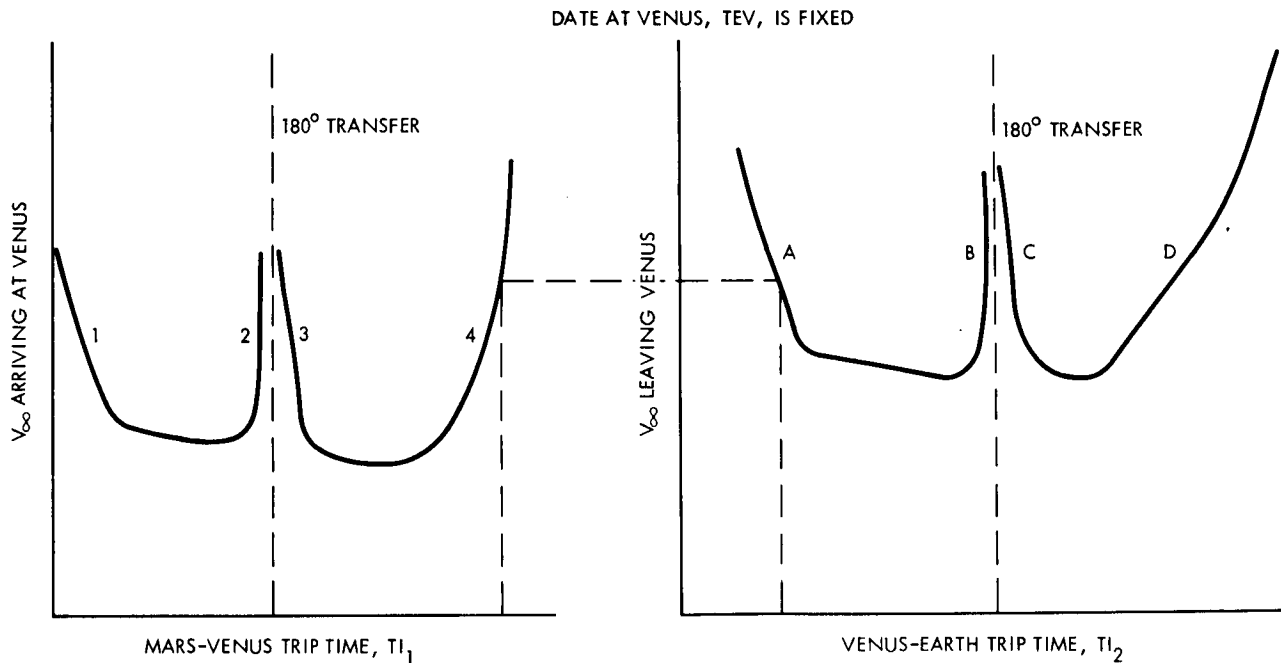


Figure II-3. Typical Possible Gravity Turn Swingby Trajectories

Figure II-4 represents two typical matching combinations. However, all quantities of interest for these two combinations are continuous so the two combinations can be taken together as one set of trajectory data. The procedure for generating the swingby data is as follows:

- o TEV and TI_1 are fixed and the arrival V_∞ determined.
- o The set of Venus-Earth trajectories for the fixed TEV is searched to find a departure V_∞ matching the arrival V_∞ . Interpolation on the Venus-Earth trajectory data is required since the precise required V_∞ value is generally not found. Planet passage distance is calculated.

- o For the matched trajectory, the Mars departure, Venus encounter, and Earth arrival data are output.
- o First TI_1 and then TEV are varied incrementally and the matching procedure repeated.

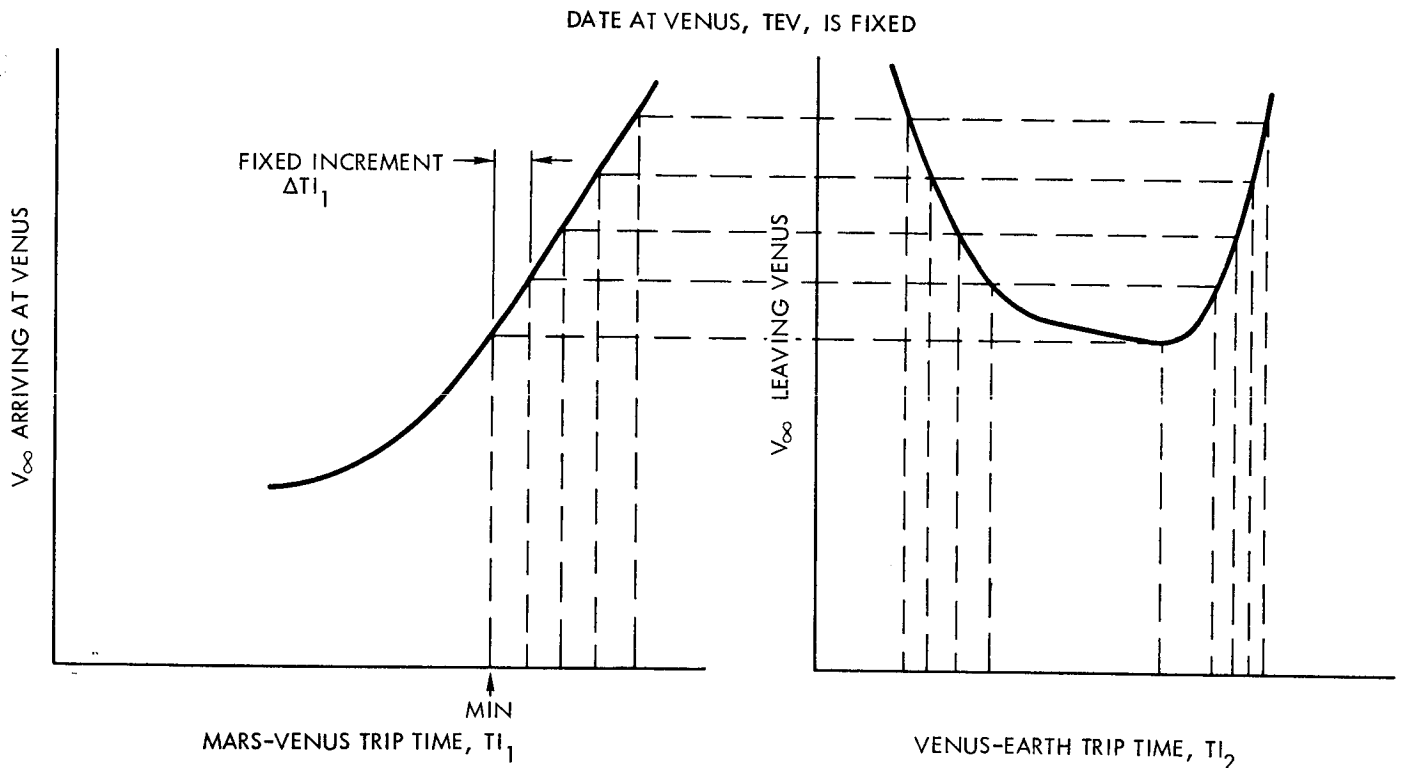


Figure II-4. Typical Matching of Gravity Turn Swingby Trajectory Legs

The data given by the solid curves of Figure II-5 (along with other associated Mars departure and Earth arrival data) represent the resulting data for a given swingby opportunity period. All of these data have been generated as a function of the two independent parameters, TEV and TI_1 , at fixed increments of these two parameters.

These data are used in the SWOP computer program with Earth-to-Mars trajectory data to optimize round-trip missions. Since SWOP mates the outbound and inbound trajectories at Mars, it is convenient in SWOP to use the Mars date as one of the independent variables defining the round trip trajectory. It was necessary, therefore, to convert the NASA-furnished data to data having the Mars departure date (TLP) as the independent parameter. This required a subtraction and a reordering of the data to obtain sets of constant TLP. The broken curves of Figure II-5 (along with the associated Mars departure and Earth arrival data)

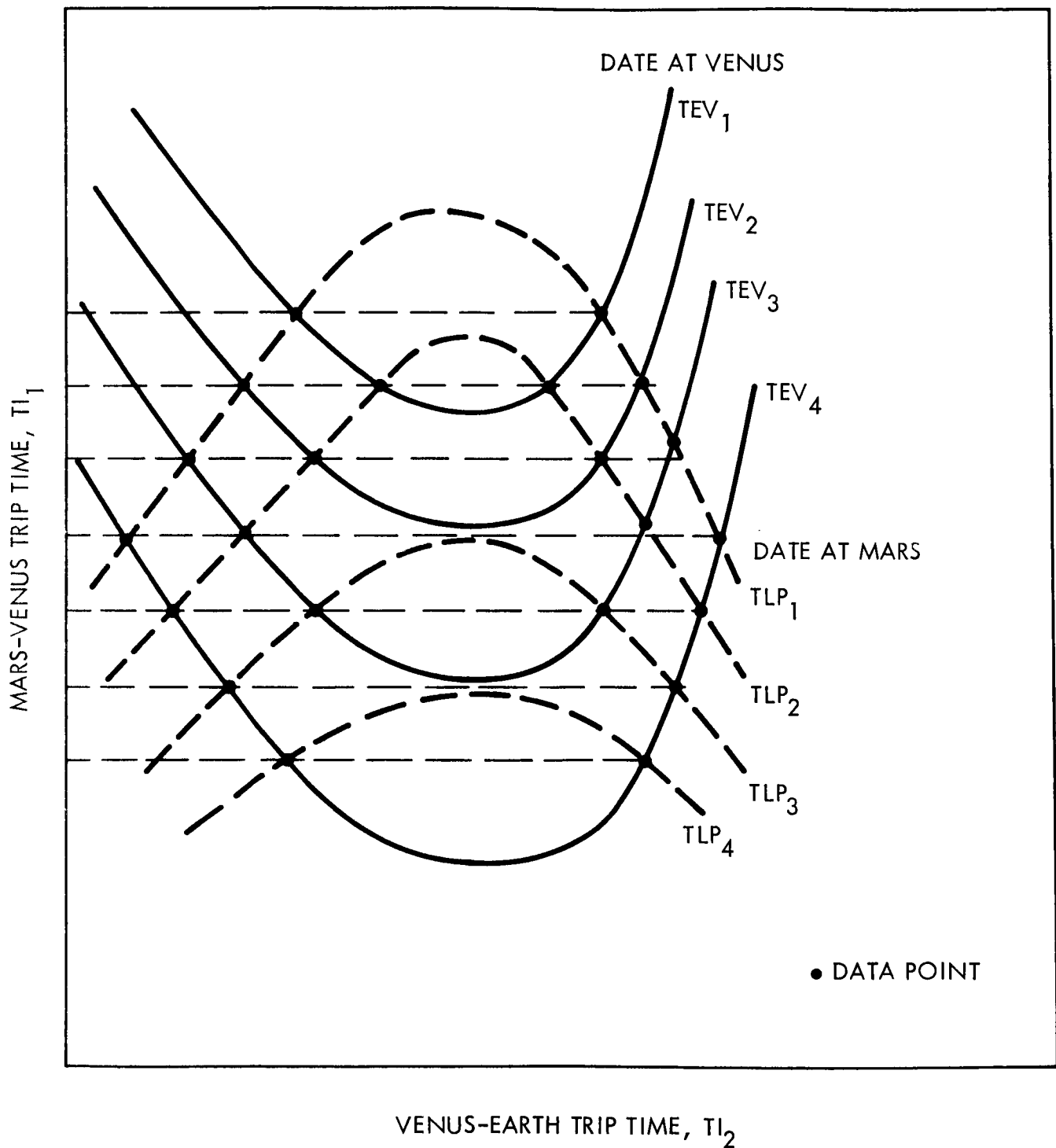


Figure II-5. Typical Matched Gravity Turn Swingby Trajectory

represent the resulting data. However, TI_1 is unsatisfactory as an independent parameter since for each TLP and TI_1 , TI_2 (as well as all of the other data) is double valued. Therefore, an interpolation was required to obtain fixed increments of TI_2 so that TI_2 can be used as the second independent parameter. Note from Figure II-5 that there exist large gaps in the data as a function of TI_2 in the region of maximum TI_1 (for each fixed TLP). In general, the minimum velocity requirements at Earth and Mars also occur in these gaps, so the data in these regions are very important and must be determined as precisely as possible. However, interpolation provides only a curve of best fit to the data points available; it cannot fill in physical data where it does not exist.

The output from the above procedure required very careful manual checking before the data could be finally approved for use in the SWOP program. The data for interplanetary trajectories can change rapidly in slope in a small time interval (e.g., near 180 degree transfer "ridges") and any interpolation procedure which uses data from both sides of this abrupt slope change can yield erroneous interpolated values. It was, therefore, necessary to thoroughly scan the data to verify that interpolated values were within the range of values used in the interpolation and fit the general curve. Erroneous data was eliminated or adjusted by manual plotting and other procedures.

The procedure for preparing the outbound unpowered swingby data for use in the SWOP program was the same as outlined above with one additional step. Since the data was generated with fixed increments of TEV and Earth departure date (TLE) and since SWOP requires fixed increments of Mars arrival date (TAP), an additional interpolation was required to obtain fixed increments of TAP.

Figures II-6 and II-7 illustrate typical sets of trajectory data as they have been finally prepared for mission analysis using SWOP. In the nomenclature of Ross and Gillespie (Reference 3), these represent a type 1 swingby and a type 3 swingby, respectively. They differ primarily with respect to the effect of the planet passage distance constraint. In the type 1 swingby (Figure II-6), the minimum planet passage distance is encountered before the minimum ΔV 's at Mars and Earth are reached; whereas in the type 3 swingby (Figure II-7), practical swingby trajectories containing the lowest ΔV 's at Mars and Earth are feasible because they lie outside the region restricted due to the planet passage distance constraint. A third practical swingby type, (type 5) also occurs. It differs

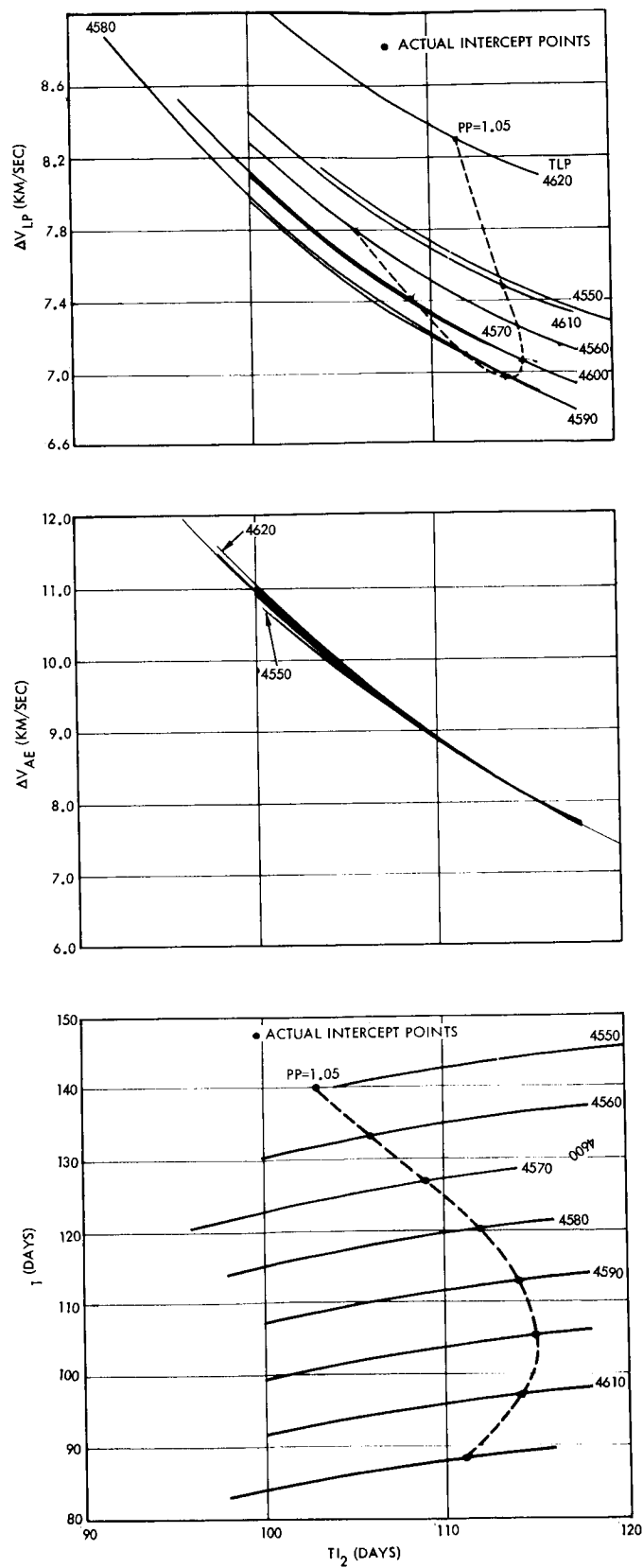


Figure II-6. Velocity Date for 1980 Inbound Gravity Turn Swingby Trajectory

1982 INBOUND GRAVITY TURN SWINGBY, TYPE 3

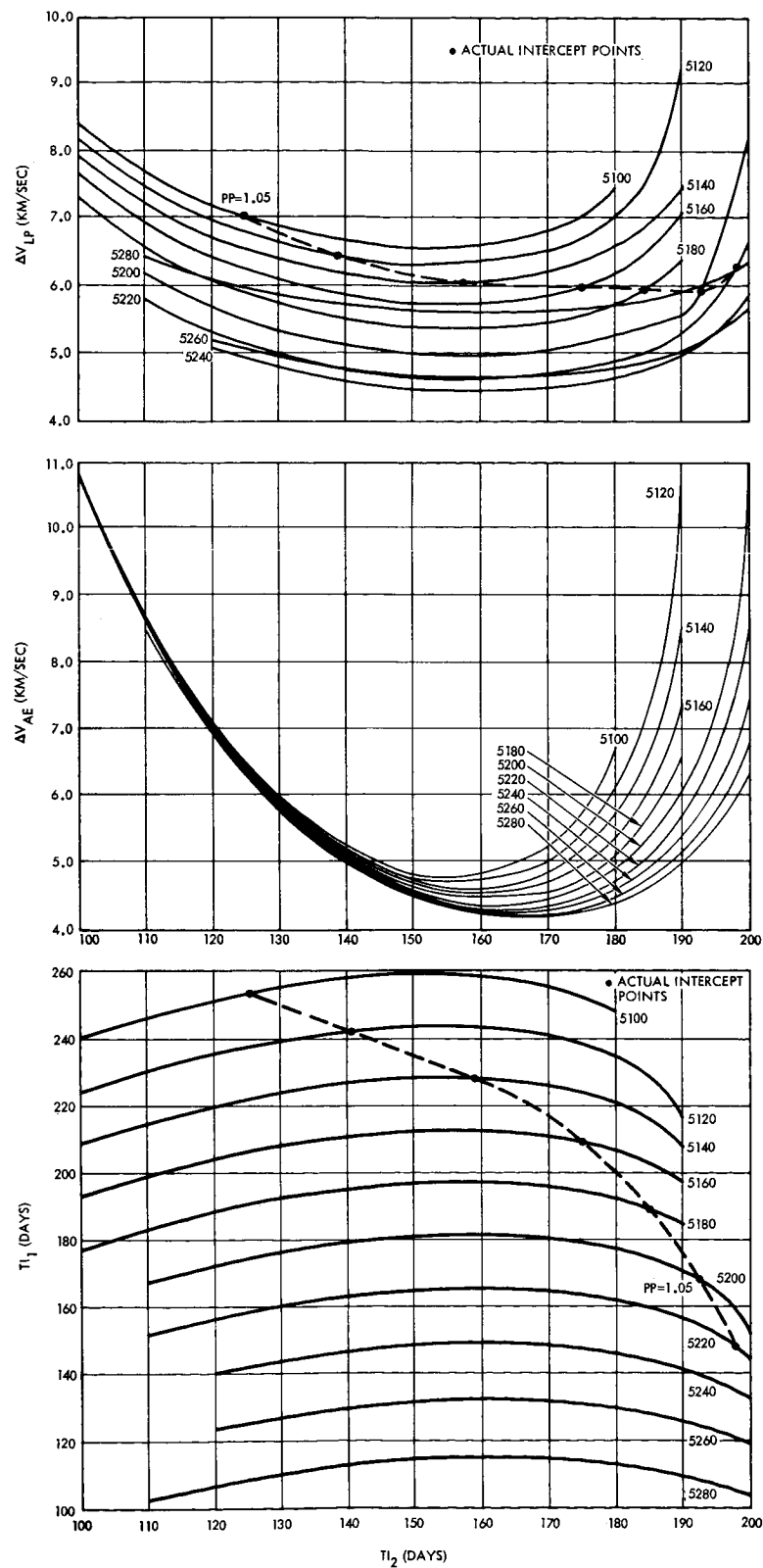


Figure II-7. Velocity Data for 1982 Inbound Gravity Turn Swingby Trajectory

appreciably from the types 1 and 3 since it results from a much different alignment of the three planets than that yielding the types 1 and 3. A more comprehensive discussion of the swingby types, the differences between them, and their merits is available in Reference 3.

The unpowered swingby data received from NASA and processed as outlined above consisted of eight sets as summarized in Table II-9.

Table II-9 Available Swingby Trajectory Data

<u>Year</u>	<u>Direction</u>	<u>Type</u>
1980	Outbound	3
1980	Inbound	1
1982	Outbound	1
1982	Inbound	3
1984	Outbound	5
1984	Inbound	5
1986	Outbound	3
1986	Inbound	1

Each line in the table above represents one set of data received and processed. For both the 1984 inbound swingby and the 1986 outbound swingby part of a second set was received, but the second set was inadequate in both cases for processing. It appeared that these two incomplete sets could be competitive with the other swingby sets, and they should be analyzed at a later date when the complete data are available.

Results and Discussion

The results of the gravity turn swingby analyses for this task are presented in the following order. First, the initial vehicle weights data are presented for the mission combinations and vehicle configurations represented in the mission and vehicle mode matrices shown previously in Table II-1, page II-4 and Table II-8, page II-19. Next, the gravity turn swingby results are evaluated and the various types of swingby round trip missions are compared in order to categorize them as to their relative merits. Finally, the more promising swingby type missions are compared to the opposition and conjunction class missions.

Initial Vehicle Weight Data - Table II-10, page II-30 to II-38, contains the complete set of data generated for this task for the gravity turn swingby, oppositions class, and conjunction class missions. The data consist of the initial vehicle weight in Earth orbit in millions of pounds and the optimum number of clustered engines (C-1, C-2, C-3, or C-4) in the leave Earth stage for those modes employing nuclear engines. Each segment of this table contains information describing the opportunity year, mission mode, and trajectory types for which the data apply. The nomenclature employed for the vehicle modes was previously defined in Table II-8, page II-19.

Cases for which no data were obtained were the result of either 1) one or more vehicle propulsive stages had a mass ratio and stage mass fraction combination which precluded the attainment of the characteristic velocity with a single stage propulsion system or 2) the optimum (minimum weight) trajectory exists outside of the trajectory data available for this study.

Figure II-8, page II-39 to II-50, is a graphical presentation of all the available data of Table II-10. The data in each separate graph of the figure are for one of the vehicle modes. Each graph in turn presents the vehicle weight requirement for the 1983 conjunction class mission and the opposition and swingby class missions for the years 1980 to 1986. The swingby missions are divided into six categories, viz, the six combinations possible from the three swingby types (1, 3, and 5) and the two direct leg types (I or B, long and II or A, short). The circle or square symbols at the top of the swingby data indicate outbound and inbound swingby legs, respectively. Finally, for the nuclear propulsive cases, the initial vehicle weight is given for both 800 and 850 sec specific impulse for some of the more favorable trajectory types.

Table II-10. Gravity Turn Swingby Mission Analysis Results

YEAR MODE OUTBOUND LEG TYPE INBOUND LEG TYPE
1980 Swingby I 1

Vehicle Configuration	NNN		NAS		CCC	CAS
Specific Impulse Arrive Earth	800	850	800	850		
A - MF #2	2.806 C-2		18.109 C-4		14.262	21.526
CM or MF #3	3.995		*		*	*
S(P) - MF #2	6.358 C-4				27.047	
CM or MF #3	7.755				*	

YEAR MODE OUTBOUND LEG TYPE INBOUND LEG TYPE
1980 Swingby 3 A

Vehicle Configuration	NNN		NAS		CCC	CAS
Specific Impulse Arrive Earth	800	850	800	850		
A - MF #2	1.909 C-2	1.717 C-2	*	*	4.919	*
CM or MF #3	2.577	2.322	*	*	6.814	*
S(P) - MF #2	1.980 C-2	1.778 C-2			5.161	
CM or MF #3	2.648	2.388			7.184	

*No data obtained

Cases where no data or symbol appears were not included in the matrix (see text)

Table II-10. Gravity Turn Swingby Mission Analysis Results (Continued)

<u>YEAR</u>	<u>MODE</u>	<u>OUTBOUND LEG TYPE</u>		<u>INBOUND LEG TYPE</u>		
1980	Swingby	3		B		
Vehicle Configuration	NNN		NAS		CCC	CAS
Specific Impulse (Nuclear) Arrive Earth	800	850	800	850		
A - MF #2	1.669 C-2	1.509 C-2	1.403 C-2	1.334 C-1	3.705	2.092
	CM or MF #3	2.293	2.040	1.717	4.953	2.555
S(P) - MF #2	1.884 C-2	1.709 C-2			4.391	
	CM or MF #3	2.519	2.293		6.183	

<u>YEAR</u>	<u>MODE</u>	<u>OUTBOUND LEG TYPE</u>		<u>INBOUND LEG TYPE</u>		
1982	Swingby	I		3		
Vehicle Configuration	NNN		NAS		CCC	CAS
Specific Impulse Arrive Earth (Nuclear)	800	850	800	850		
A - MF #2	1.482 C-1	1.340 C-1	2.352 C-2	2.263 C-2	3.513	3.352
	CM or MF #3	1.882	1.703	3.133	3.010	4.785
S(P) - MF #2	1.567 C-1	1.433 C-2			3.770	
	CM or MF #3	1.960	1.772		5.176	

Table II-10. Gravity Turn Swingby Mission Analysis Results (Continued)

<u>YEAR</u>		<u>MODE</u>		<u>OUTBOUND LEG TYPE</u>		<u>INBOUND LEG TYPE</u>	
1982		Swingby		II		3	
Vehicle Configuration		NNN		NAS		CCC	CAS
Specific Impulse Arrive Earth (Nuclear)		800	850	800	850		
A -	MF #2	1.702 C-2	1.527 C-2	2.548 C-2	2.450 C-2	4.390	3.742
	CM or MF #3	2.186	1.988	3.450	3.265	6.348	4.879
S(P) -	MF #2	1.797 C-2	1.610 C-2			4.722	
	CM or MF #3	2.340	2.073			6.871	

<u>YEAR</u>		<u>MODE</u>		<u>OUTBOUND LEG TYPE</u>		<u>INBOUND LEG TYPE</u>	
1984		Swingby		I		5	
Vehicle Configuration		NNN		NAS		CCC	CAS
Specific Impulse Arrive Earth (Nuclear)		800	850	800	850		
A -	MF #2	1.978 C-2	1.764 C-2	2.223 C-2	2.119 C-2	5.609	3.434
	CM or MF #3	2.609	2.344	2.843	2.701	8.186	4.420
S(P) -	MF #2	2.048 C-2	1.827 C-2			5.864	
	CM or MF #3	2.678	2.405			8.559	

Table II-10. Gravity Turn Swingby Mission Analysis Results (Continued)

YEAR MODE OUTBOUND LEG TYPE INBOUND LEG TYPE
 1984 Swingby II 5

Vehicle Configuration	NNN		NAS		CCC	CAS
Specific Impulse (Nuclear) Arrive Earth	800	850	800	850		
A - MF #2	2.044 C-2	1.807 C-2	1.994 C-2	1.919 C-2	6.152	2.870
	CM or MF #3	2.684	2.288	2.529	2.373	9.448 3.575
S(P) - MF #2	2.118 C-2	1.872 C-2			6.425	
	CM or MF #3	2.758	2.352		9.898	

YEAR MODE OUTBOUND LEG TYPE INBOUND LEG TYPE
 1984 Swingby 5 A

Vehicle Configuration	NNN		NAS		CCC	CAS
Specific Impulse (Nuclear) Arrive Earth	800	850	800	850		
A - MF #2	3.206 C-3		3.464 C-4		12.313	5.756
	*		4.937		22.159	8.437
S(P) - MF #2	4.006 C-4				*	
	*				*	

Table II-10. Gravity Turn Swingby Mission Analysis Results (Continued)

<u>YEAR</u>	<u>MODE</u>	<u>OUTBOUND LEG TYPE</u>		<u>INBOUND LEG TYPE</u>	
1984	Swingby	5		B	
Vehicle Configuration		NNN		NAS	
Specific Impulse Arrive Earth (Nuclear)		800	850	800	850
A - MF #2		2.408 C-3		1.907 C-2	6.866
	CM or MF #3	3.240		2.400	10.243
S(P) - MF #2		3.031 C-3			9.111
	CM or MF #3	4.087			14.788

<u>YEAR</u>	<u>MODE</u>	<u>OUTBOUND LEG TYPE</u>		<u>INBOUND LEG TYPE</u>	
1986	Swingby	I		1	
Vehicle Configuration		NNN		NAS	
Specific Impulse Arrive Earth (Nuclear)		800	850	800	850
A - MF #2		2.273 C-2		6.405 C-4	8.970
	CM or MF #3	3.045		*	19.387
S(P) - MF #2		*			*
	CM or MF #3	*			*

Table II-10. Gravity Turn Swingby Mission Analysis Results (Continued)

<u>YEAR</u>	<u>MODE</u>	<u>OUTBOUND LEG TYPE</u>		<u>INBOUND LEG TYPE</u>		
1986	Swingby	II		1		
Vehicle Configuration	NNN		NAS		CCC	CAS
<div>Specific Impulse Arrive Earth</div> <div>(Nuclear)</div>	800	850	800	850		
A - MF #2	2.433 C-2		6.865 C-4		9.944	9.719
CM or MF #3	3.345				22.118	27.927
S(P) - MF #2	*				*	
CM or MF #3	*				*	

<u>YEAR</u>	<u>MODE</u>	<u>OUTBOUND LEG TYPE</u>		<u>INBOUND LEG TYPE</u>		
1986	Swingby	3		A		
Vehicle Configuration	NNN		NAS		CCC	CAS
<div>Specific Impulse Arrive Earth</div> <div>(Nuclear)</div>	800	850	800	850		
A - MF #2 CM or MF #3	1.565 C-2	1.425 C-1	1.189 C-1	1.139 C-1	3.370	1.742
	2.119	1.946	1.462	1.402	4.575	2.016
S(P) - MF #2 CM or MF #3	1.634 C-2	1.492 C-2			3.572	
	2.249	2.006			4.868	

Table II-10. Gravity Turn Swingby Mission Analysis Results (Continued)

YEAR MODE OUTBOUND LEG TYPE INBOUND LEG TYPE
 1986 Swingby 3 B

Vehicle Configuration		NNN		NAS		CCC	CAS
Arrive Earth	Specific Impulse (Nuclear)	800	850	800	850		
A -	MF #2	1.585 C-2	1.444 C-1	1.250 C-1	1.197 C-1	3.449	1.830
	CM or MF #3	2.139	1.963	1.523	1.460	4.682	2.182
S(P) -	MF #2	1.693 C-2	1.533 C-2			3.727	
	CM or MF #3	2.296	2.047			5.158	

YEAR MODE OUTBOUND LEG TYPE INBOUND LEG TYPE
 1980 Opposition II B

Vehicle Configuration		NNN		NAS		CCC	CAS
Arrive Earth	Specific Impulse (Nuclear)	800	850	800	850		
A -	MF #2	2.042 C-2	1.788 C-2	2.977 C-3	2.849 C-3	6.684	4.395
	CM or MF #3	2.818	2.518	4.017	3.811	12.230	6.125
S(P) -	MF #2	*	*	*		*	*
	CM or MF #3	*	*	*		*	*

Table II-10. Gravity Turn Swingby Mission Analysis Results (Continued)

<u>YEAR</u>	<u>MODE</u>	<u>OUTBOUND LEG TYPE</u>		<u>INBOUND LEG TYPE</u>		
1982	Opposition	II		B		
Vehicle Configuration	NNN		NAS		CCC	CAS
Specific Impulse Arrive Earth (Nuclear)	800	850	800	850		
A - MF #2	1.904 C-2	1.705 C-2	2.402 C-2	2.387 C-2	5.835	3.436
	CM or MF #3	2.652	2.175	3.249	3.104	9.239
S(P) - MF #2	4.485 C-4	*	16.849 C-4		29.291	20.269
	*	*	*		*	*

<u>YEAR</u>	<u>MODE</u>	<u>OUTBOUND LEG TYPE</u>		<u>INBOUND LEG TYPE</u>		
1984	Opposition	II		B		
Vehicle Configuration	NNN		NAS			
<div>Specific Impulse Arrive Earth</div> <div>(Nuclear)</div>	800	850	800	850	CCC	CAS
A - MF #2	1.721 C-2	1.544 C-1	2.166 C-2	2.080 C-2	4.832	3.105
	CM or MF #3	2.209	2.003	2.788	2.667	7.137
S(P) - MF #2	2.826 C-2	2.489 C-2	3.424 C-3		9.225	4.917
	CM or MF #3	3.580	3.190	4.753 C-4	*	7.746

Table II-10. Gravity Turn Swingby Mission Analysis Results (Continued)

YEAR MODE OUTBOUND LEG TYPE INBOUND LEG TYPE
 1986 Opposition II B

Vehicle Configuration		NNN		NAS		CCC	CAS
Arrive Earth	Specific Impulse (Nuclear)	800	850	800	850		
	A - MF #2	1.502 C-1	1.358 C-1	2.060 C-2	1.991 C-2	3.850	2.980
	CM or MF #3	1.969	1.724	2.675	2.563	5.598	3.811
S(P) -	MF #2	2.140 C-2	1.946 C-2	2.686 C-2		6.166	3.885
	CM or MF #3	2.831	2.376	3.417 C-3		9.819	5.235

YEAR MODE OUTBOUND LEG TYPE INBOUND LEG TYPE
 1983 Conjunction I A

Vehicle Configuration		NNN		NAS		CCC	CAS
Arrive Earth	Specific Impulse (Nuclear)	800	850	800	850		
	A - MF #2	1.679 C-2	1.565 C-1	1.637 C-2	1.575 C-1	3.023	2.293
	CM or MF #3	2.212	2.071	1.899	1.803	3.579	2.577
S(P) -	MF #2	1.748 C-2	1.632 C-2			3.186	
	CM or MF #3	2.287	2.140			3.790	

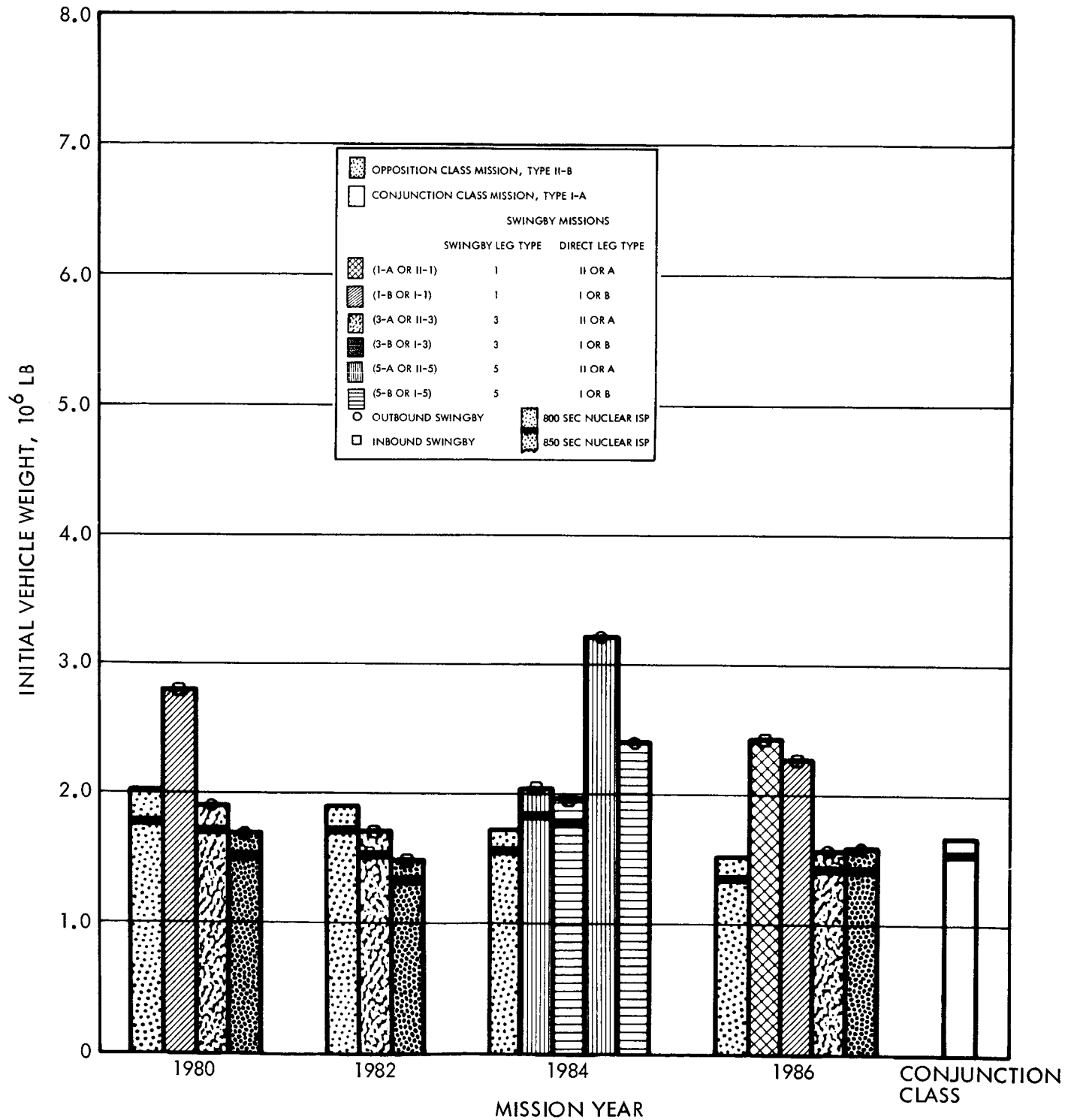


Figure II-8. Gravity Turn Swingby Mission Analysis Results

NNNA CONNECTING MODE

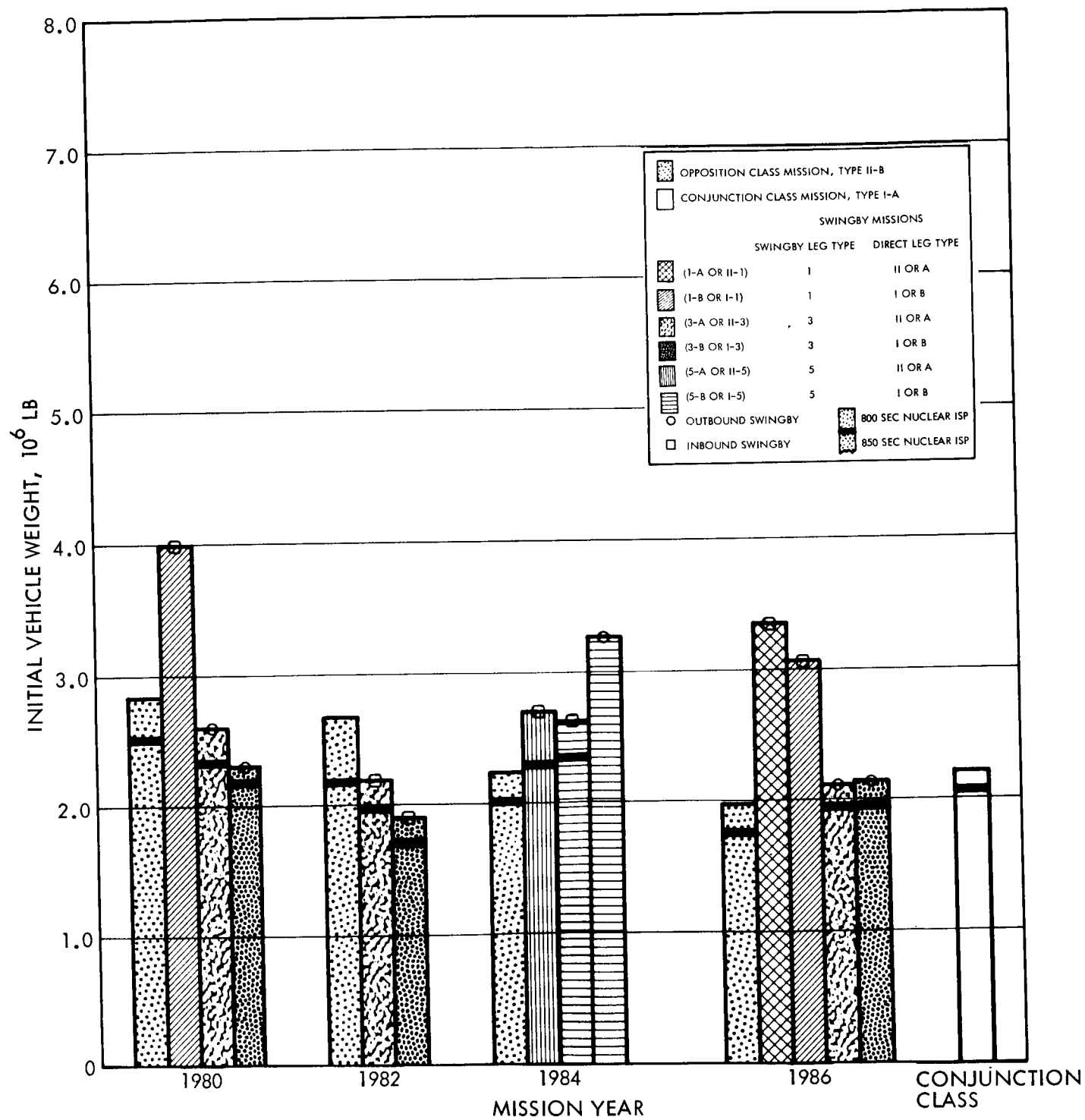


Figure II-8. Gravity Turn Swingby Mission Analysis Results (Continued)

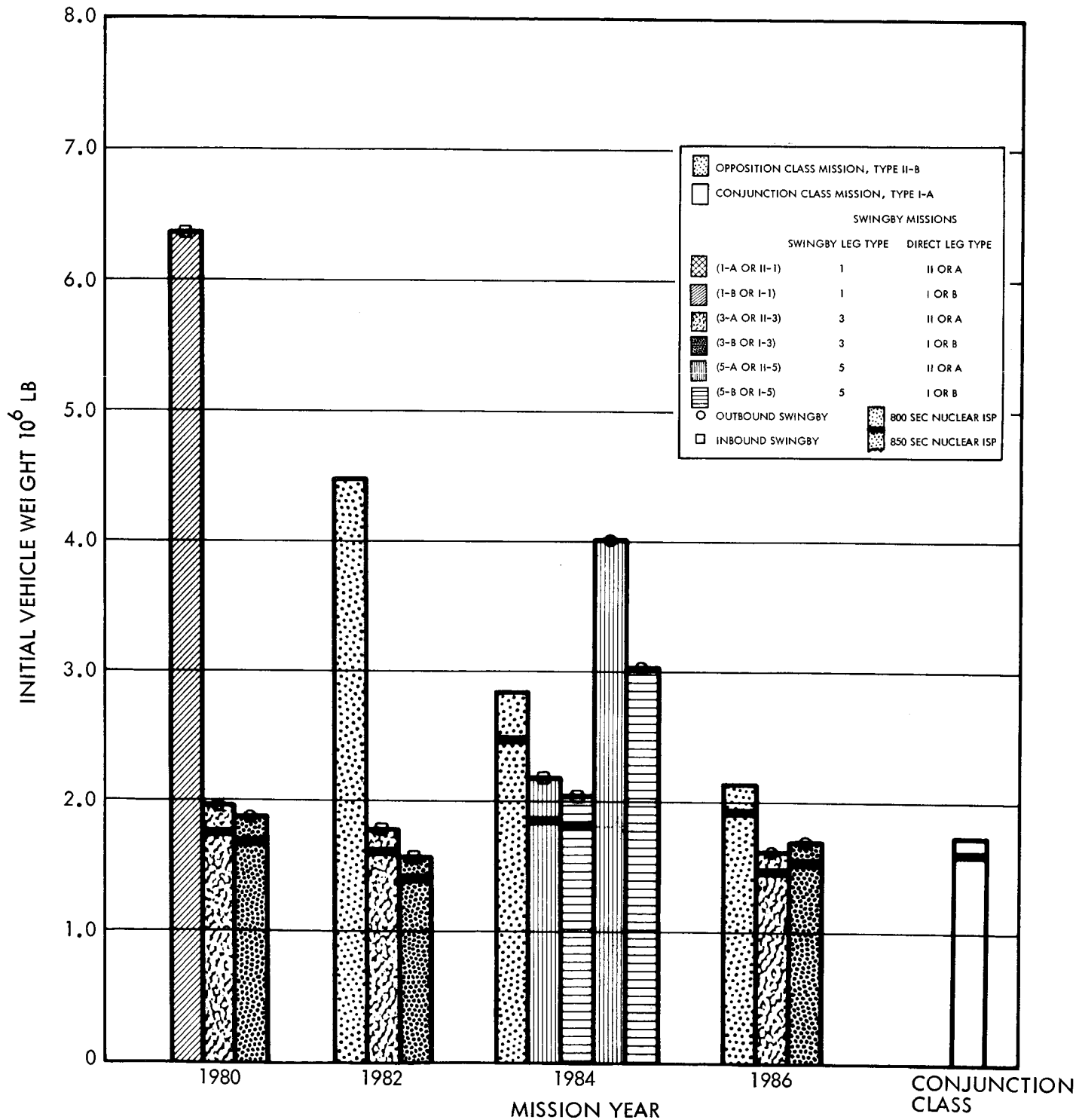


Figure II-8. Gravity Turn Swingby Mission Analysis Results (Continued)

NNNS(P) CONNECTING MODE

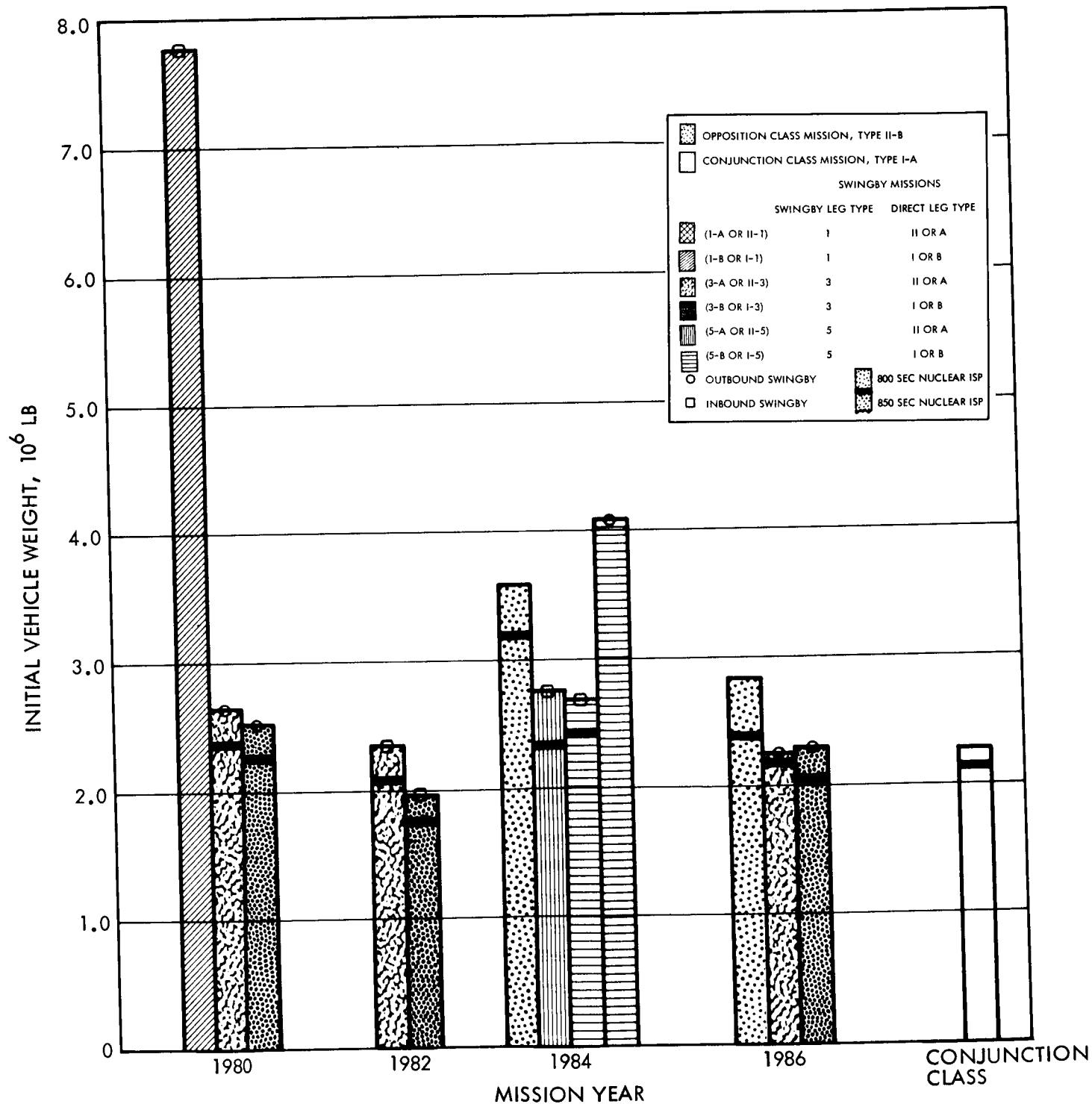


Figure II-8. Gravity Turn Swingby Mission Analysis Results (Continued)

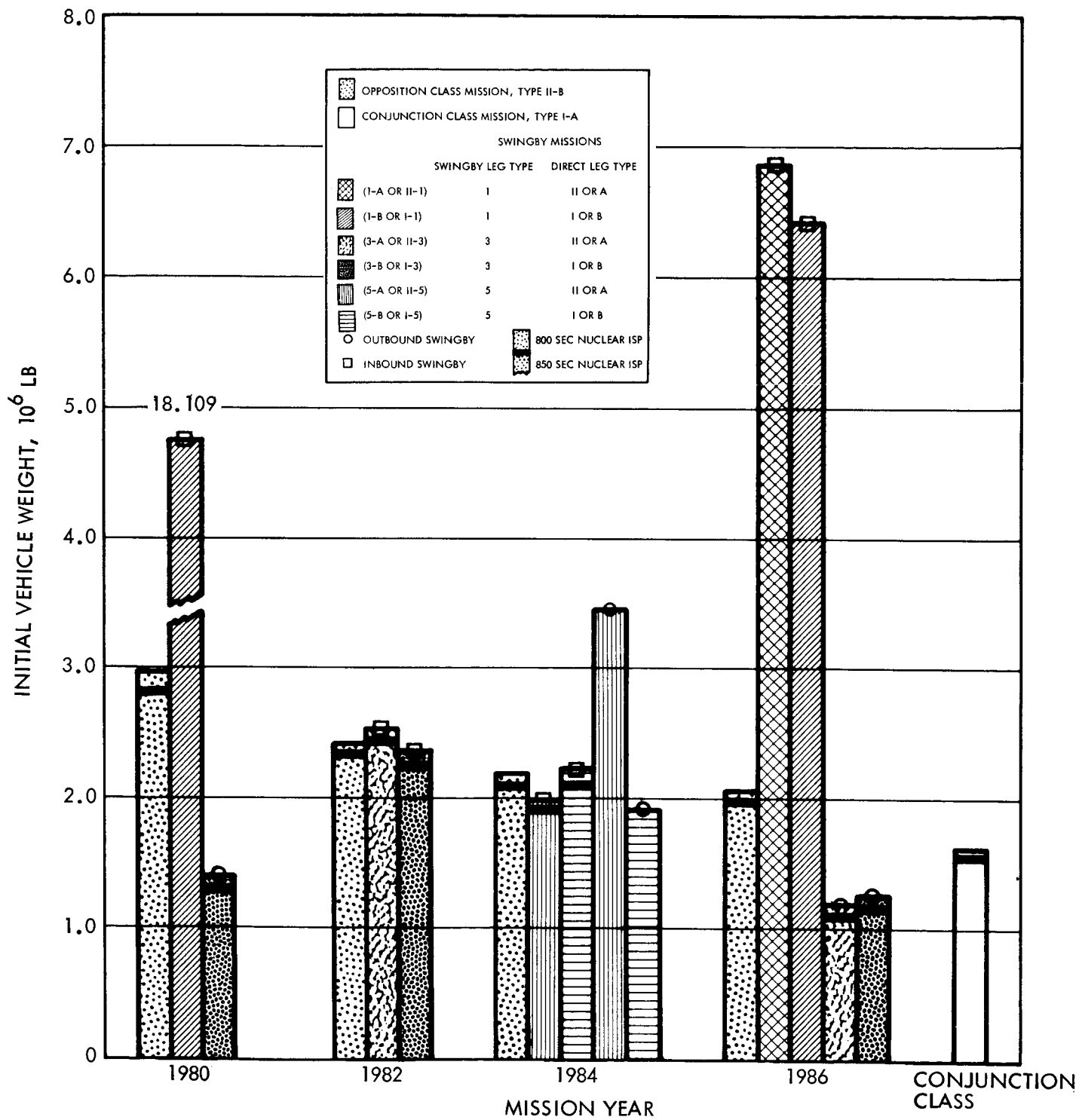


Figure II-8. Gravity Turn Swingby Mission Analysis Results (Continued)

NASA CONNECTING MODE

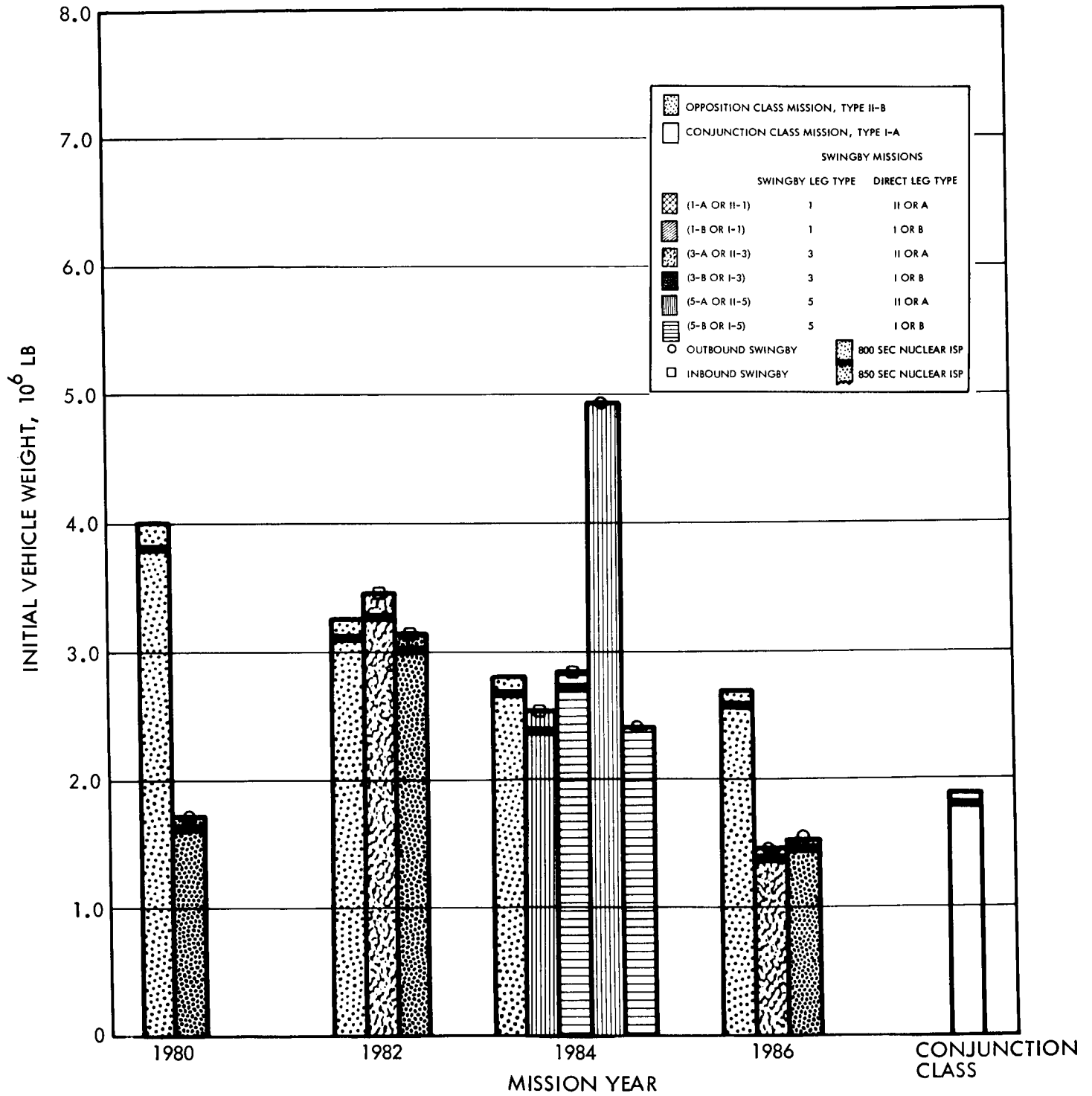


Figure II-8. Gravity Turn Swingby Mission Analysis Results (Continued)

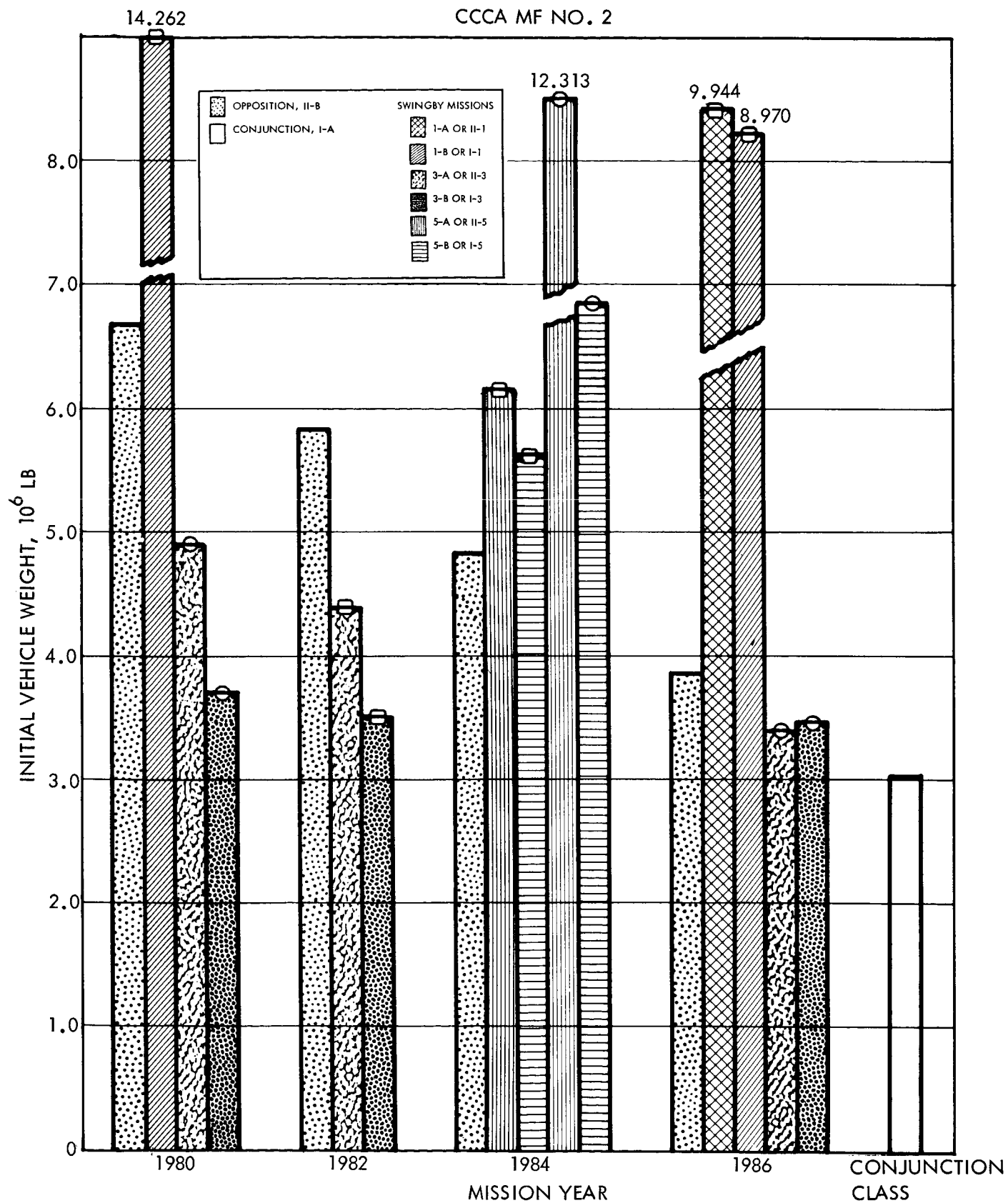


Figure II-8. Gravity Turn Swingby Mission Analysis Results (Continued)

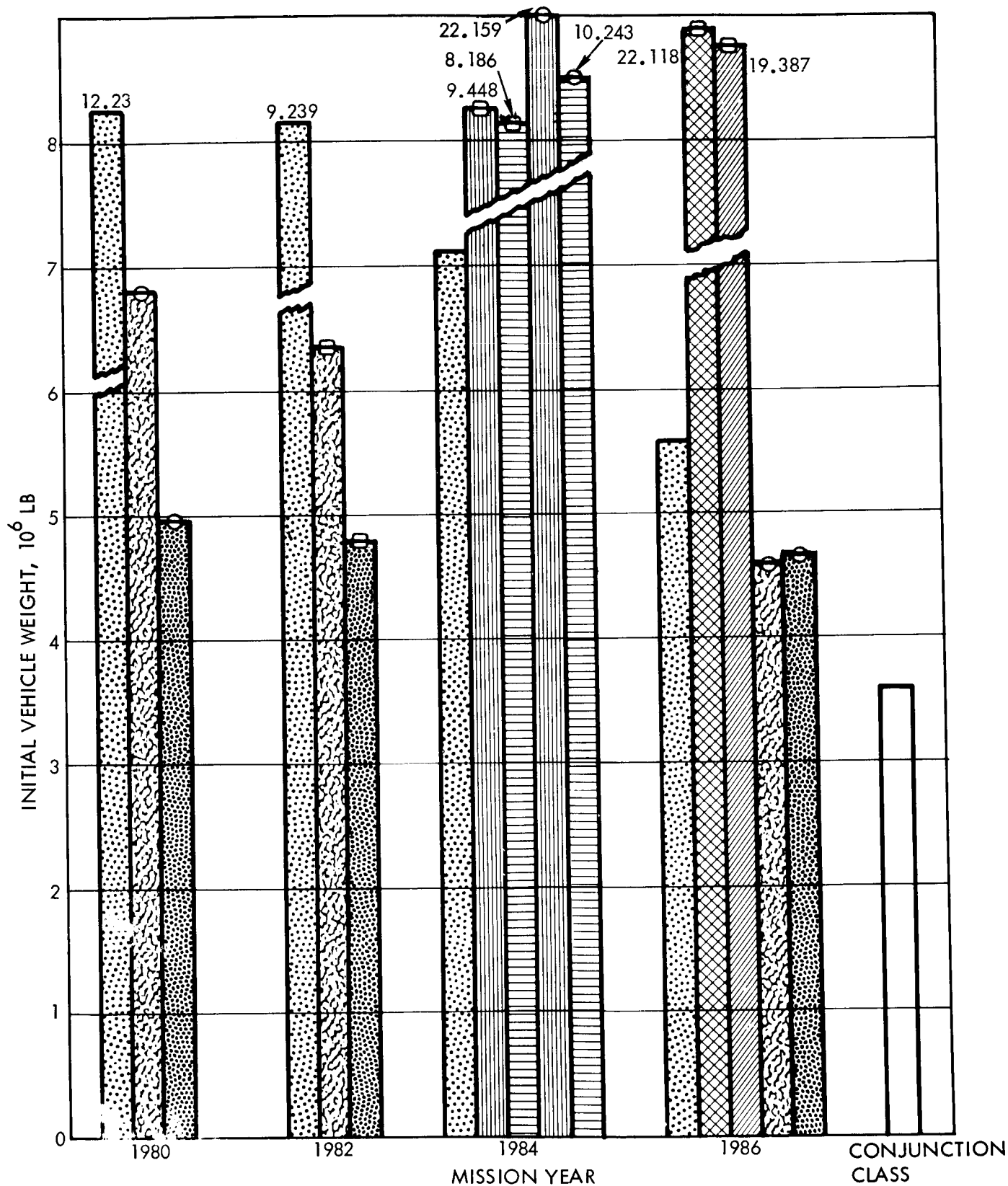


Figure II-8. Gravity Turn Swingby Mission Analysis Results (Continued)

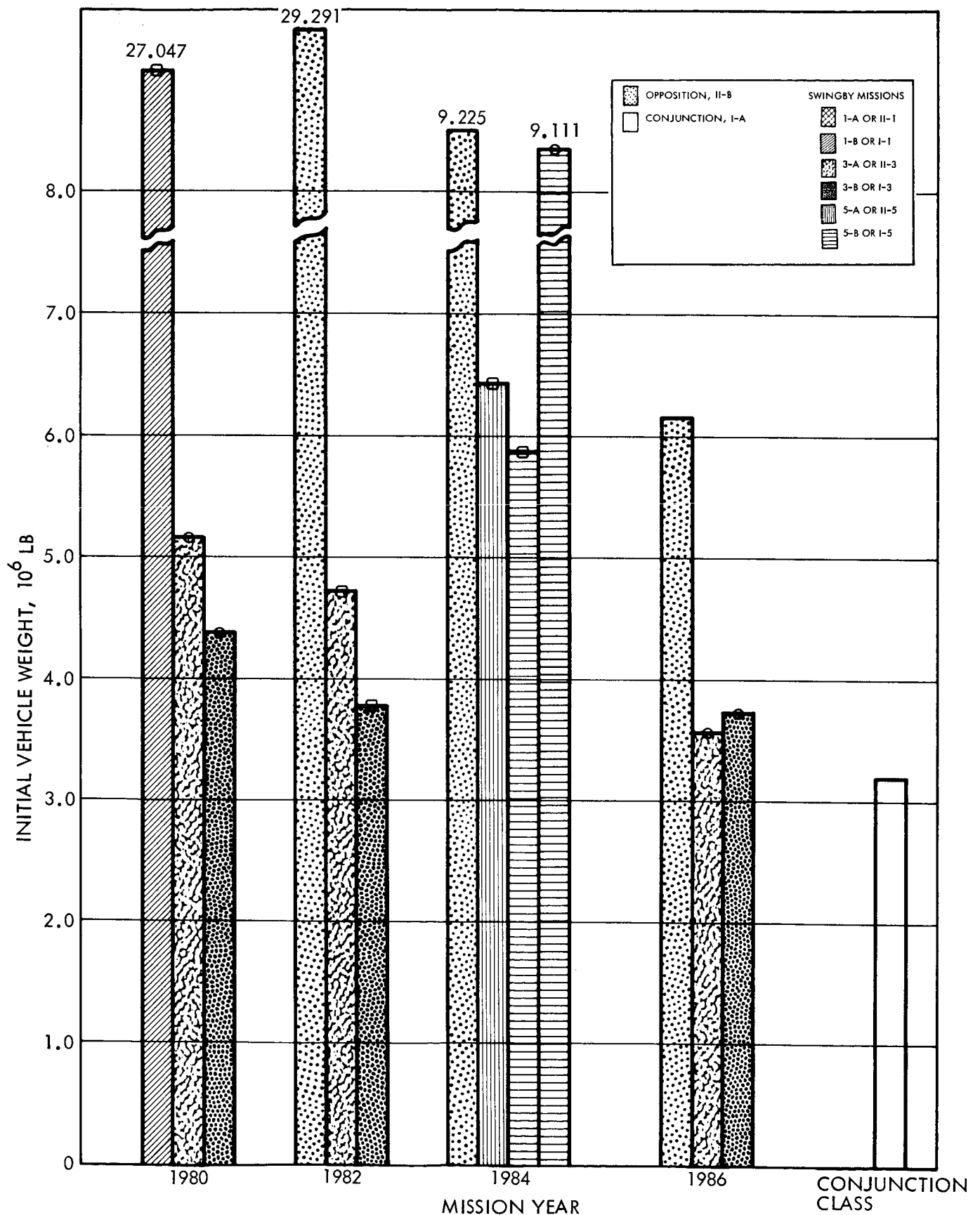


Figure II-8. Gravity Turn Swingby Mission Analysis Results (Continued)

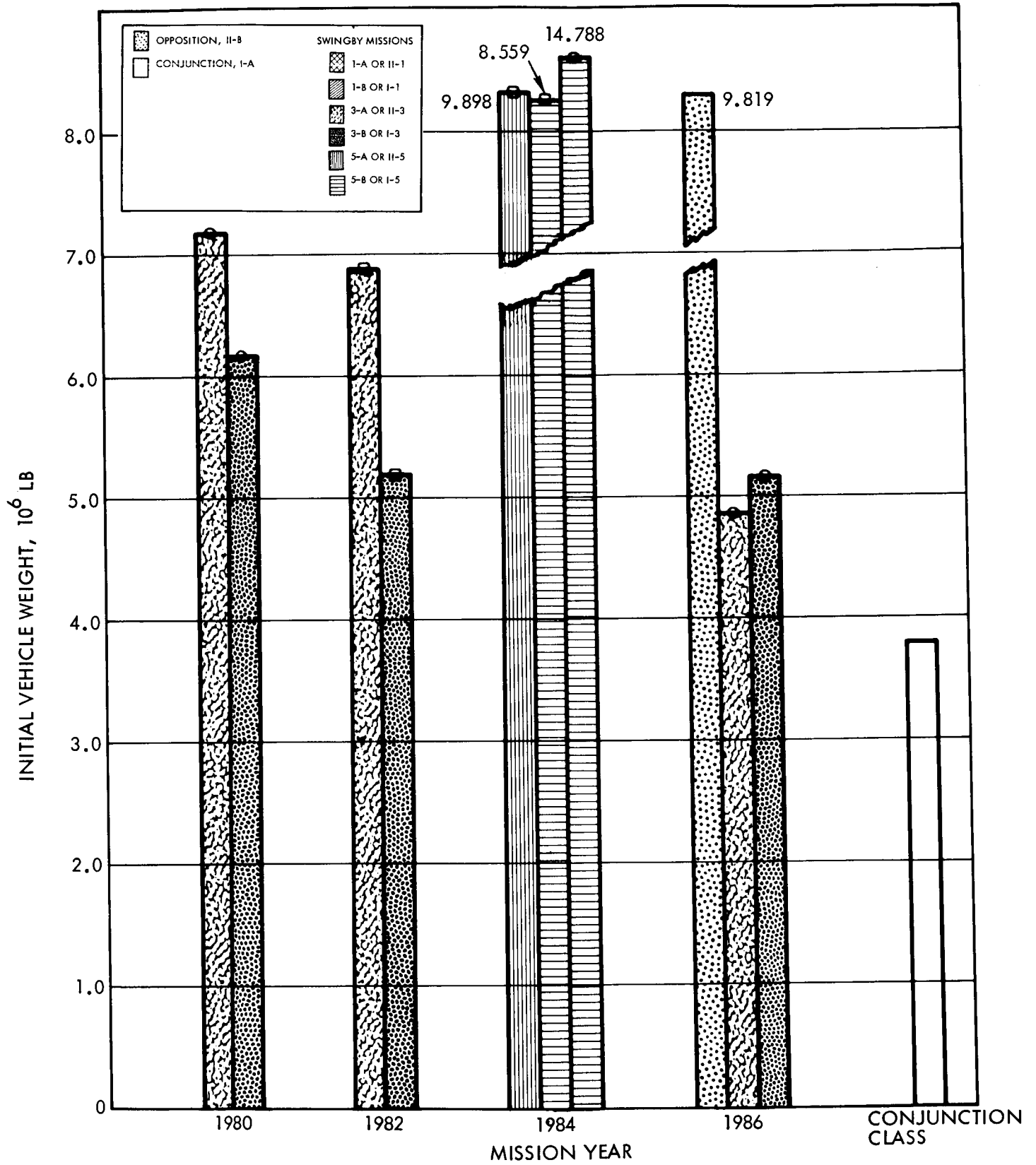


Figure II-8. Gravity Turn Swingby Mission Analysis Results (Continued)

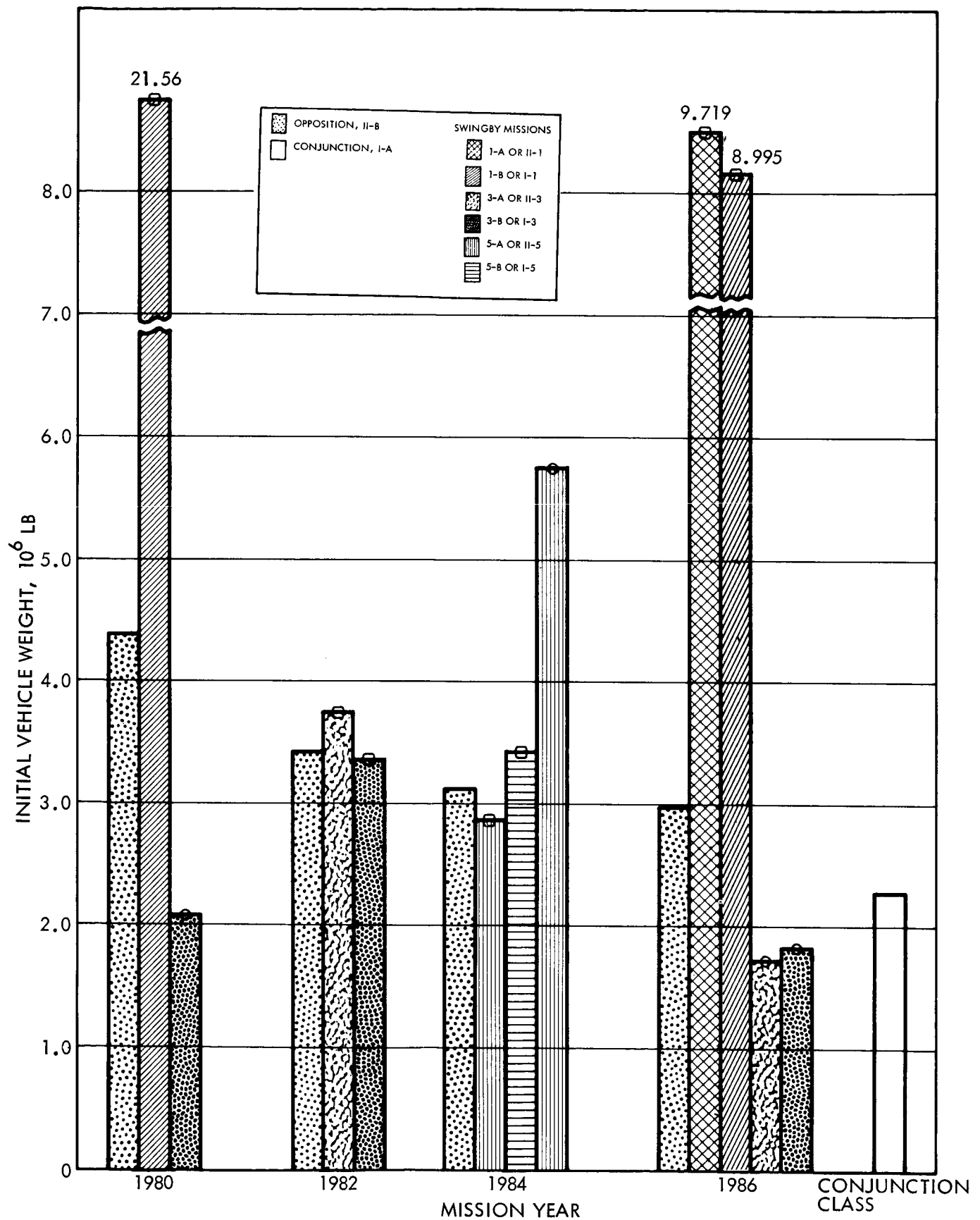


Figure II-8. Gravity Turn Swingby Mission Analysis Results (Continued)

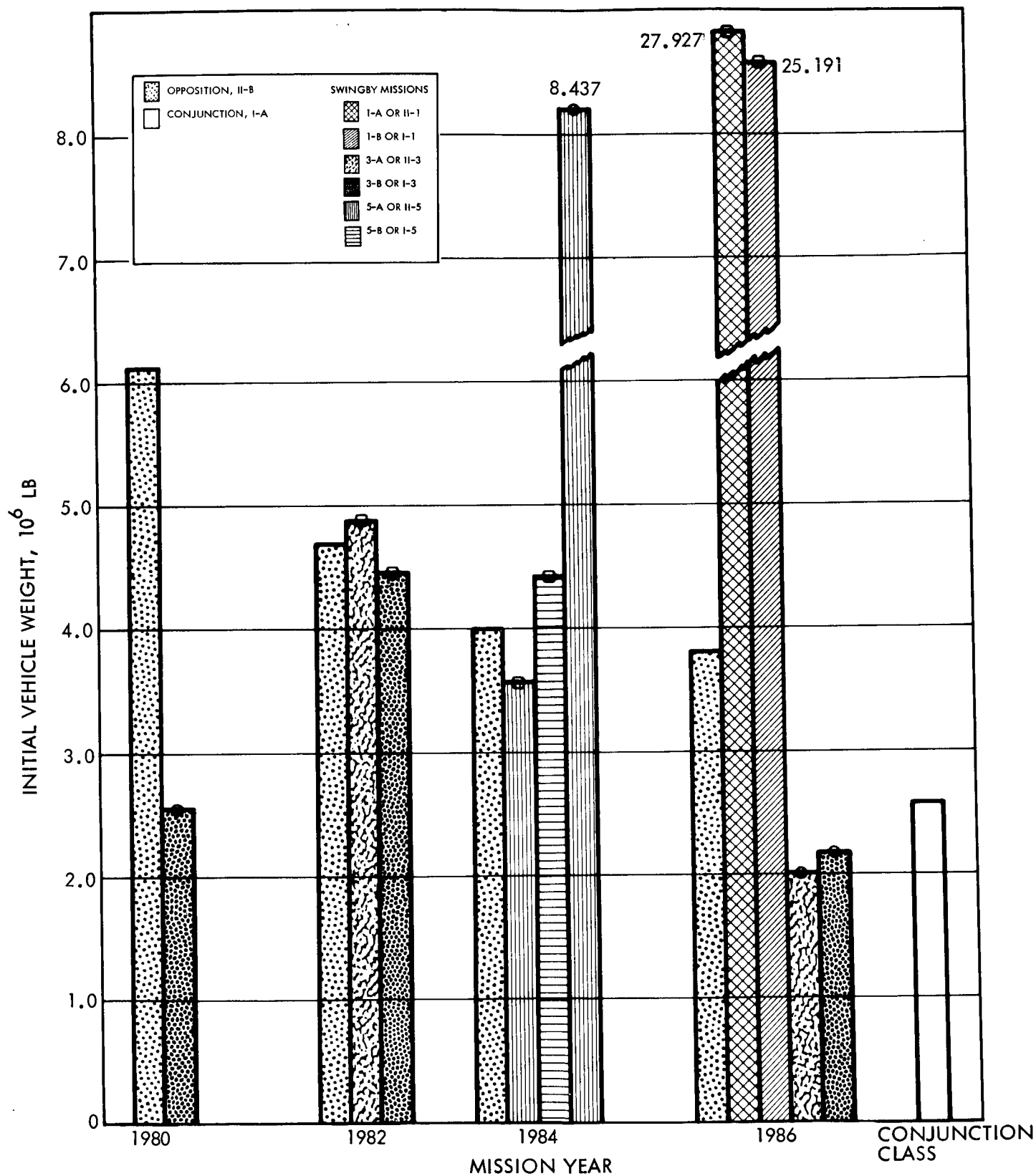


Figure II-8. Gravity Turn Swingby Mission Analysis Results (Continued)

Gravity Turn Swingby Evaluation - The gravity turn swingby missions are evaluated on the basis of several levels of trajectory and vehicle characteristics. First, the different types of swingby trajectories are compared; second, the use of the short or long direct leg with a swingby leg is evaluated; third, a comparison of the results for the various mission years is made; and finally, the results for the different vehicle modes are discussed.

The graphs in Figure II-8 indicate that the type 3 gravity turn swingby trajectories lead to lower weight vehicles than the type 1 trajectories for the years 1980, 1982, and 1986. The superiority of the type 3's over the type 1's is consistent regardless of the direct leg type or vehicle mode. In 1984, the inbound type 5 yields lower weight vehicles for all vehicle modes except those employing aerodynamic braking for the capture maneuver at Mars. For these Mars aerodynamic braking configurations, the outbound type 5 swingby trajectories with a long (type B) direct inbound leg show a slightly lower vehicle weight. Results are available only for the two NASA, 800 sec cases due to the tendency for these vehicle modes to optimize outside of the available range of the 1984 outbound type 5 trajectory data.

The type 3 trajectories for the years 1980 and 1982 yield a lower weight vehicle by employing a long trajectory for the direct leg. That is, a 1980 outbound type 3 swingby leg with a type B inbound direct leg (3-B) and a 1982 inbound type 3 swingby leg with a type I outbound direct leg (I-3) are the best swingby trajectories for those two years. The use of the long instead of the short direct leg tends to increase the total trip time by 128 and 50 days for 1980 and 1982, respectively, but reduces the gross vehicle weight by approximately 15 percent.

The long direct leg also yields the minimum weight vehicles when coupled with the type 5 trajectories for 1984. For those vehicles employing propulsive braking at Mars, the longer inbound swingby or type I-5 round trip trajectory results in a vehicle weight approximately five percent less than that given by the shorter II-5 trajectory. As previously shown for vehicles utilizing aerodynamic braking in 1984, the longer outbound swingby mission, type 5-B is best; the vehicle weight is about five percent lower than for the next best swingby (II-5).

In 1986 the shorter type 3 swingby mission (3-A) yields slightly lower weight vehicles than the longer type 3-B. This lower weight and the shorter trip time (49 days less), therefore, make the type 3-A trajectory the preferred swingby mission for this year.

A summary of the minimum weight swingby round trip trajectories for each year is given in Table II-11.

Table II-11. Minimum Weight Swingby Trajectories

<u>Mission Year</u>	<u>Trajectory Type</u>	
	<u>Outbound</u>	<u>Inbound</u>
1980	3	B
1982	I	3
1984 (Mars Propulsive Braking)	I	5
1984 (Mars Aero Braking)	5	B
1986	3	A

A typical comparison of swingby missions on the basis of the mission year or opportunity is shown in Figure II-9 for the NNNA, NASA, CCCA, and CASA modes. Plotted on this graph are the vehicle weights for the best (minimum weight) trajectories as previously discussed. The vehicle weights for the NNNA mode increase in the following order; 1982 (minimum), 1986, 1980, and 1984 (maximum). For the NASA mode, the weight is a minimum in 1986 and increases in 1980, 1984, and 1982 (maximum). The results for the other analogous nuclear and chemical propulsive modes have vehicle weights that vary through the years in the same order except that for the CCCA and CCCS(P) modes, 1986 is the minimum weight year followed by 1982 which has only a slightly greater weight.

The weight differences on the basis of the yearly variations are quite significant. For example, the vehicle weight for the maximum year is from 30 to 40 percent greater than the minimum year for the NNNA and NNNS(P) modes; and from 65 to 80 percent for the CCCA and CCCS(P) modes. The increase from minimum to maximum for the modes utilizing aerodynamic braking at Mars is 88 to 120 percent.

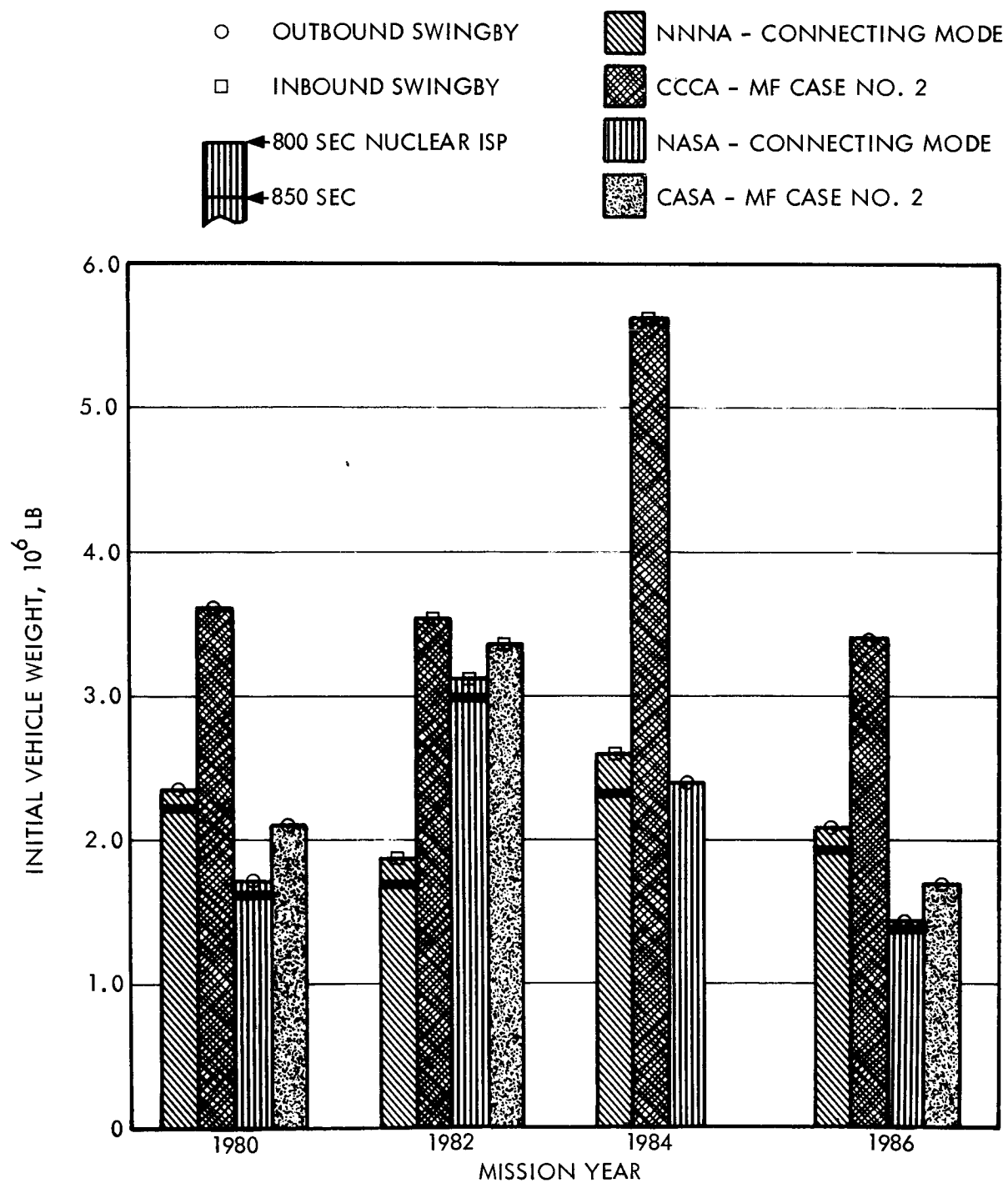


Figure II-9. Launch Opportunity Comparison for Gravity Turn Swingby Missions

Although the characteristics of swingby trajectories repeat on a cycle of approximately 6.4 years, it does not necessarily follow that favorable (or unfavorable) round trip missions will occur at like intervals. It might be expected that the Earth-Mars opposition characteristics, which vary over a 15-year cycle, will influence the overall missions or vehicle weights differently over succeeding swingby cycles (6.4 years) (e.g., compare the results for the years 1980 and 1986 in Figure II-9). Therefore, any conclusions reached by comparing the results for the years 1980 through 1986 may not necessarily apply for preceding or succeeding six-year periods.

An evaluation of the results on the basis of the vehicle modes and performances reveals the not surprising fact that the vehicle weight is severely influenced by the propulsive specific impulses. The results on Figure II-9 show that the modes employing chemical cryogenic propulsion stages require vehicles whose weights are from 15 to 110 percent greater than the nuclear vehicles depending on the particular vehicle mode and structural scaling laws being compared. In addition, a decrease in specific impulse from 850 to 800 sec for the NNNA or NNNS(P) mode increases the vehicle weight by 10 to 20 percent; and 5 to 10 percent for the NASA mode.

The arrival velocities at Earth for the best swingby trajectories in any year are generally only slightly greater than parabolic velocity. Therefore, there is seen to be only a slight difference in weight between the all aerodynamic braking at Earth modes and those modes employing a retrostage to decelerate the vehicle to parabolic entry velocity.

Mission Modes Comparison - The comparison of the mission modes or types, i.e., conjunction, opposition, and gravity turn swingby class missions, was made primarily for the NNNA, CCCA, NASA, and CASA vehicle modes.

A comparison of modes utilizing a retro stage at Earth for braking to parabolic velocity does not appear meaningful for two reasons. First, the application of this limited Earth aerodynamic braking capability to the opposition class missions of 1980 and 1982, yields vehicles with unreasonably high initial weights that require "staging" of individual propulsion systems. Second, since the Earth arrival velocities for the conjunction and swingby modes are only slightly greater than parabolic velocity, a comparison of these two mission modes for the S(P) vehicle mode yields essentially the same results as for the aerodynamic braking or "A" vehicle mode.

A comparison of the three mission modes or types is presented by first comparing the conjunction and opposition class missions, then the conjunction and swingby class missions, and finally the opposition and swingby class missions. Figure II-10 presents the initial vehicle weight for the NNNA mode for all three classes of missions. The minimum weight swingby and the II-B opposition class missions are shown for the years 1980 through 1986. The conjunction class mission is given for the conjunction year of 1983; the initial vehicle weight varies only slightly for other conjunction years. It should be remembered that the payloads for the conjunction class mission have been increased by 50 percent over the other two types of missions to account for the approximately double total trip time and extremely long Mars dwell time.

A comparison of the conjunction and opposition class missions shows that the vehicle weight for the conjunction class mission is essentially equal to that for the opposition class mission in 1984 and an average of 16 percent greater than the 1986 opposition vehicle; but the 1980 and 1982 opposition class missions have greater vehicle weights than the conjunction class mission; 25 percent greater in 1980 and 12 percent greater in 1982.

A comparison of the conjunction and swingby class missions shows that the swingby mission yields a lower weight vehicle for the years 1982 and 1986; 17 percent less in 1982 and approximately 5 percent less in 1986. In 1980, the swingby mission is essentially equal to the conjunction class and in 1984, approximately 16 percent greater.

A comparison of the opposition and swingby class missions shows that the swingbys give lower vehicle weights in 1980 and 1982, 20 percent less in 1980 and 30 percent less in 1982. In 1984 and 1986, the swingby missions yield greater vehicle weights than the opposition class missions; 18 percent greater in 1984 and approximately 10 percent greater in 1986.

Similar comparisons of mission classes for the CCCA vehicle mode (Figure II-11) reveal that the conjunction class mission yields a vehicle weight lower than either the opposition or swingby class mission for all years. In the comparison of the opposition and swingby class missions, the swingby mission has a lower weight vehicle in all years except 1984.

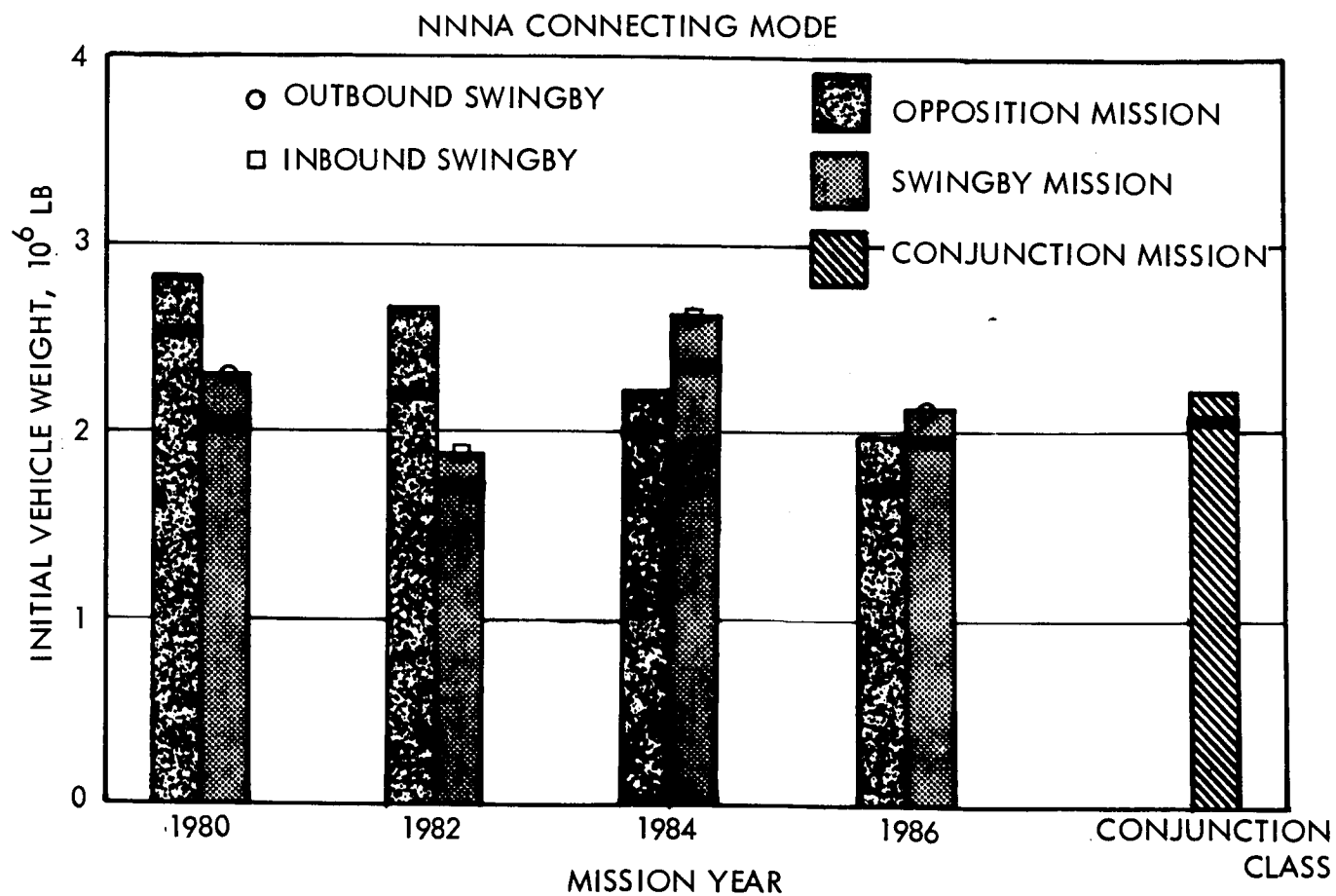


Figure II-10. Mission Mode Comparison, NNNA Vehicle Configuration

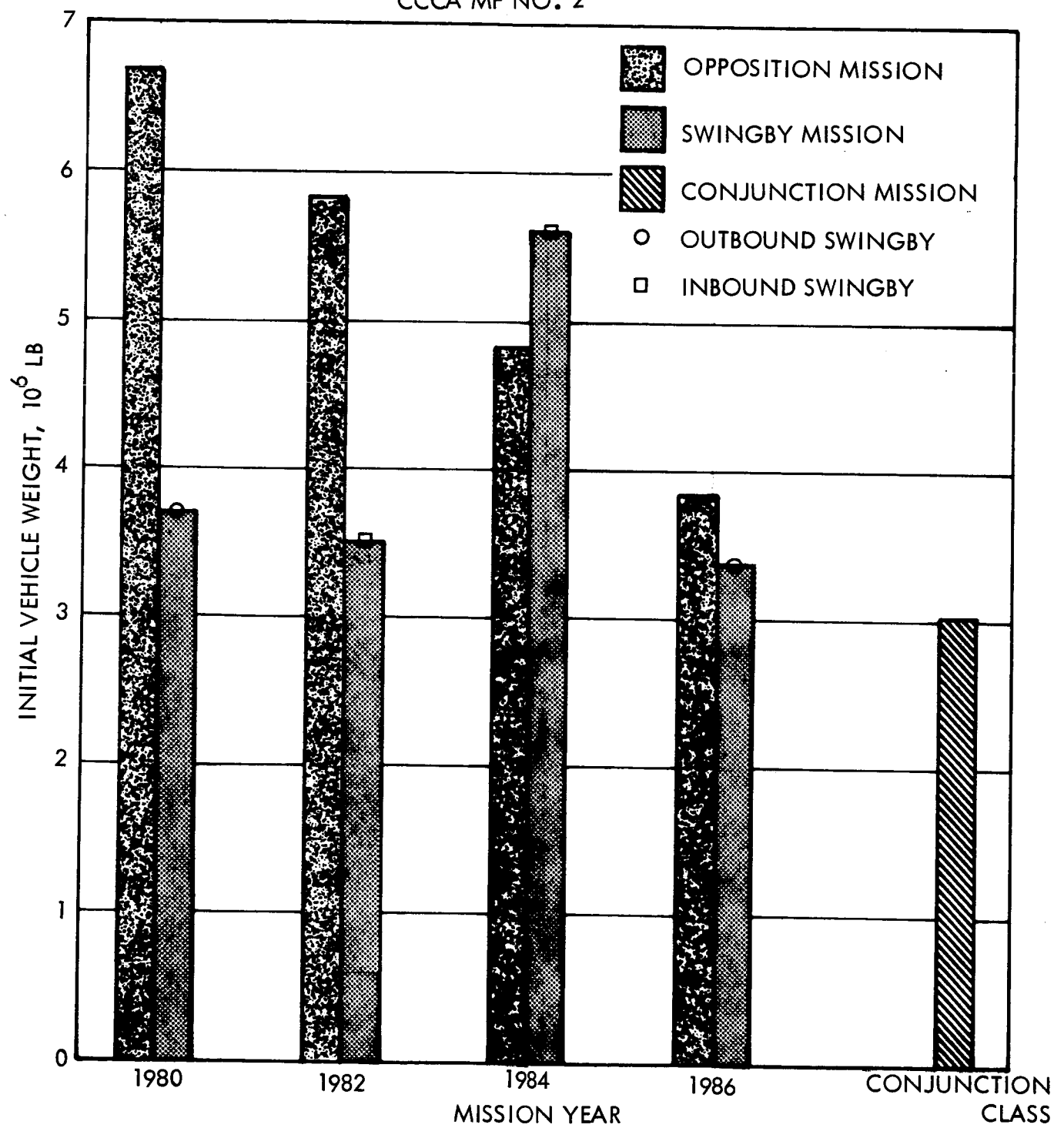


Figure II-11. Mission Mode Comparison, CCCA Vehicle Configuration

An extension of the comparisons to vehicles employing aerodynamic braking at Mars is shown in Figure II-12 for the NASA mode. A comparison of the conjunction and opposition class missions for this mode shows that the vehicle weights for all years of the opposition class missions are greater than for the conjunction class mission. The opposition class vehicle weights are 112 percent greater in 1980, 70 percent in 1982, 48 percent in 1984, and 40 percent in 1986.

A comparison of the conjunction and swingby class missions shows that the swingby missions of 1980 and 1986 yield lower weight vehicles; 9 percent less in 1980 and 23 percent less in 1986. In 1982 and 1984, the swingby mission vehicles are greater in weight; 65 percent greater in 1982 and 48 percent in 1984.

A comparison of the opposition and swingby class missions shows that the swingby missions yield lower vehicle weights in all years. The vehicle weights for the swingby class missions are 57 percent less in 1980, 3 percent in 1982, 14 percent in 1984, and 45 percent in 1986.

Similar comparisons of mission modes for the CASA vehicle mode (Figure II-13) reveal that qualitatively the results are identical to those of the NASA mode.

Although the preceding comparisons are relatively lengthy and detailed, they were made to permit a full exploration of the weight advantages and disadvantages inherent in the use of the gravity turn swingby mission mode. A contracted summarization of these comparisons is given in Table II-12. The table compares the opposition, conjunction, and swingby mission types, separately for each of the four basic vehicle modes. The weights for each vehicle mode are normalized to the mission mode that yields the minimum weight.

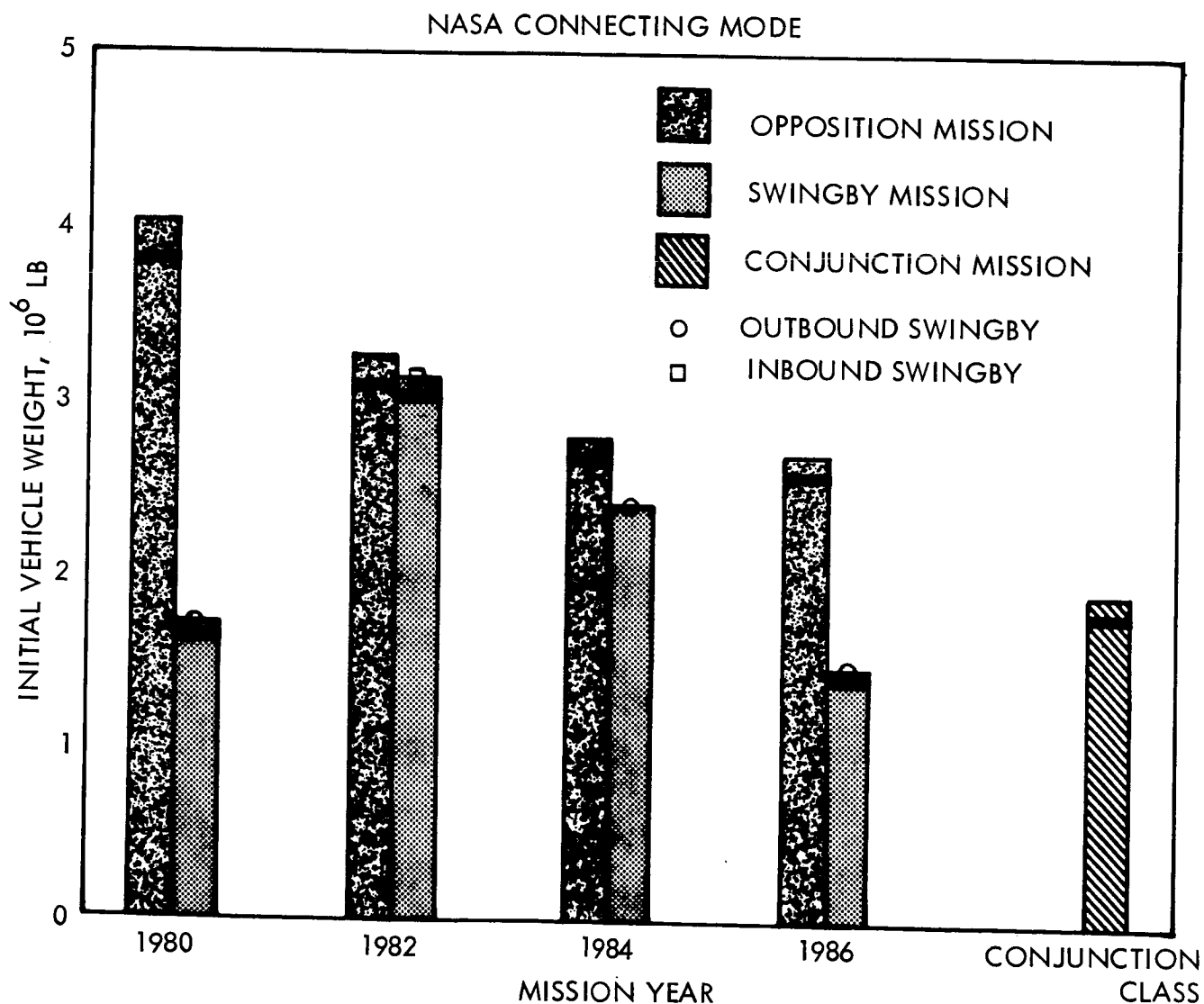


Figure II-12. Mission Mode Comparison, NASA Vehicle Configuration

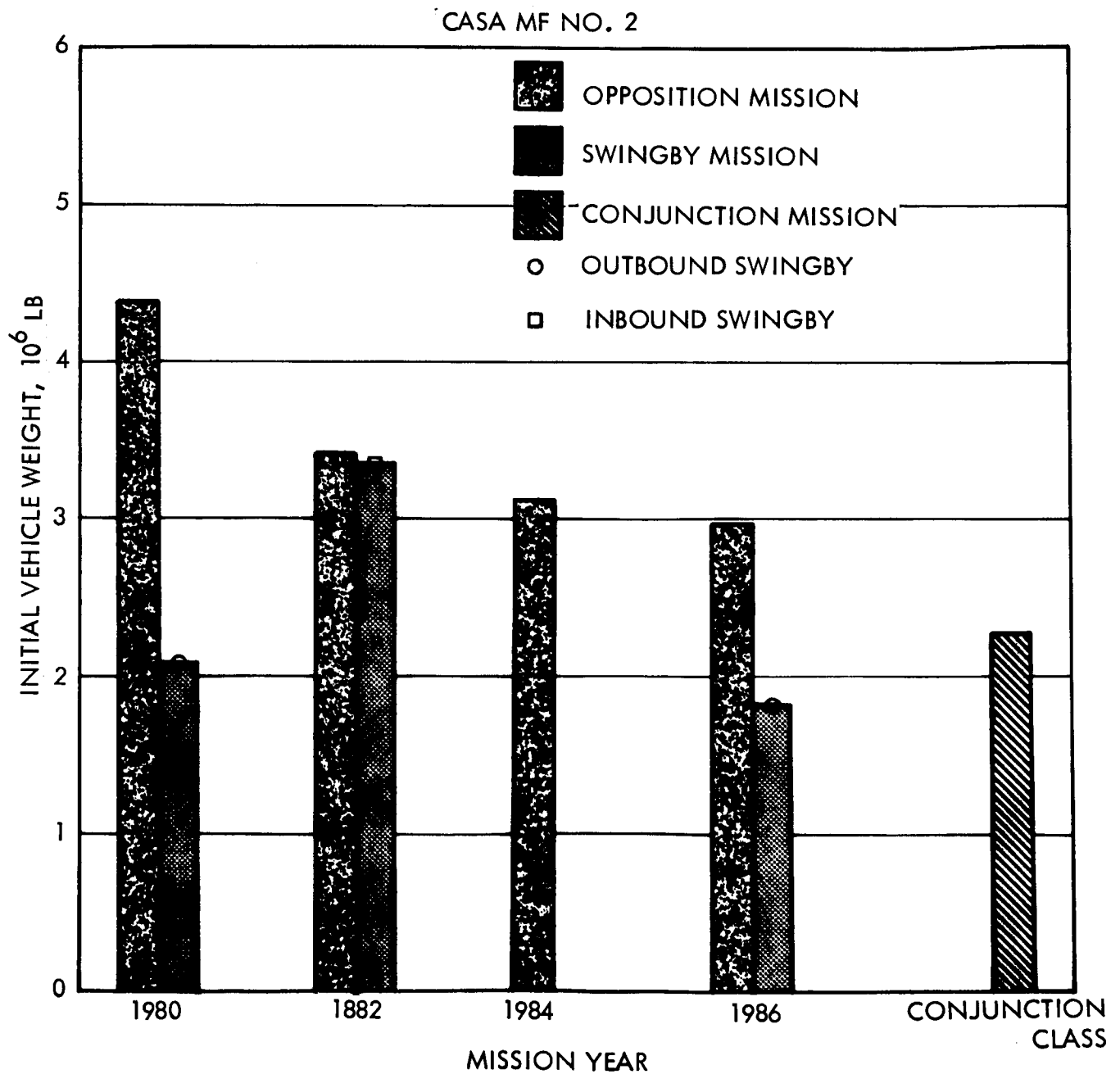


Figure II-13. Mission Mode Comparison, CASA Vehicle Configuration

Table II-12. Mission Mode Comparison

Mission Mode Vehicle Mode	Conj. Class	Opposition Class				Swingby Class			
		1980	1982	1984	1986	1980	1982	1984	1986
NNNA *(1.70 x 10 ⁶ lbs)	1.22	1.48	1.28	1.18	1.02	1.20	1.00	1.38	1.15
CCCA *(3.02 x 10 ⁶ lbs)	1.00	2.21	1.94	1.60	1.28	1.23	1.16	1.86	1.12
NASA *(1.46 x 10 ⁶ lbs)	1.30	2.75	2.22	1.91	1.89	1.18	2.14	1.64	1.00
CASA *(1.74 x 10 ⁶ lbs)	1.32	2.53	1.98	1.79	1.70	1.20	1.93	--	1.00

*Weights normalized to this value

POWERED TURN SWINGBY MISSIONS

A number of investigators have found that using a powered turn at Mars can provide significant reductions in the total velocity requirements for the nonstop Mars flyby mission. Hollister (Ref 4) suggested that a powered turn might also offer an improvement to the unpowered or gravity turn Venus swingby missions. Hollister compared some powered to unpowered Venus swingbys on the basis of total impulsive velocity (ΔV) requirement and found that in some cases the best powered swingbys did require a few hundred feet per second less total ΔV than did the best unpowered swingbys. However, a comparison on the basis of total ΔV is not sufficient to determine whether the addition of the powered turn at Venus (which requires an additional vehicle stage) will improve the mission in terms of reduced vehicle weight or increased mission flexibility. It is necessary to actually size vehicles for the powered swingby mission to determine whether it offers any advantages over the unpowered swingbys and other mission modes.

A comparison was made of powered with unpowered swingbys for the 1980 (type 1) inbound swingby and the 1982 (type 3) inbound swingby. The vehicle mode used in the comparison was the NNNA connecting mode with 850 sec specific impulse for the nuclear stages, and the powered turn at Venus was performed by a 440 second chemical cryogenic stage.

Trajectory Data

A subroutine was developed for the TRW/AIP computer program (Ref 5) to generate the required powered swingby trajectory data. The data generation method and assumptions used were essentially those of Hollister (Ref 4), which are based on the analytical work and conclusions of Gobetz (Ref 6). The planet passage distance (PP) was constrained to be greater than or equal to 1.05 radii. Whenever the optimum (minimum) swingby ΔV required a lower passage distance, the passage distance was fixed at 1.05 radii and the corresponding (non-optimum) ΔV was computed. Trajectory data were generated and prepared for the SWOP program for the 1980 inbound powered swingby and the 1982 inbound powered swingby.

Figure II-14 illustrates the ΔV data for the powered turn at Venus for one Mars departure date. The three-dimensional isometric graph is not easily visualized on a two-dimensional page. However, the surface is more easily visualized if it is thought of as a dome-shaped amphitheater in the foreground with a hill sloping up behind it. The intersection of the amphitheater and the hill is a valley with ΔV equal to zero to the left of the PP = 1.05 line; the ΔV along the valley (the portion of the valley line that is dashed) increases above zero to the right of the PP = 1.05 line. The line representing PP = 1.05 and the line of the valley are shown in a view from above in Figure II-15. In Figure II-14 and II-15 all points to the right of the PP = 1.05 line have a PP equal to 1.05 radii. The segment of the valley line that lies in the plane of $\Delta V = 0$ is simply the locus of unpowered swingbys for the given Mars departure date. This is apparent from a comparison of Figure II-15 with the appropriate curve in Figure II-6, page II-26.* To the right of the PP=1.05 line the dashed line would represent unpowered swingbys with a PP less than 1.05 radii. However, in the generation of the

*In Figure II-6 the entire valley curve does not appear as in Figure II-15 because the data to the right of the PP = 1.05 line was unusable and, therefore, not generated.

9.0

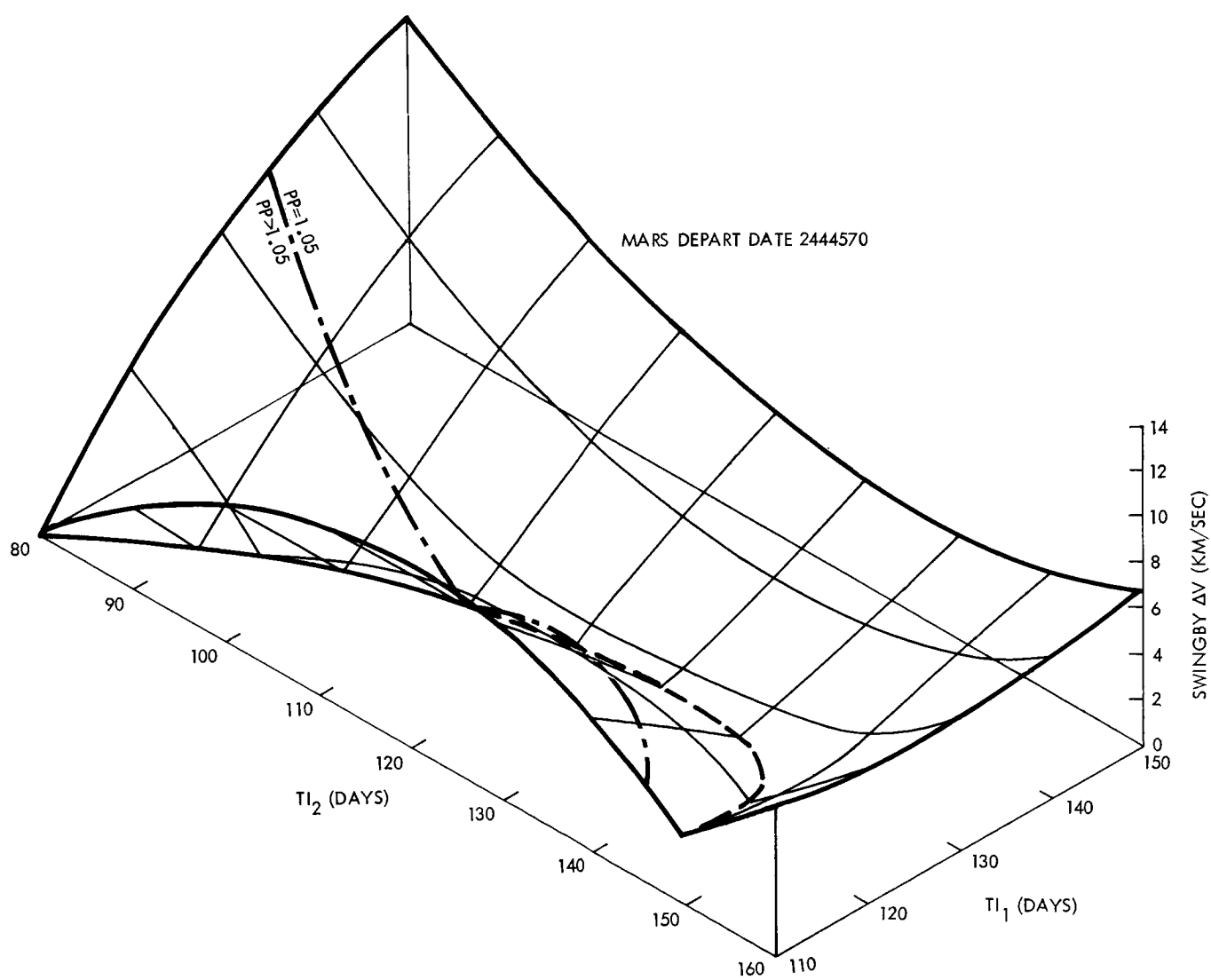


Figure II-14. Surface of Powered Swingby Velocities

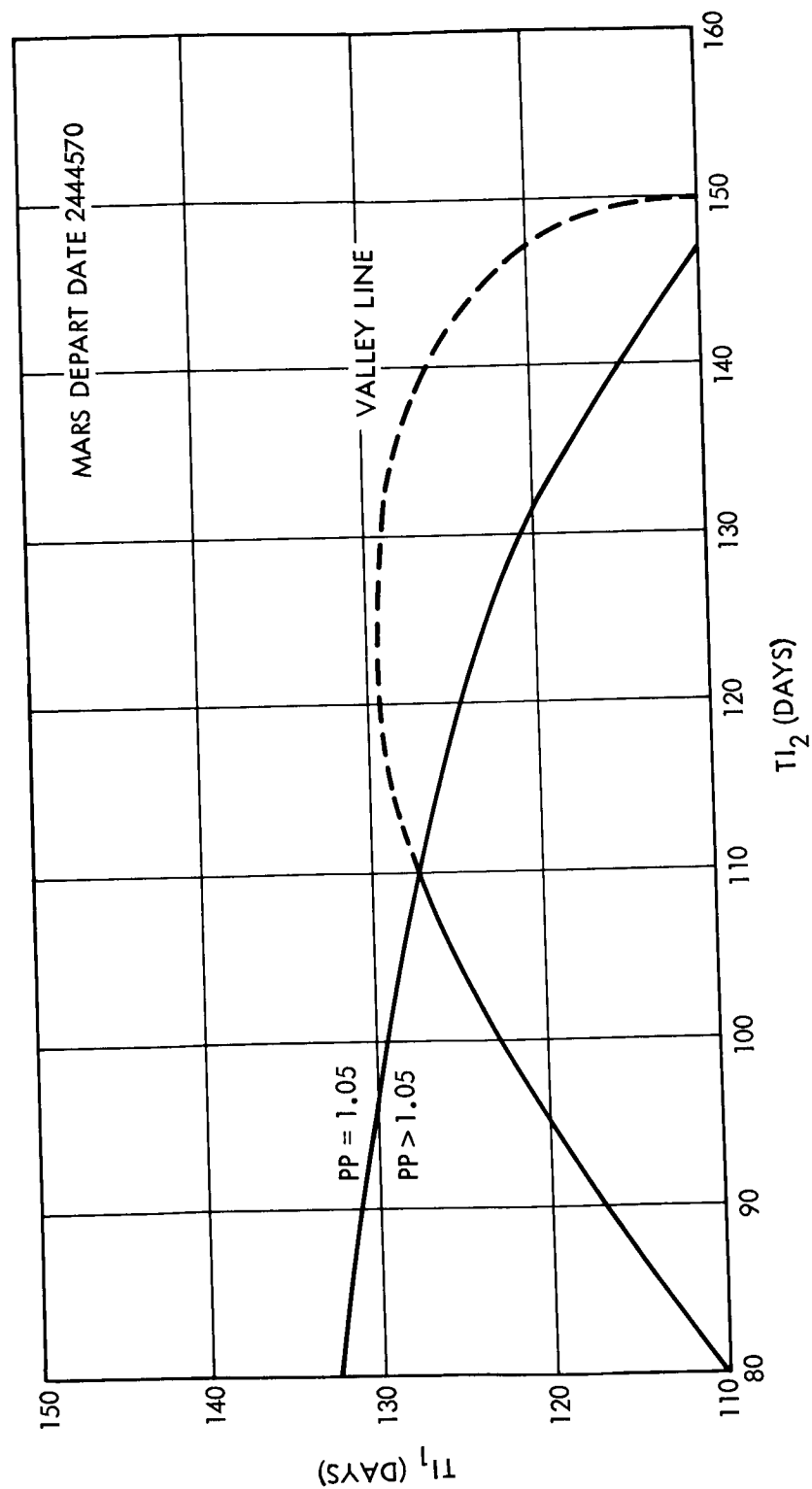


Figure II-15. Characteristics of Powered Swingby Velocity Surface

powered swingby data, PP was not allowed to go below 1.05 radii and so a ΔV is required to maintain the passage distance at 1.05 radii.

Figure II-16 shows two cross-sections of Figure II-14 in the vicinity of the gravity turn along with the corresponding ΔV 's leaving Mars (ΔV_{LP}) and arriving at Earth (ΔV_{AE}). Figure II-17 shows the values of the swingby ΔV , ΔV_{LP} , and ΔV_{AE} along the valley line of Figure II-14.

Optimization Technique

The SWOP computer program was designed to optimize powered swingby missions, as well as gravity turn swingby and opposition class missions. The optimization approach used in SWOP is simply the differential calculus approach to minimizing a function of several variables (Ref 1). For an inbound powered swingby mission, the vehicle primarily is a function of the mission ΔV 's, which are in turn, functions of the outbound and two inbound leg times plus the planet arrival date. After application of the chain rule for derivatives, the optimization equation will include terms involving the partial derivatives of the ΔV 's with respect to the leg times and planet arrival date. The approach used in SWOP requires that the partial derivatives be continuous in the domain of the optimum. It is apparent from Figures II-14 and II-16 that the partials of the swingby ΔV with respect to TI_1 and TI_2 are discontinuous across the valley line.

The powered swingby portion of the SWOP program was written assuming that powered swingby missions would be sufficiently superior to unpowered swingby missions so that the program would optimize well away from the region of discontinuity of the partials (as is the case with powered Mars flybys). An attempt to run the SWOP program using the trajectory data for the 1980 and 1982 inbound powered swingbys made it apparent that the optimum (minimum vehicle weight) point would lie on or very near the region of discontinuity of the partials. The program failed to operate, and in all cases entered an infinite loop, jumping back and forth across the discontinuity.

Since it became obvious that the optimum point in the powered swingby data would apparently lie on, or very near, the discontinuity of the partial derivatives, it became necessary to find the optimum point manually by using SWOP in a mode in which the program simply computes the vehicle weight for a given set of dates, ΔV 's, etc., without optimizing. This procedure first required

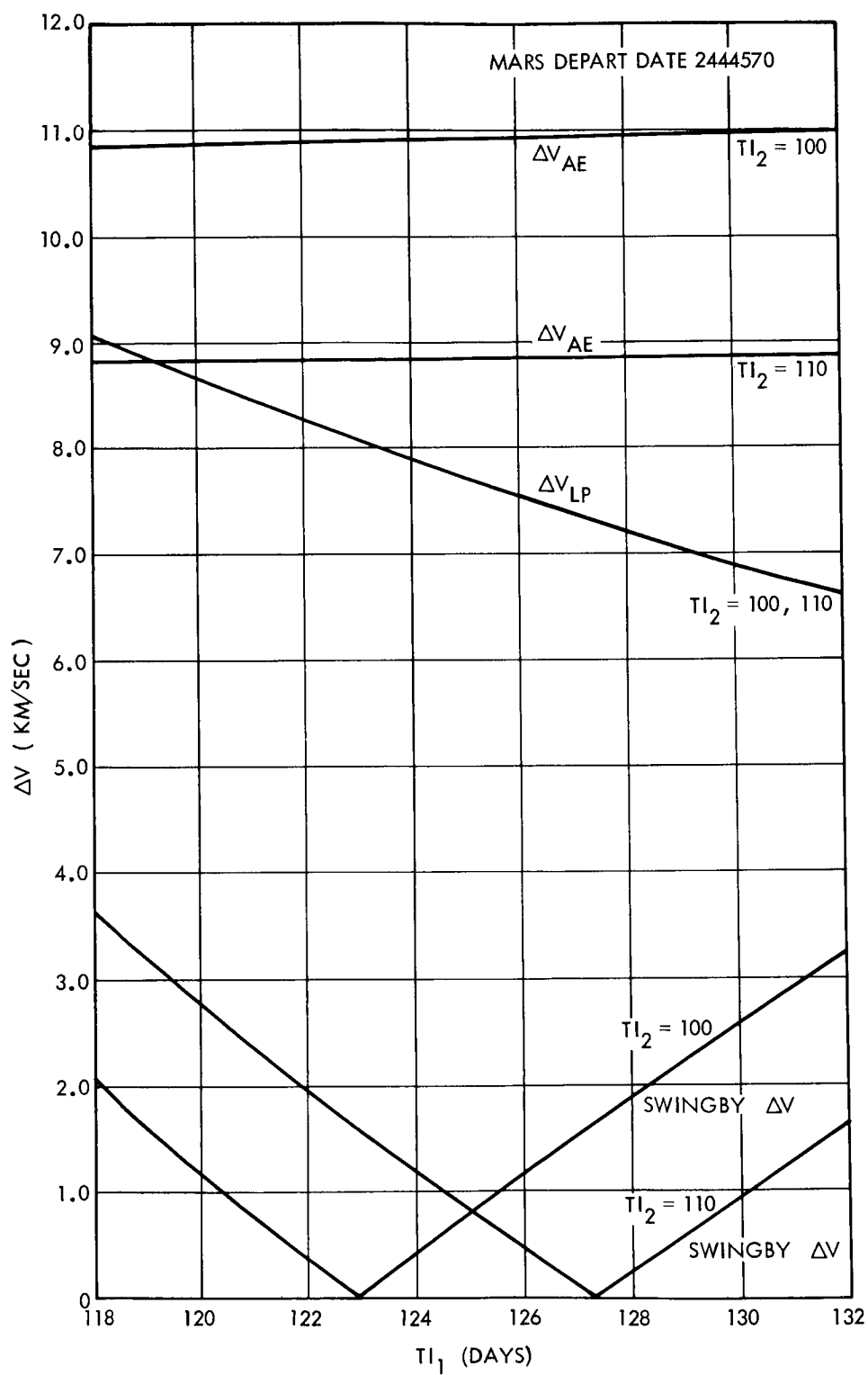


Figure II-16. Typical Powered Swingby Velocity Data

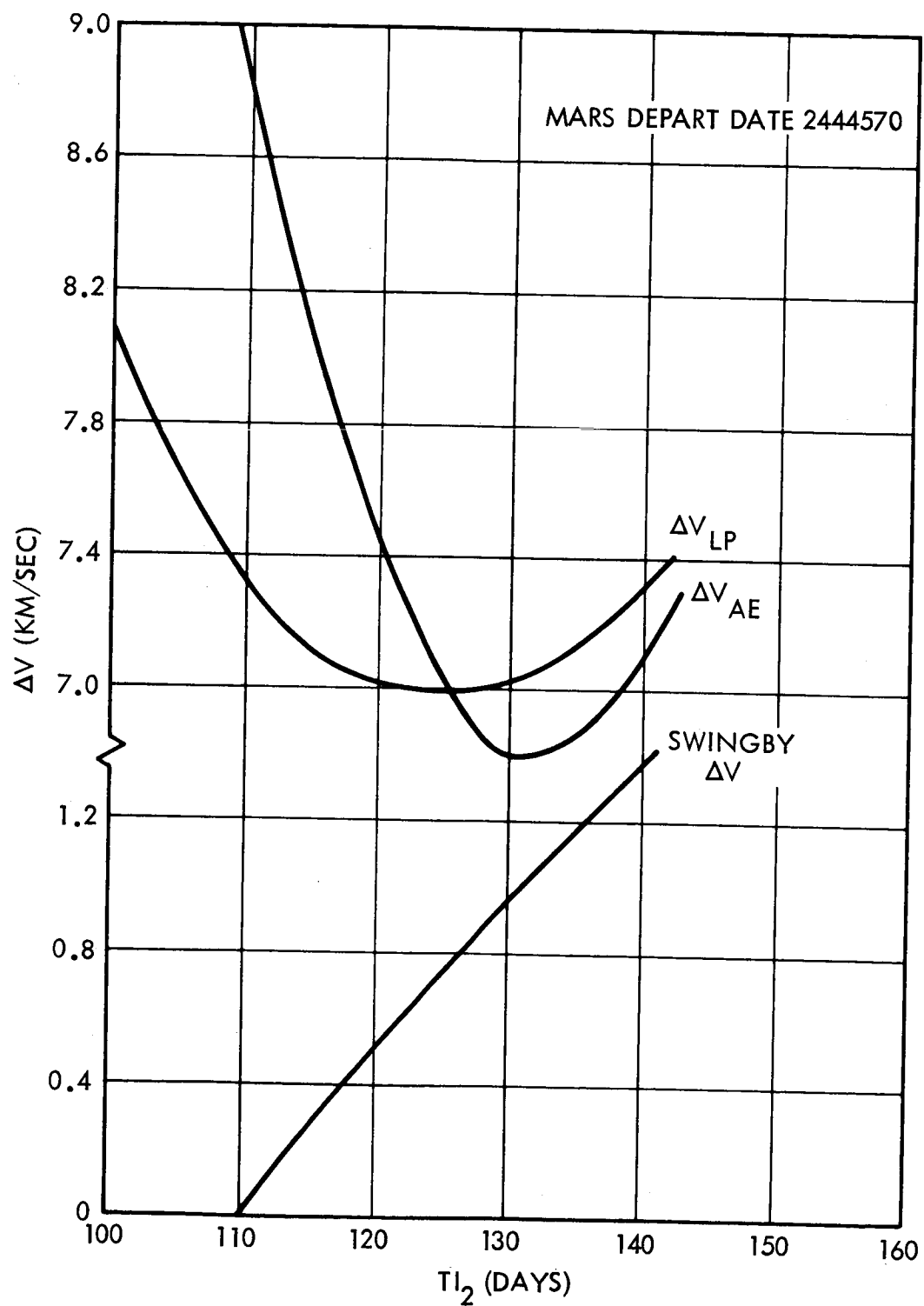


Figure II-17. Powered Swingby Velocity Data Along Valley Line

narrowing down the region where the optimum may lie by hand analysis of the data. The data in that region was then regenerated with a finer division (one day) of dates and trip times. The resulting data were then sequentially inputted into SWOP and the minimum weight vehicles selected from the output. The approach taken was to start with the optimum point for an unpowered swingby and then attempt to decrease the vehicle weight by moving from that point with the planet arrival date (and, therefore, the planet departure date) fixed. This was done for several planet arrival dates and the results were plotted yielding the optimum powered swingby.

Figures II-14 to II-17 were very helpful in this manual optimization process. For 1980, the best unpowered swingby always will be at the intersection of the valley line and the $PP = 1.05$ radii line.* It is apparent from Figure II-16 that moving normal to the valley line will not decrease the vehicle weight. However, Figure II-17 indicates that some improvement may be possible moving to the right along the valley line.** In the manual optimization, vehicle weights were computed for a narrow band of data along the valley line to the right of the $PP = 1.05$ radii line.

Graphs analogous to Figures II-14 to II-17 for the 1982 inbound powered swingby contain curves that are very similar to those of Figures II-14 to II-17 except that in Figure II-15 the $PP = 1.05$ radii line would intersect the valley line to the right of its maximum TI_1 for the best planet departure dates (see Figure II-7, page II-27). Therefore, in Figure II-17 the swingby ΔV curve would shift to the right and the swingby ΔV would be zero on to the right of the minimum of the other two ΔV curves (along the valley line). Therefore, the region of possible gravity swingbys for that planet arrival date would include the minima of the ΔV_{LP} and ΔV_{AE} curves, and the gravity swingbys would have optimized in the vicinity of the minima of the ΔV_{LP} and ΔV_{AE} curves. It would appear, then, that for 1982 inbound swingbys no improvement is possible over the optimum unpowered swingby.

*The reason for this is apparent from Figure II-6, page II-26.

**This is equivalent to moving below the $PP = 1.05$ radii line in Figure II-6, which would have been impossible for unpowered swingbys.

Results and Discussion

Figures II-18 and II-19 give the results of the manual optimization for the 1980 and 1982 inbound powered swingbys and a MNNA vehicle mode. Similar curves for the unpowered swingby are included for comparison. The curves for the powered swingbys represent an envelope of the minima of the computed points obtained by using a one-day grid. The minimum weight obtained by using a one-day grid for any given planet arrival date will generally be greater than the true optimum for that date (slightly greater or much greater depending on whether the true optimum for that date lies near the one-by-one-day grid point in the data). It is only very rarely that the exact optimum point is hit using a one-day grid. The unpowered swingby curves, on the other hand, represent the exact optima.

It appears from Figures II-18 and II-19 that the powered swingby offers no advantage over the unpowered swingby in either case. Hollister (Ref 4) stated that total ΔV savings of "a few hundred feet per second" are possible in some cases using the powered swingby. Figures II-20 and II-21 give the total ΔV requirements for the two years for both powered and unpowered swingbys. For 1980, the powered swingbys do indeed require a lower total ΔV than do the unpowered swingbys. However, Figure II-18 does not indicate any corresponding savings in weight. In order to perform the powered swingby mission the vehicle must carry an additional stage for the maneuver at Venus. Since this additional fixed weight must be carried through three previous propulsion maneuvers, a lower vehicle weight is not obtained.

The results of the powered swingby mission analysis indicate that the powered swingby mission offers no advantage over the unpowered swingby mission for the type 3 swingby trajectories because there is no reduction in total mission characteristic velocity or initial vehicle weight. (The type 5 swingby missions have trajectory characteristics similar to those of the type 3 missions and would, therefore, also not obtain any benefit from the use of a powered turn at Venus.)

For the type 1 inbound swingby, use of the powered turn at Venus reduces the total mission characteristic velocity by about 4 percent, but no reduction in vehicle weight results. The major effect obtained from the use of a powered turn with the type 1 inbound trajectory is a reduction in the Earth arrival velocity. Since this maneuver is performed by a low weight aerodynamic braking system that is relatively insensitive to arrival velocity, only a small weight reduction is obtained for this stage. On the other hand, for an outbound type 1 swingby the major velocity reductions obtained from a powered Venus flyby apply to maneuvers performed by propulsion systems. However, for the 1982 outbound type 1 gravity swingby (the only outbound type 1 swingby occurring in the 1980 to 1986 period) the total mission characteristic velocity is approximately twice that for the 1982 inbound (type 3) gravity swingby. Therefore, the use of a powered Venus swingby for this launch opportunity would have to reduce the total velocity of the outbound swingby by 50 percent to make it competitive with the inbound gravity swingby. Since a reduction of this magnitude is not apparently feasible, it is concluded that the best gravity swingby (outbound or inbound with short or long connecting leg) would be superior to the best powered swingby for any given year in the 1980 to 1986 time period.

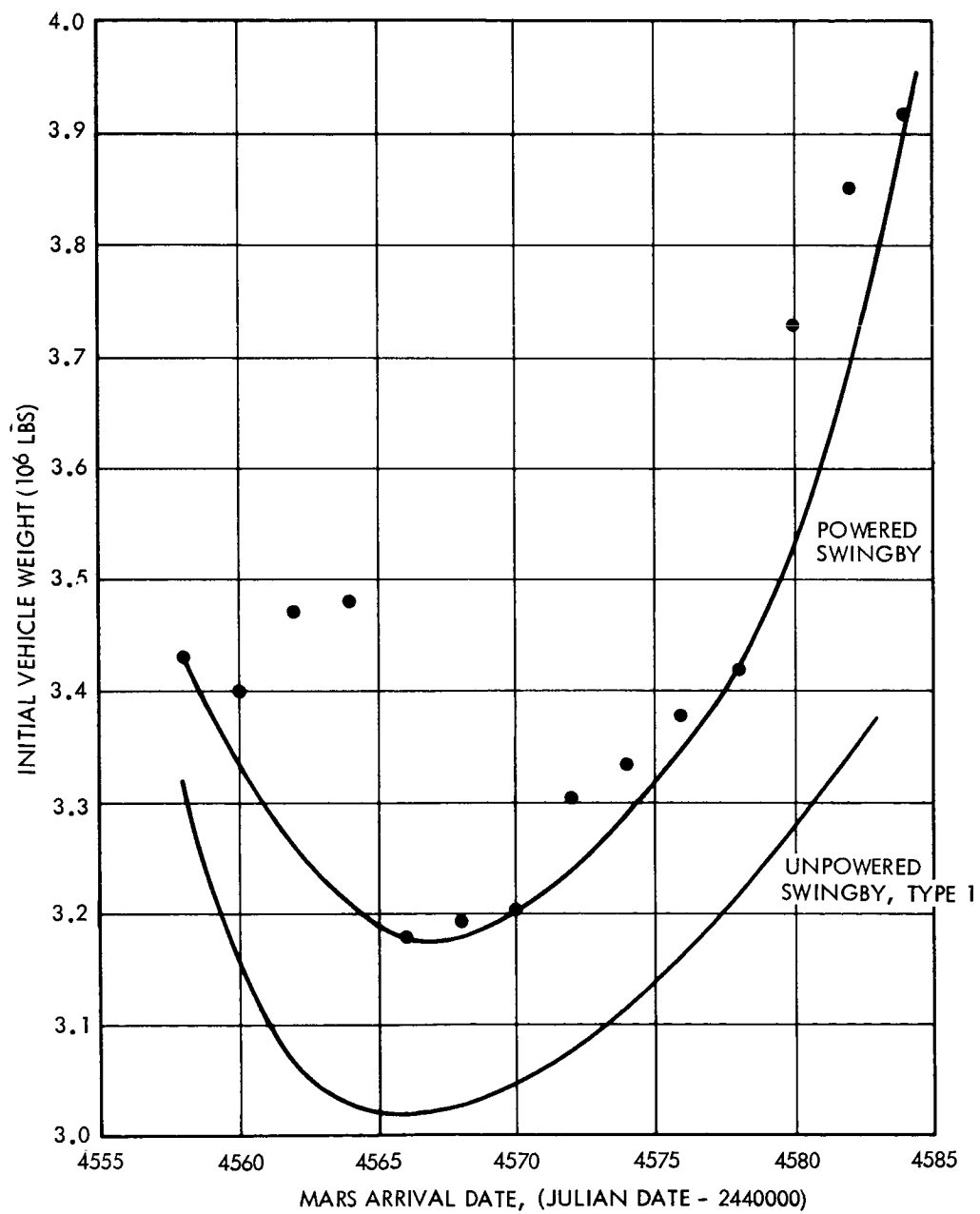


Figure II-18. 1980 Inbound Swingby Mission Weight Comparison

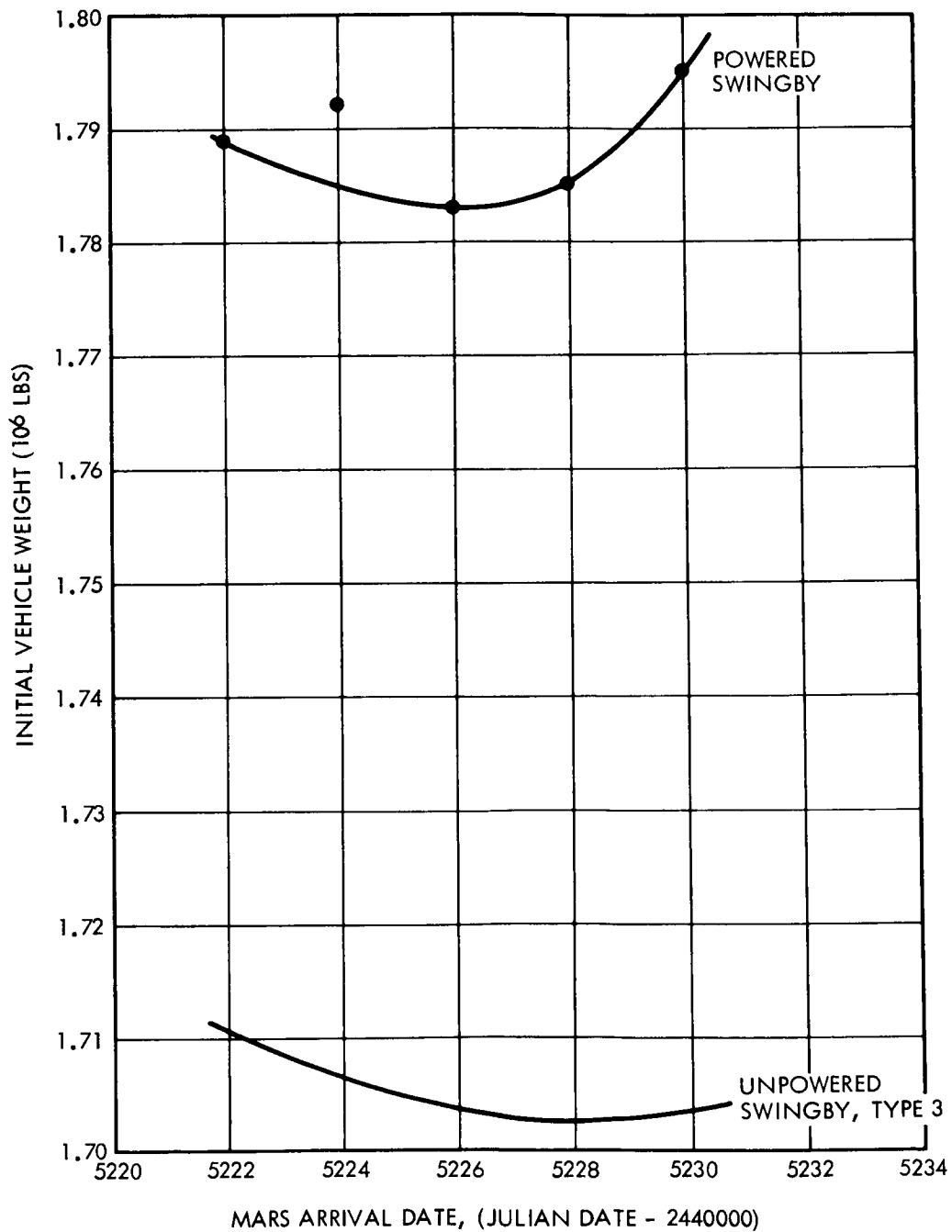
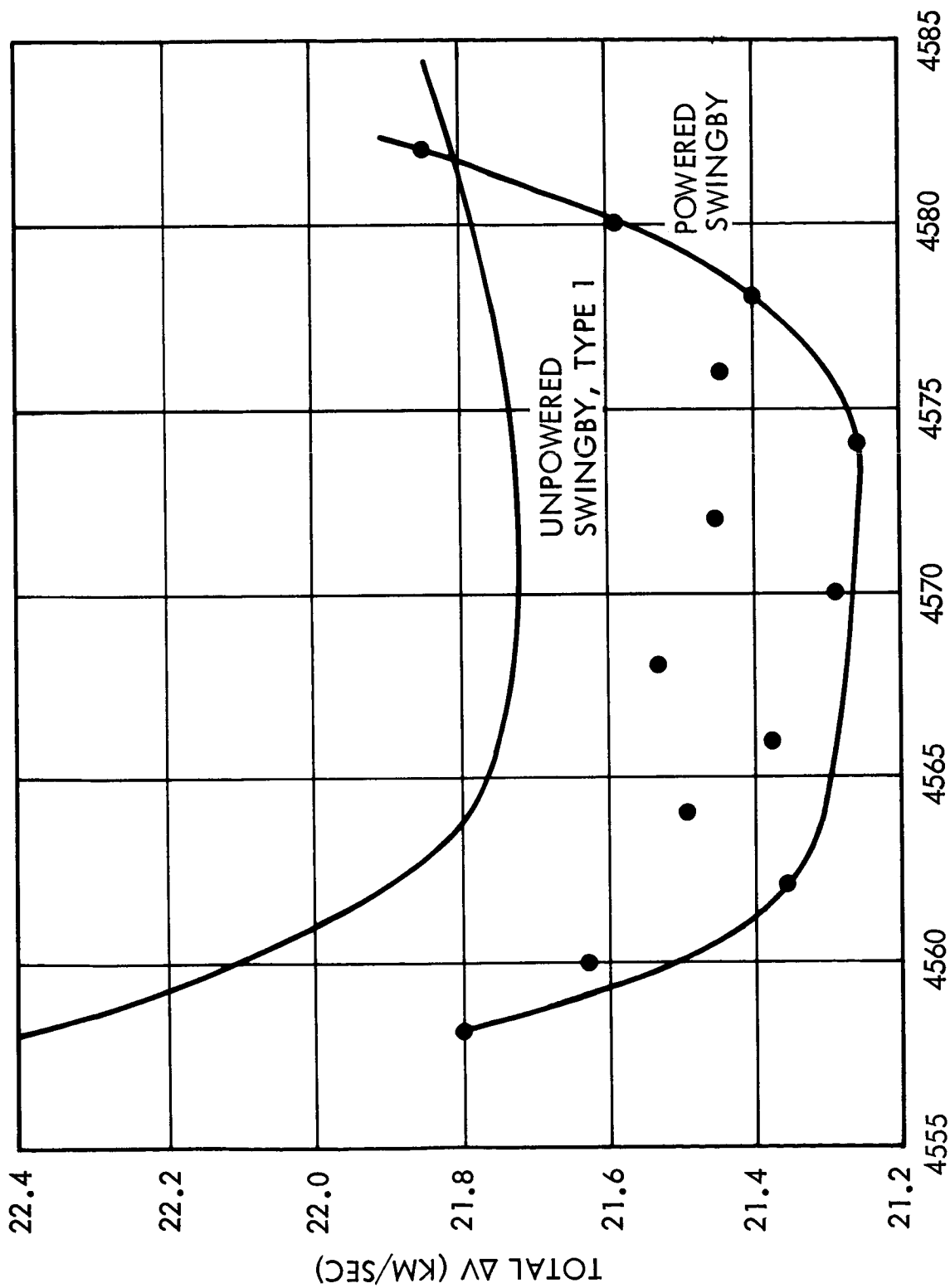


Figure II-19. 1982 Inbound Swingby Mission Weight Comparison



MARS ARRIVAL DATE, (JULIAN DATE - 2440000)

Figure II-20. 1980 Inbound Swingby Mission Velocity Comparison

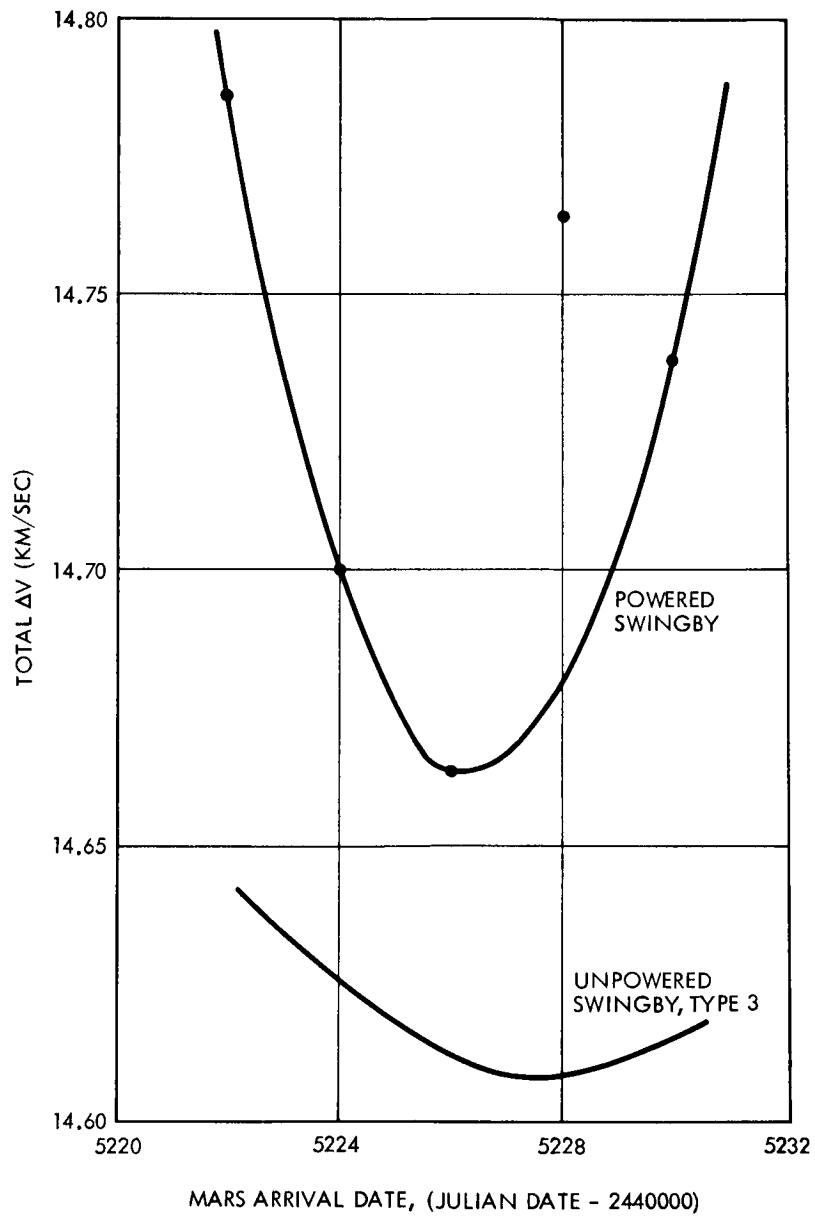


Figure II-21. 1982 Inbound Swingby Mission Velocity Comparison

III. CONJUNCTION CLASS MISSION ANALYSIS

TASK DESCRIPTION

The Swingby Optimization Program (SWOP) was utilized to determine the initial weight requirements in Earth orbit for conjunction class, manned Mars stopover missions. The mission opportunity of the 1983 Earth-Mars conjunction was selected as typical and the necessary free flight trajectory data were generated for the various types of trajectories for that opportunity. All four combinations of the short and long, outbound and inbound trajectories were analyzed.

These investigations included parametric variations of the vehicle and propulsive modes, structural scaling laws, and payload weights in order to illustrate their effect on initial vehicle weight.

ASSUMPTIONS AND CONSTRAINTS

The set of assumptions and constraints that was postulated for this task in order to circumscribe the vehicle's performance, operation, and system weights is essentially the same as that of the Swingby Mission Analysis with only a few exceptions or additions.

Therefore, the basic set of assumptions, constraints, and definitions are set forth in detail in Section II and only those peculiar to this task are given below.

Mission and Trajectory Description

The conjunction class mission is designed to take advantage of the lowest possible energy requirements for both the outbound trip and the return trip. The opposition class mission is characterized by short stopover periods at Mars and, therefore, cannot take advantage of minimum energy trips. The minimum energy return trip occurs before rather than after the nearest minimum energy outbound trip. Therefore, the opposition class trips are a compromise combination of outbound and inbound energy requirements close to the time of the Earth-Mars opposition. The rectangular region outlined by the heavy line in the upper right-hand corner of Figure III-1 is the region of interest for the 1984 opposition class mission.

EARTH-MARS-EARTH, CONJUNCTION 3.4 JUNE 1983

HYPERBOLIC EXCESS SPEED CONTOURS
NORMALIZED WITH RESPECT TO 0.1 EARTH'S
MEAN ORBITAL SPEED

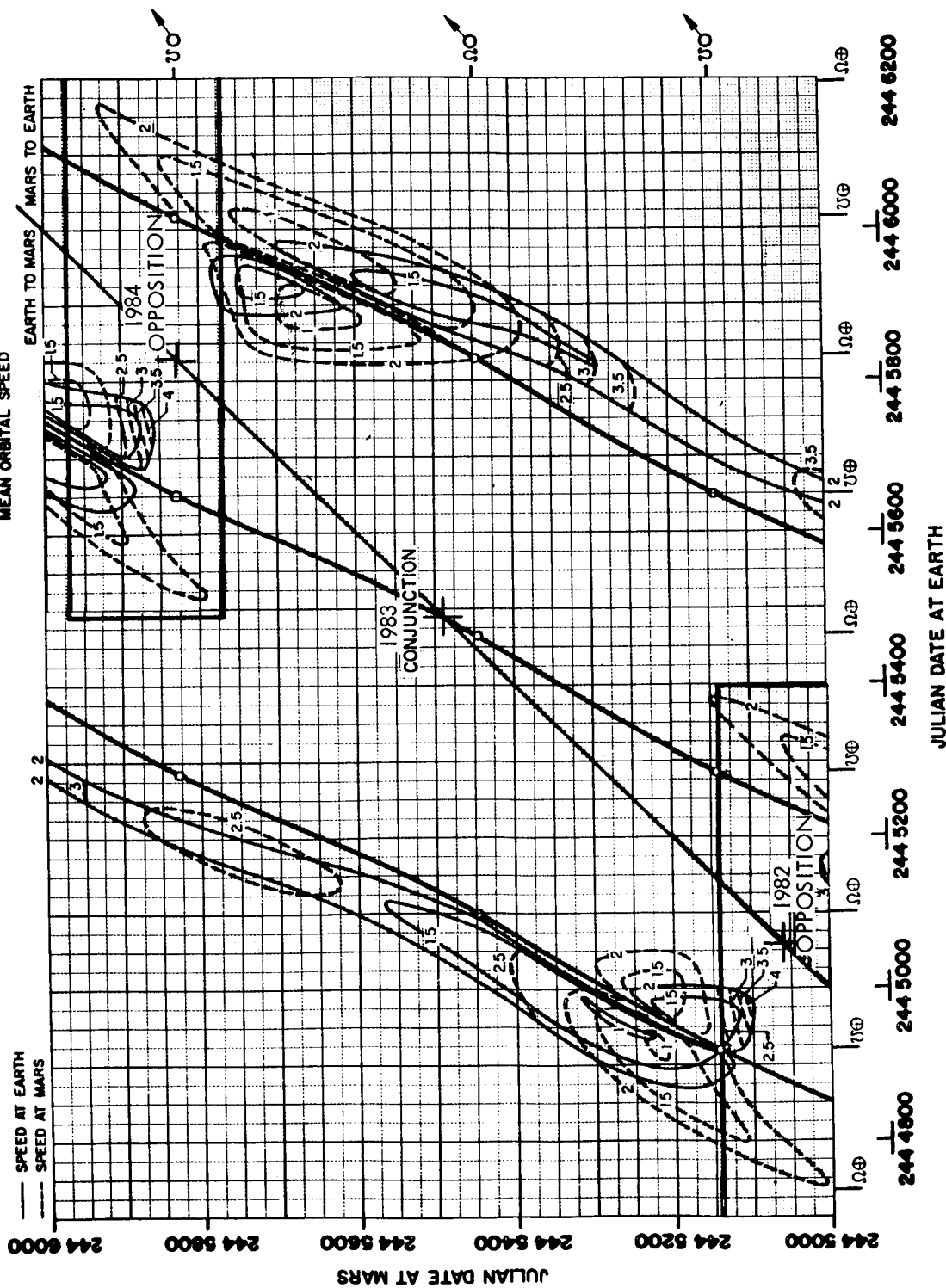


Figure III-1. Velocity Contour Map

It is possible to utilize the minimum energy trips, but to do so requires long stopover periods at Mars (as is apparent from Figure III-1). These missions using the minimum energy trips are referred to as conjunction class because the Earth-Mars conjunction occurs during the stopover period and the mission is approximately symmetrical about the conjunction. The energy requirements for the conjunction class missions vary much less from year to year than do the requirements for other mission types. Therefore, one year, 1983, was taken as typical and vehicles were analyzed for only that year.

For both the outbound and inbound legs of the round trip trajectory, two types of trajectories were considered, viz, the short and the long one-way transfers. Therefore, four types of round trip missions were investigated; type IA (long outbound leg, short inbound leg), type IB (long, long), type IIA (short, short), and type IIB (short, long).

Vehicle Configuration and System Weights

The scaling laws and system weights used to define the mission payloads, propellant tanks, propulsion systems, secondary spacecraft systems, and operational modes are essentially the same as those for the Swingby Mission Analysis except for the qualifications and exceptions noted below.

Propulsion System Weight Scaling Laws - Only the tanking mode configuration was employed in the mission analyses conducted for this task. The sets of scaling laws used were the mass fraction cases Nos. 2 and 3 for the vehicles employing chemical cryogenic propulsion systems for the main stages and mass fraction case No. 2 for vehicles employing nuclear propulsion systems. These scaling laws were previously given in Section II in Tables II-2 and II-3 on pages II-8 and II-9. In addition, the mass fraction case No. 3 was also used for the vehicles employing nuclear propulsion systems. The additional scaling laws for this latter case are shown in Table III-1.

An additional weight was added to the planet depart stage for all cases to account for the increased micrometeoroid protection required due to the longer planet stopover period. This weight varied with the assumed payload and is given in Table III-2 which follows in this section.

Table III-1 Mass Fraction Case No. 3

<u>Mode</u>	<u>Equation (lbs)</u>	<u>Single Tank Max Propellant Capacity (lbs)</u>
Earth Depart		
Nuclear Propulsion	$W_j = .22208 W_p + 7010$	342,540
Midcourse Correction Outbound		
Storable Propulsion	$W_j = .12888 W_p + 1652$	
Planet Braking		
Nuclear Propulsion	$W_j = .25043 W_p + 3531$	342,540
Aero Capture Circularizing		
Storable Propulsion	$W_j = .12888 W_p + 1652$	
Planet Depart		
Nuclear Propulsion	$W_j = .25043 W_p + 3531$	342,540
Storable Propulsion	$W_j = .12385 W_p + 18,131$	800,000
Midcourse Correction Inbound		
Storable Propulsion	$W_j = .10094 W_p + 1021$	
Earth Braking		
Storable Propulsion	$W_j = .14973 W_p + 4215$	

Notes:

1. Includes micrometeoroid protection
2. Includes insulation for Earth depart stages
3. Does not include insulation for all other stages
4. Includes engine weight for all non-nuclear stages
5. Does not include engine weight for all nuclear stages

A single nuclear engine weight of 38,000 pounds was used and each engine was assumed to have 230,000 pounds of thrust. The engine weight and thrust for clusters of two or more nuclear engines were taken as direct multiples of these values. A single nuclear engine was assumed for the arrive and depart Mars stages and the optimum number of engines was determined and used for the depart Earth stage, i.e., the number of engines that yield the minimum initial vehicle weight.

Payload and Expendable Weights - The stopover time at Mars is about 400 days for the conjunction class mission compared to 20 days for the other mission types. The longer stopover time will tend to increase some of the module and life support weights due to increases in crew size and requirements. Also an increase in the payload weights is desirable to allow for more extensive experiments and shelters at the planet. Four payload sets were postulated as shown in Table III-2. They represent a range of values obtained from interplanetary mission studies performed by NASA, TRW, and industry in the past years. The first set is identical to that used for the missions in the other study tasks which use a 20-day stopover time. The other three sets represent increased weights to account for added experiments and crew. Payload set 3 was used in the comparisons of the conjunction class mission to the other mission types in the other four study tasks.

Table III-2 Conjunction Mission Payloads

Payload Set	Crew	Earth Return Module (lb)	Mission Module (lb)*	Mars Excursion Module (lb)	Orbit Return Weight (lb)	Life Support Expendables (lb/day)	Additional Micrometeoroid Protection (lb)
1	8	10,000	68,734	80,000	1500	50	
2	8	11,500	75,000	109,000	2500	50	27,500 + 27 T _{SO}
3	12	15,000	100,000	135,000	3100	75	38,000 + 40 T _{SO}
4	20	27,000	150,000	178,600	7500	120	57,000 + 60 T _{SO}

*Does not include solar flare shield

As mentioned previously, the additional weight which was added to the planet depart stage to account for increased micrometeoroid protection is also given in Table III-2. This weight is added to the tank weight for all sets of scaling laws, i.e., mass fraction cases Nos. 2 and 3, and is jettisoned prior to Mars departure.

The solar flare radiation shielding scaling law which was used in this task was that given in Section II for an active solar flare activity. This weight is added to the mission module weight to determine the total weight to be jettisoned prior to Earth arrival. A perihelion distance of 1.0 AU was used.

Aerodynamic Braking Scaling Laws - The scaling laws for aerodynamically braking the Earth return module are given below for the four module weights used in this task.

$$W_R = 10,000$$

$$W_{ERM} = 46.71 V_{AE}^2 - 1042.3 V_{AE} + 20,122$$

$$W_R = 11,500$$

$$W_{ERM} = 43.75 V_{AE}^2 - 947.3 V_{AE} + 21,170$$

$$W_R = 15,000$$

$$W_{ERM} = 55.82 V_{AE}^2 - 1237.7 V_{AE} + 27,384$$

$$W_R = 27,000$$

$$W_{ERM} = 46.25 V_{AE}^2 - 756.3 V_{AE} + 35,960$$

where

W_R - Recovered or useable payload weight after Earth entry (lbs)

W_{ERM} - Gross vehicle weight or Earth entry module weight (lbs)

V_{AE} - Entry velocity relative to a non-rotating Earth at an altitude of 100 km (km/sec)

The weight scaling law for aerodynamic braking at Mars is identical to that given in Section II.

Secondary Spacecraft Systems - The weight expenditures for the secondary spacecraft systems including midcourse corrections, attitude control, and orbit adjustment for modes employing aerodynamic braking at Mars were the same as those outlined in Section II for the Swingby Mission Analysis with one exception. In order to account for the prolonged stay time at Mars, the attitude control provisions during the planetary stopover period were computed on the basis of one percent of the vehicle weight in planetary orbit.

Cryogenic Propellant Vaporization - The computational techniques employed for this task for determining the propellant vaporized during the interplanetary trip were identical to those described in Section II for the tanking mode. That is, the tankage insulation and propellant boiloff during the mission were calculated separately for each stage on the basis of the optimum trade-off equations which yield a minimum overall vehicle weight.

Vehicle Mode Matrix

The conjunction class missions for 1983 were analyzed for a variety of vehicle modes, trajectory types, propulsion systems, engine performance parameters, and stage scaling laws. Table III-3 shows the matrix of cases investigated.

Table III-3 Vehicle Mode Matrix

<u>Year</u>	<u>Trajectory Types</u>	<u>Vehicle Modes</u>	<u>Scaling Laws</u>	<u>Payloads</u>
1983	IA Long, Short	NNNA	MF No. 2	Sets 1, 2, 3 and 4
	IB - Long, Long	NNNS(P)	MF No. 3	
	IIA - Short, Short	NASA		
	IIB - Short, Long	CCCA		
		CCCS(P)		
		CASA		

N - Nuclear Propulsion (800 sec)

C - Chemical Cryogenic Propulsion, H_2/O_2 (440 sec)

S - Liquid Storable Propulsion (330 sec)

A - Aerodynamic braking

S(P) - Liquid storable propulsion (330 sec) to parabolic entry velocity followed by aerodynamic braking.

RESULTS AND DISCUSSION

The results of the mission analyses for this task are presented in the following order. First, the initial vehicle weights data are presented for the mission and vehicle mode combinations shown previously in Table III-3. Next the results for various types of trajectories are evaluated to illustrate their various characteristics. Finally, the results for the various vehicle modes and payload weights are compared.

Initial Vehicle Weight Data

Table III-4 contains the minimum initial vehicle weights and total trip times for the 1983 conjunction class mission. These data are presented for the matrix of four payload sets, six vehicle modes, and four trajectory types analyzed. All these results are for the mass fraction case No. 2 structural scaling laws.

An examination of the results in Table III-4 showed that in all cases the trajectory type IA (long outbound leg, short inbound leg) yielded the overall minimum vehicle weight. This trajectory type, therefore, was selected as the preferred trajectory and was used to analyze the vehicle mode matrix for mass fraction case No. 3. The results of this analysis is given in Table III-5.

Trajectory Type Comparison

As mentioned previously, a comparison of the four combinations of trajectory types shows that the type IA gives the lowest vehicle weight as shown in Figure III-2 for the NNNA mode, mass fraction case No. 2, and payload set 3. The type IIA trajectory, on the other hand, gives the shortest trip but with the greatest vehicle weight. Therefore, the type IA was selected as the best overall compromise since it requires 11 percent less vehicle weight than type IIA with only 4 percent longer total trip time. The type IA trajectory was used in the comparisons of the conjunction class mission to the other mission types in the other four study tasks.

A comparison of trajectory types for the other vehicle modes and payload weights results in identical comparative conclusions.

Table III-4. 1983 Conjunction Class Mission Initial Vehicle Weights

PAYLOAD CASE NO.	TRAJECTORY TYPE	NNNA		NNNS(P)		CCCA		CCCS(P)		NASA		CASA	
		Initial Weight (10 ⁶ lbs)	Total Trip Time (Days)	Initial Weight (10 ⁶ lbs)	Total Trip Time (Days)	Initial Weight (10 ⁶ lbs)	Total Trip Time (Days)	Initial Weight (10 ⁶ lbs)	Total Trip Time (Days)	Initial Weight (10 ⁶ lbs)	Total Trip Time (Days)	Initial Weight (10 ⁶ lbs)	Total Trip Time (Days)
1	IA	1.238	956	1.287	968	1.873	957	1.994	968	1.150	950	1.465	950
	IB	1.251	1024	1.293	1025	1.903	1024	2.005	1025	1.160	1029	1.485	1029
	IIA	1.389	927	1.455	941	2.271	918	2.551	941	1.173	932	1.502	933
	IIB	1.369	1004	1.428	970	2.369	974	2.456	964	1.187	1008	1.523	1008
2	IA	1.469	955	1.526	968	2.345	956	2.485	968	1.374	947	1.807	948
	IB	1.480	1025	1.527	1006	2.371	1025	2.493	1014	1.389	1030	1.829	1025
	IIA	1.634	922	1.700	935	2.886	925	3.051	935	1.411	933	1.863	933
	IIB	1.630	992	1.698	980	2.915	996	3.065	982	1.426	1009	1.884	1009
3	IA	1.755	955	1.822	967	3.009	956	3.171	968	1.690	948	2.282	946
	IB	1.773	1025	1.828	1014	3.051	1025	3.193	1014	1.714	1018	2.316	1018
	IIA	1.978	921	2.058	935	3.632	925	3.823	935	1.737	932	2.353	933
	IIB	1.976	992	2.058	960	3.685	1005	3.884	972	1.760	1008	2.386	1008
4	IA	2.348	954	2.448	968	4.233	956	4.466	967	2.345	946	3.279	946
	IB	2.378	1025	2.457	1006	4.301	1025	4.501	1014	2.382	1017	3.335	1018
	IIA	2.683	921	2.814	935	5.196	925	5.519	934	2.413	932	3.383	933
	IIB	2.708	971	2.847	990	5.292	984	5.604	1002	2.452	1008	3.450	1010

All results are for mass fraction case No. 2

Table III-5. 1983 Type IA Conjunction Class Mission Initial Vehicle Weights

Vehicle Code	Payload Set							
	1		2		3		4	
	Initial Weight (10^6 lbs)	Total Trip Time (Days)	Initial Weight (10^6 lbs)	Total Trip Time (Days)	Initial Weight (10^6 lbs)	Total Trip Time (Days)	Initial Weight (10^6 lbs)	Total Trip Time (Days)
NNNA	1.330	957	1.578	955	1.900	955	2.533	954
NNNS(P)	1.388	969	1.645	969	1.980	968	2.651	969
CCCA	2.237	957	2.839	956	3.562	956	5.002	956
CCCS(P)	2.396	968	3.023	968	3.773	969	5.442	967
NASA	1.239	951	1.476	947	1.817	946	2.523	946
CASA	1.662	951	2.035	947	2.565	946	3.682	946

All results are for mass fraction case No. 3.

1983 CONJUNCTION MISSION

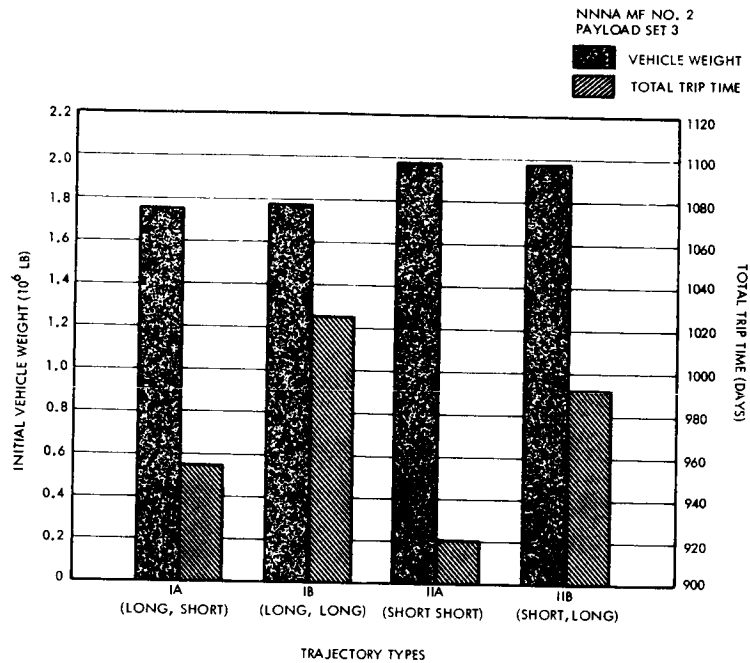


Figure III-2. Conjunction Mission Trajectory Type Comparison

Vehicle Mode Comparisons

Figure III-3 shows the increased vehicle weight that results from increases in payload weights for the various vehicle modes based on the mass fraction case No. 2 structural scaling laws. Figure III-4 is the analogous results for mass fraction case No. 3. The vehicle weights corresponding to payload set 1 (which is the same as that used for all other mission types) are extremely low. A comparison among mission modes in the other study tasks based on this set would show the conjunction class mission requiring considerably lower vehicle weights than the other modes for all years and vehicles. However, payload sets 2, 3, and 4 are probably more realistic for comparisons involving the conjunction class mission.

1983 CONJUNCTION (TYPE IA) MISSION

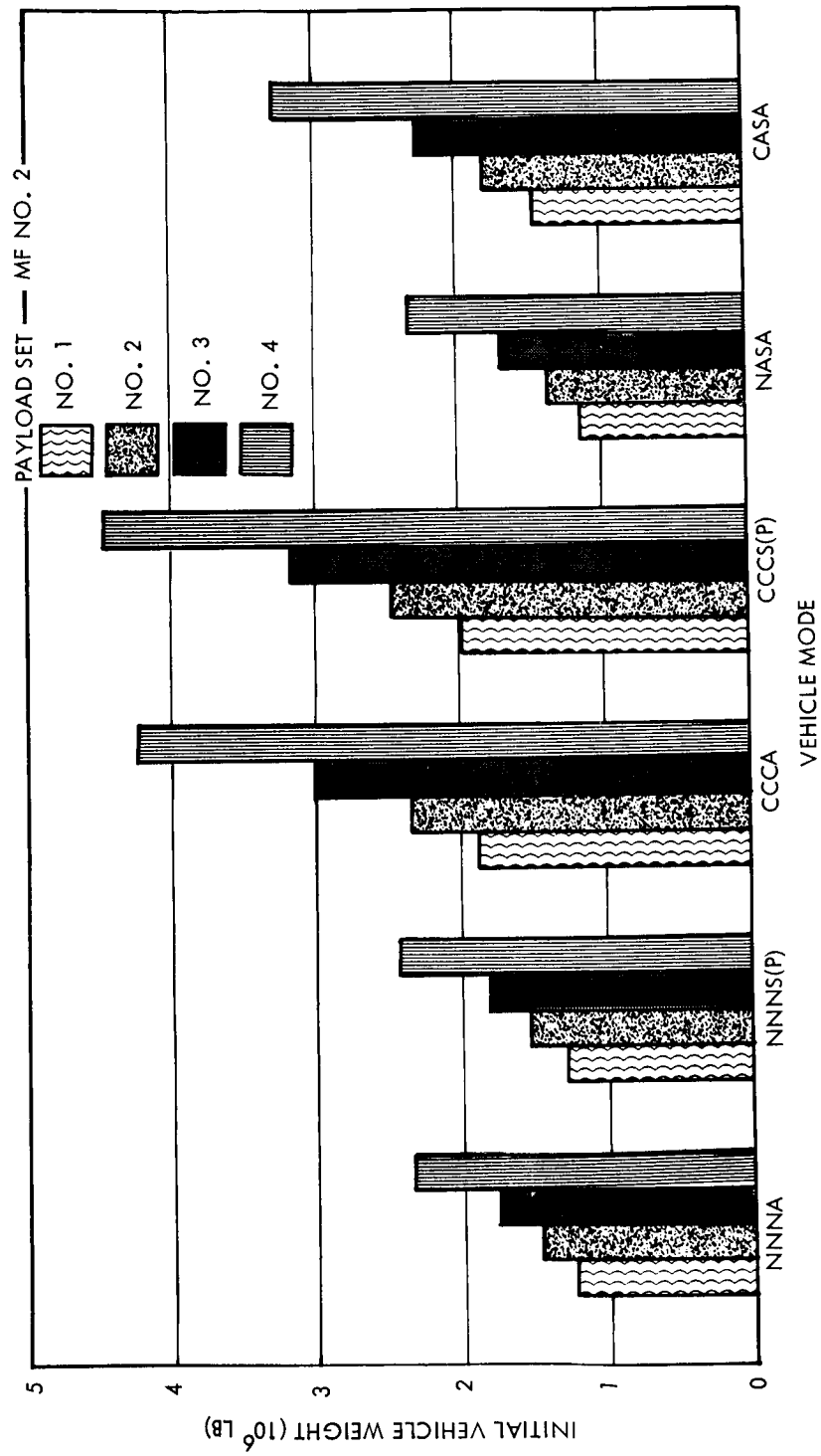


Figure III-3. Conjunction Mission Mass Fraction No. 2 Payload Comparison

1983 CONJUNCTION (TYPE IA) MISSION

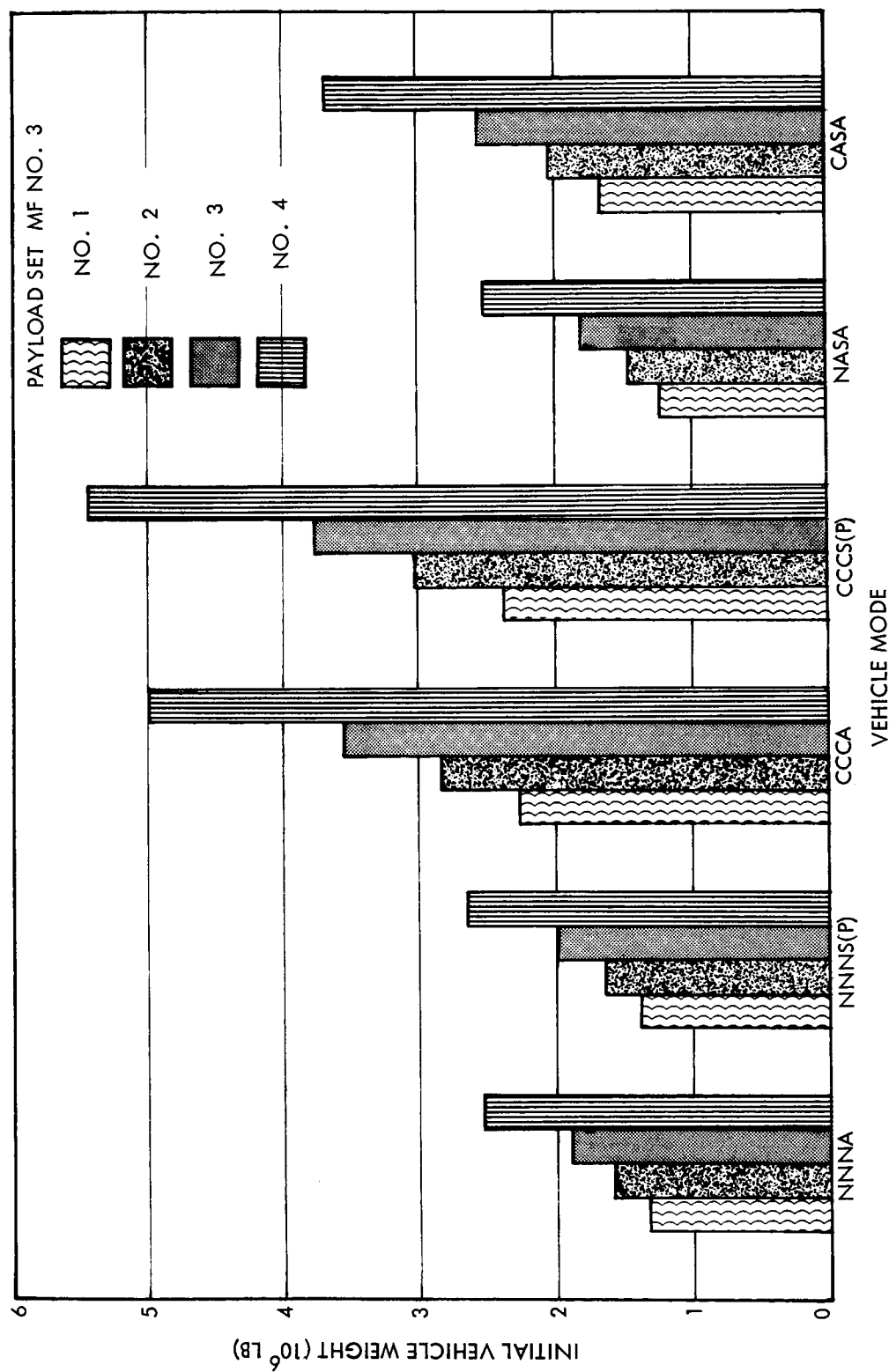


Figure III-4, Conjunction Mission Mass Fraction No. 3 Payload Comparison

IV. MISSION ABORT ANALYSIS

TASK DESCRIPTION

An investigation was made of opposition, swingby, and conjunction class missions to determine the abort capability of the vehicle from various points along the outbound trajectory using the available vehicle propulsive systems. Abort trajectories were determined from various points along the Earth to Mars outbound trajectory and various combinations of the vehicle propulsive systems were considered for providing the abort velocity increment and the Earth deceleration requirements. Velocity contour maps were constructed indicating the vehicle abort capabilities, Earth entry velocities, and Earth rescue requirements.

ASSUMPTIONS AND CONSTRAINTS

The four missions and vehicles used for the abort analysis are shown in Table IV-1.

Table IV-1. Abort Analysis Vehicles

<u>Mission</u>	<u>Year</u>	<u>Vehicle Mode</u>
Oppositon, IIB	1982	NNNS(15)
Conjunction, IA	1983	NNNS(P)
Inbound Swingby, I3	1982	NNNS(P)
Outbound Swingby, 3A	1986	NNNS(P)

The connecting mode vehicle configuration was used for all vehicle weight calculations. The scaling laws and payload system weight assumptions are those listed in Section II. A specific impulse of 850 sec was used for all nuclear propulsion stages.

ANALYSIS APPROACH

In the final selection of trajectories for manned interplanetary missions, many factors other than vehicle weight must be considered. One of these factors, which is associated with the mission success probability and safety of the crew is the abort capability of the vehicle.

It is impossible to plan a mission and build the required vehicle so that the probability of success of the mission is 100 percent. For manned missions it becomes necessary, therefore, to plan and prepare for the possibility of irreparable failure at some point in the mission. It should be recognized at the outset that for a mission as complex as the manned Mars mission there will inevitably be possible modes of failure for which return to Earth by the crew or rescue will be impossible. In other words, the probability of a safe return to Earth by the crew (regardless of success or failure of the mission) can never be 100 percent. The objective in planning the mission will be to make this figure as close to 100 percent as possible.

For convenience of discussion we can divide the manned Mars mission into five general phases: launch, outbound leg, near planet and surface maneuvers, inbound leg, and capture and landing. At the present time, abort during launch from Earth is provided by a launch escape system consisting of adequate propulsion to separate the manned capsule from the launch vehicle and a landing system (usually aerodynamic) for the capsule or its occupants. It is assumed that such a system will continue as the means of abort in the event of failure during launch from Earth.

Once the vehicle has reached the necessary energy to escape the Earth (at which point the launch escape system will no longer be of any use) it can be considered to be on its outbound trip, and abort analysis for the beginning of the outbound trip will then be applicable. During the outbound trip, the vehicle is carrying the propulsive capability to be used for the Mars arrival and departure and Earth arrival maneuvers. Therefore, during the outbound trip, the vehicle has propulsive capability which could possibly be adequate for a return to Earth if it was necessary to abort the mission.

The operations near Mars and on its surface consist of a complicated series of maneuvers for which certain failures could terminate the mission, e.g., propulsion failures on the surface of the planet or during escape from the planet.

The only possible abort mode for such failures would be redundant propulsion systems which would greatly increase the total vehicle weight to the point of being unreasonable. However, in most cases, it would be possible to return to Earth if the failure occurred in the Mars parking orbit and did not involve the depart Mars propulsion system. An early departure from Mars requires a lower propulsive capability for the opposition class missions and would, therefore, always be possible. For conjunction class missions, there would be a long period of time after arriving at Mars during which return to Earth from the Mars parking orbit would be impossible. However, the launch window provisions would make it possible to depart a few days earlier than the nominal depart date (probably less than ten days) if it became necessary to do so. For Venus swingby missions, it may or may not be possible to return to Earth early using the available depart Mars propulsive capability. For these latter missions, the effects of early departure change from year to year as well as for the nominal depart date in any given year, and it would be necessary to analyze each mission separately to determine whether early departure would be possible.

During the return trip to Earth, the only available propulsive capability is the Earth arrival stage. The vehicle would normally be traveling on a trajectory which would return it to Earth. The only possible use which could be made of the Earth arrival stage would be to provide a faster return trip or to provide additional midcourse correction capability if the midcourse correction stage failed or was inadequate. In either case, the vehicle would be left without the necessary means for its arrival maneuver at Earth. Therefore, any abort attempt during the inbound trip which employs the Earth arrival propulsion would be essentially impractical unless a rescue mode was available at Earth.

The capture and landing maneuvers at Earth involve using the last of the propulsive capability of the vehicle. Therefore, without redundant propulsive or aerodynamic braking capability there is very little the crew can do in case of failure during these maneuvers. However, at this point in the mission, it may be feasible to consider rescue of the crew by an Earth-based vehicle. In many cases, e.g., very late failures, rescue may be impossible or at least very difficult, but there may be a sufficiently large number of possible failure modes for which rescue is possible to warrant development of a rescue system.

It is clear from the above discussion that only during the outbound trip will the crew have clear alternatives for aborting the mission if the need arises. It was necessary then to analyze the requirements for abort from the outbound trajectory so that these alternatives could be compared. For each of the assumed alternatives it was possible to determine when on the trip abort would be possible and what return trajectories and trip times would be involved. The approach which was taken was to compute the impulsive abort and Earth arrival velocity requirements for aborting along the nominal outbound trajectory. The results were plotted as contours of constant ΔV on a grid of return trip time versus date of abort. It was then possible to assume the use of various combinations of the vehicle propulsive systems for abort and arriving at Earth and determine when abort would be possible for each assumed abort condition. Envelopes showing the region of possible abort were overlaid on the contour maps. The final result shows when abort will be possible for a given mission and failure mode, and the time required for the return trip. Typical examples of opposition class, conjunction class, and inbound and outbound Venus swingby missions were selected and abort analyses completed for each.

Six different combinations of the vehicle propulsive systems were assumed for abort and arriving at Earth. The ΔV capability for each of these combinations was computed as a function of mission date. That is, in determining the vehicle weight and available propellant, the daily weight loss due to life support expendables and propellant boiloff was considered and it was assumed that the outbound midcourse correction stage, the outbound attitude control system, and the Mars excursion module would be jettisoned prior to abort. In those cases in which only the leave Mars stage was employed for abort, the arrive Mars stage also was jettisoned prior to abort. However, the vehicle configuration did not allow jettison of the leave Mars stage prior to abort for those cases in which only the arrive Mars stage was used for abort.

CONTOUR MAPS

The calculation of the impulsive velocity requirements for abort and arriving at Earth were made using a special abort version of the TRW/AIP (Analytic Interplanetary Program). The standard version of the program computes the trajectory characteristics and the impulsive velocity requirements for transfer trajectories between any two planets of the solar system when the trajectory is defined by

departure and arrival dates. For this abort analysis task, the necessary logic was added to the program to permit it to (1) compute the nominal interplanetary trajectory as defined by the vehicles' departure and arrival dates; (2) set up an ephemeris for the vehicle from the elements of the transfer trajectory; and (3) compute the trajectories and velocity requirements for transfers from any point on the nominal vehicle trajectory to Earth. The inputs to the program were the dates defining the transfer trajectory, the range and increment of dates for which abort trips were to be computed, and the range and increment of return trip times to be considered. The output consisted of the abort and Earth arrival velocity requirements and the perihelion distance (if the vehicle passes through perihelion on its abort trajectory) for the range of abort dates and return trip times which were specified. These output data were plotted as contours of constant ΔV on a grid of return trip time versus date of abort for each of the four nominal mission trajectories, i.e., the 1982 opposition, the 1983 conjunction, the 1982 inbound swingby, and the 1986 outbound swingby missions. The dates which define the outbound trajectories were based on the trajectories for launching on the optimum date. A typical contour map is shown in Figure IV-1.

In the vicinity of 180° transfers a ridge of very high ΔV 's occurs since the inclination of the abort trajectory to both the Earth's orbit and the nominal interplanetary trajectory must be near 90° . Below the ridge is the region of high energy, short return time abort trajectories. Above the ridge is the region of low energy, long return time abort trajectories. Lines have been included on the contour maps to indicate the regions where the vehicle would not pass through perihelion on the abort trajectory. Also lines of constant perihelion distance equal to 0.5 A.U. and 0.75 A.U. have been included to give an indication of how near the vehicle must approach the sun when it does pass through perihelion.

1982 OPPOSITION CLASS MISSION

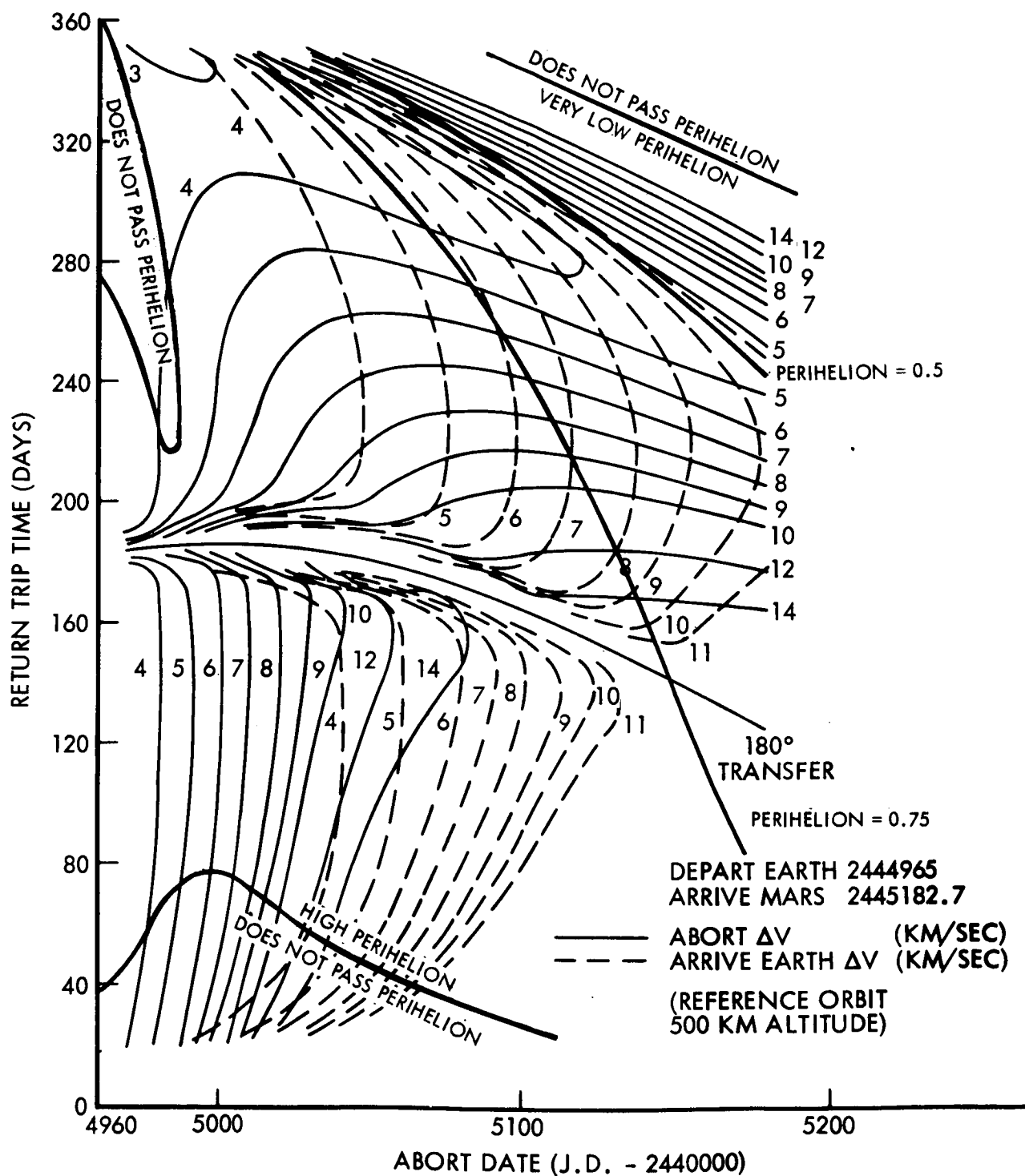


Figure IV-1. Typical Abort Velocity Contour Map

RESULTS AND DISCUSSION

The contour maps with their associated vehicle abort capability overlays for the four missions analyzed are given in Figures IV-2, IV-3, IV-4, and IV-5. (In order to permit a more perfect match of the overlay vellums with the contour maps, the reader is invited to remove the overlays from the binding and scotch tape them in exact position to the contour maps.)

When a number of choices of abort trajectory are open it is usual to inquire as to which would be the "optimum" abort trajectory to use. "Optimum" abort trajectory could mean the minimum time trajectory, the minimum fuel trajectory, the trajectory giving minimum arrival velocity at Earth, or the trajectory giving maximum perihelion distance. The greatest value of the contour maps is that all of these "optimum" abort trajectories along with all other possible trajectories are available on a single map. With the vehicle abort capability curves overlaid on the contour maps it is then immediately apparent when abort is possible and when it is impossible, which of the possible abort trips gives the quickest return to Earth, which will require the least amount of fuel, which will give the lowest arrival velocities at Earth, and which will give the greatest solar passage distance. In some instances, such as when a failure or malfunction is discovered late, it may be impossible or undesirable to follow one of these "optimum" trips. For such instances the map shows all trips that are still possible and a choice can be made.

Figure IV-2 illustrates the abort capabilities for the 1982 opposition class mission. Successful abort is possible during approximately the first half of the outbound leg for all assumed vehicle abort capabilities. (The regions of possible aborts lie to the left, within the areas that are partially enclosed by the individual capability curves.) The abort capability is extended over nearly the entire outbound trip for two of the cases which employ both the arrive Earth retro and aerodynamic braking capability for decelerating at Earth.

The abort curves for the conjunction class mission shown on Figure IV-3 indicate that at best an abort is possible only during the first third of the outbound trajectory for those cases in which both the arrive Earth propulsive retro and aerodynamic braking capability is employed for decelerating the vehicle at Earth. For those cases in which the arrive Earth propulsive retro is known to be inoperable

1982 OPPOSITION MISSION - TYPE IIB
NNNS(15) CONNECTING MODE

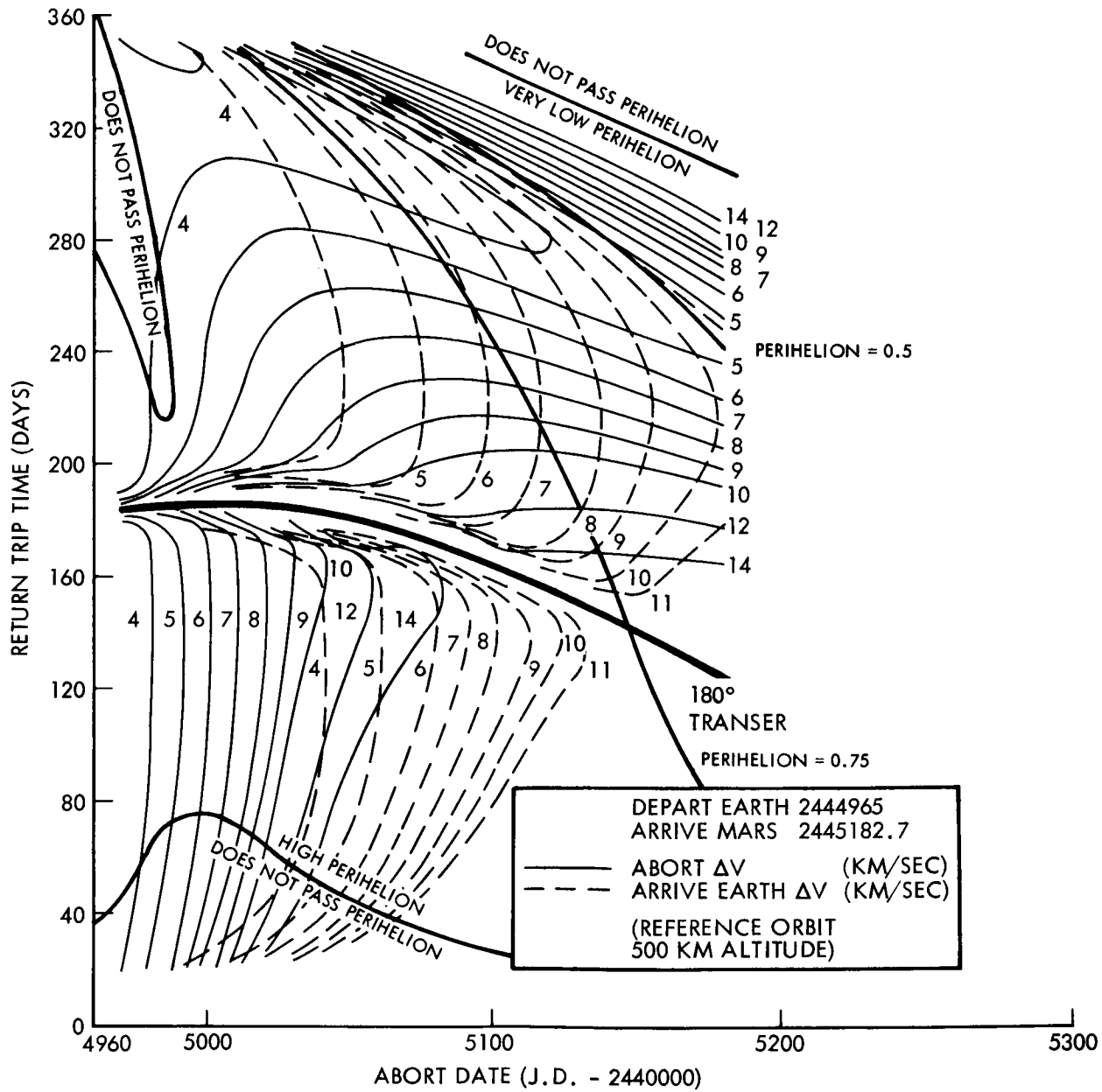


Figure IV-2b. 1982 Opposition Mission Abort Velocity Contour Map

1982 OPPOSITION MISSION - TYPE II B
NNNS(15) CONNECTING MODE

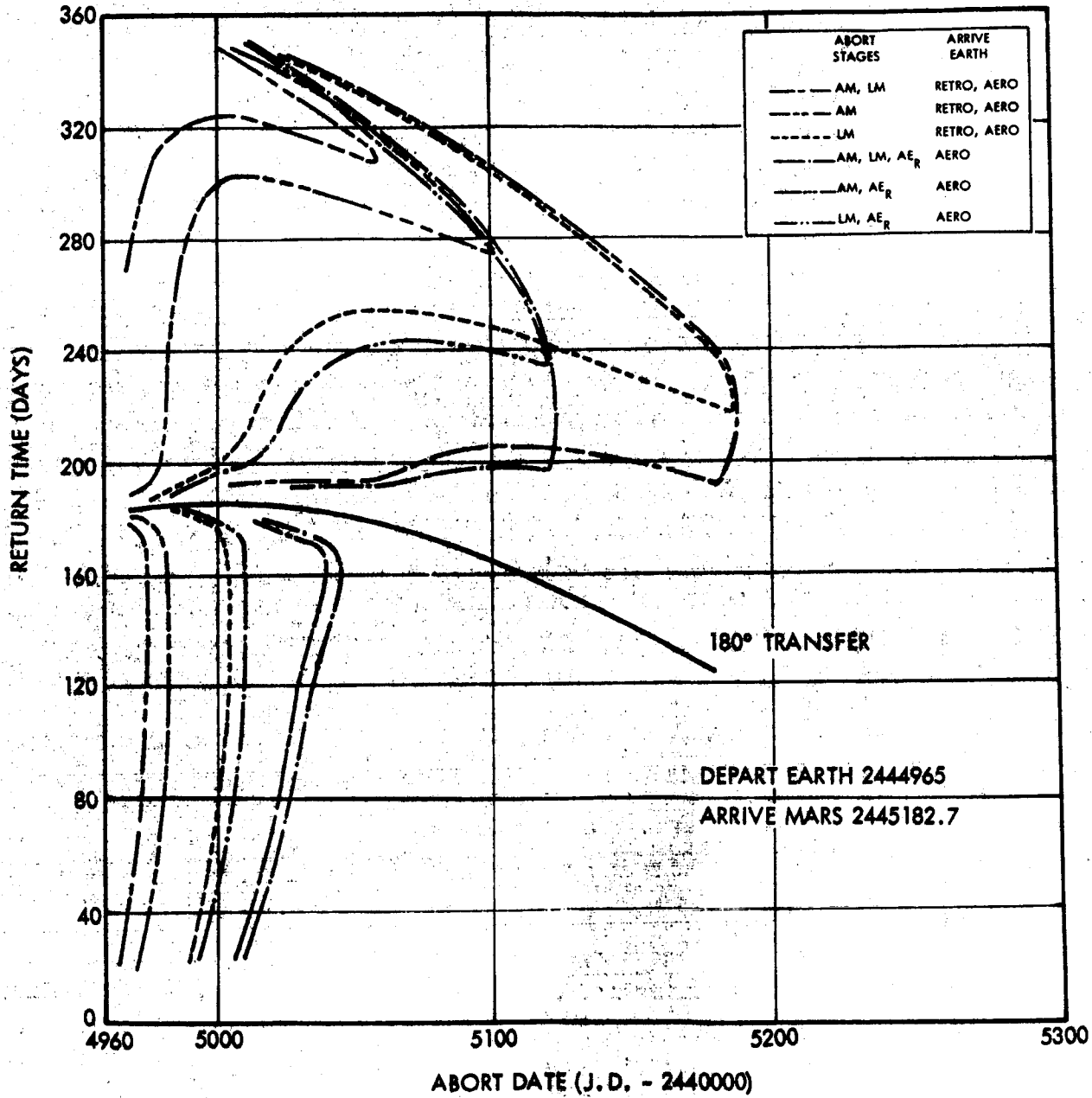


Figure IV-2a. 1982 Opposition Mission Vehicle Abort Capability

1983 CONJUNCTION MISSION - TYPE 1A
NNNS(P) CONNECTING MODE

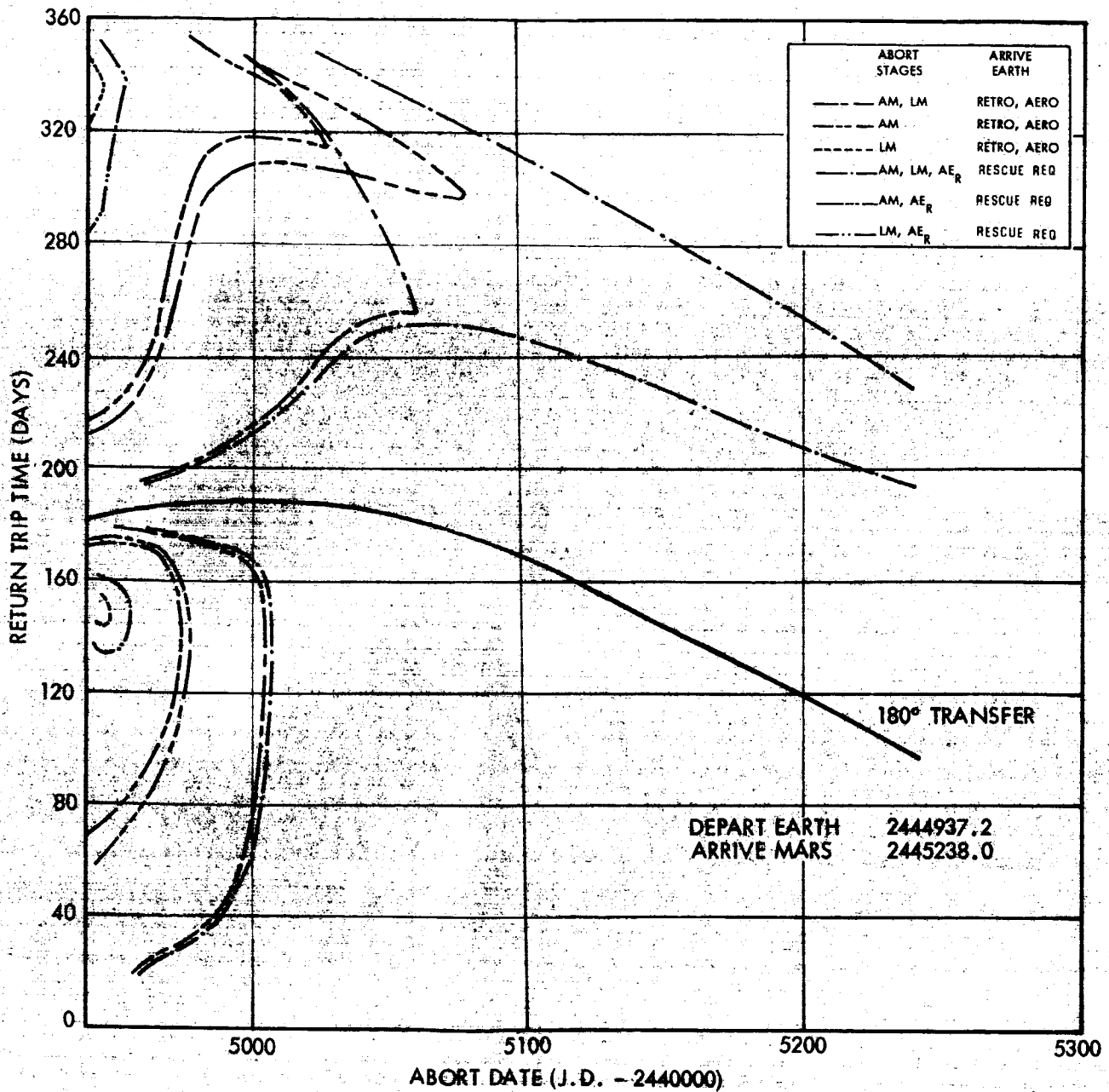


Figure IV-3a. 1983 Conjunction Mission Vehicle Abort Capability

1983 CONJUNCTION MISSION - TYPE IA
NNNS(P) CONNECTING MODE

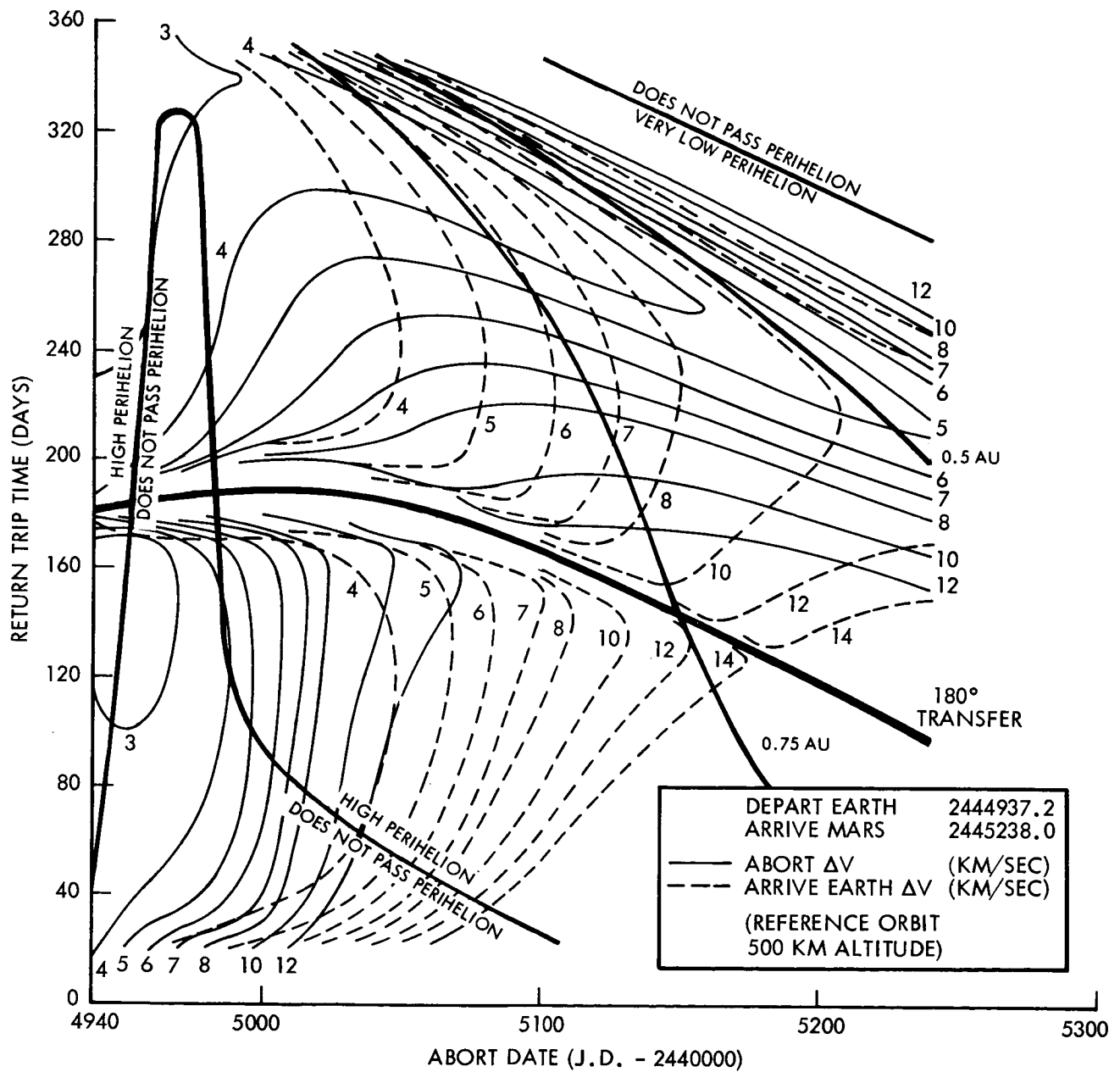


Figure IV-3b. 1983 Conjunction Mission Abort Velocity Contour Map

1982 INBOUND SWINGBY MISSION - TYPE I3
NNNS(P) CONNECTING MODE

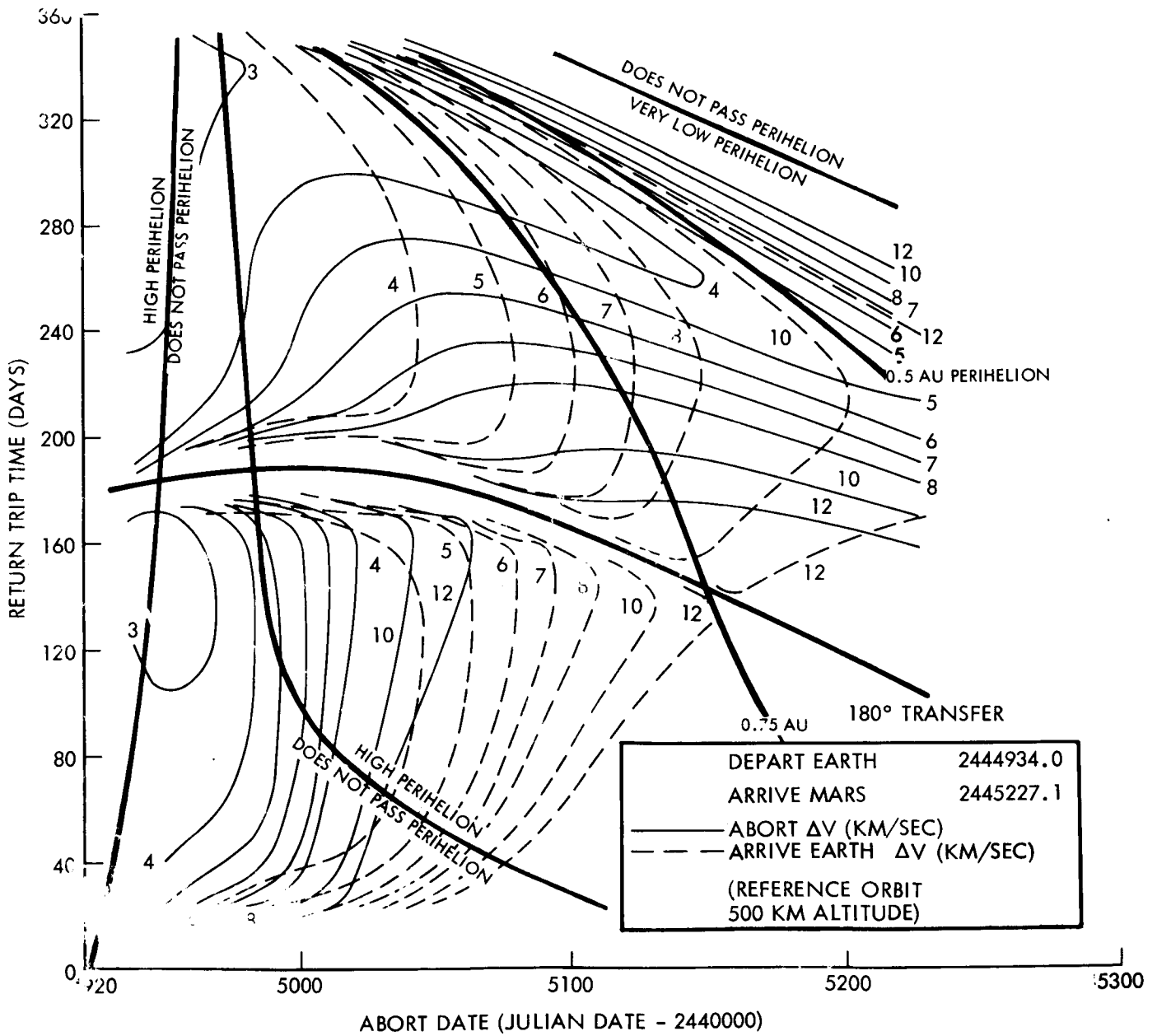


Figure IV-4b. 1982 Inbound Swingby Mission Abort Velocity Contour Map

1982 INBOUND SWINGBY MISSION - TYPE I3
NNNS(P) CONNECTING MODE

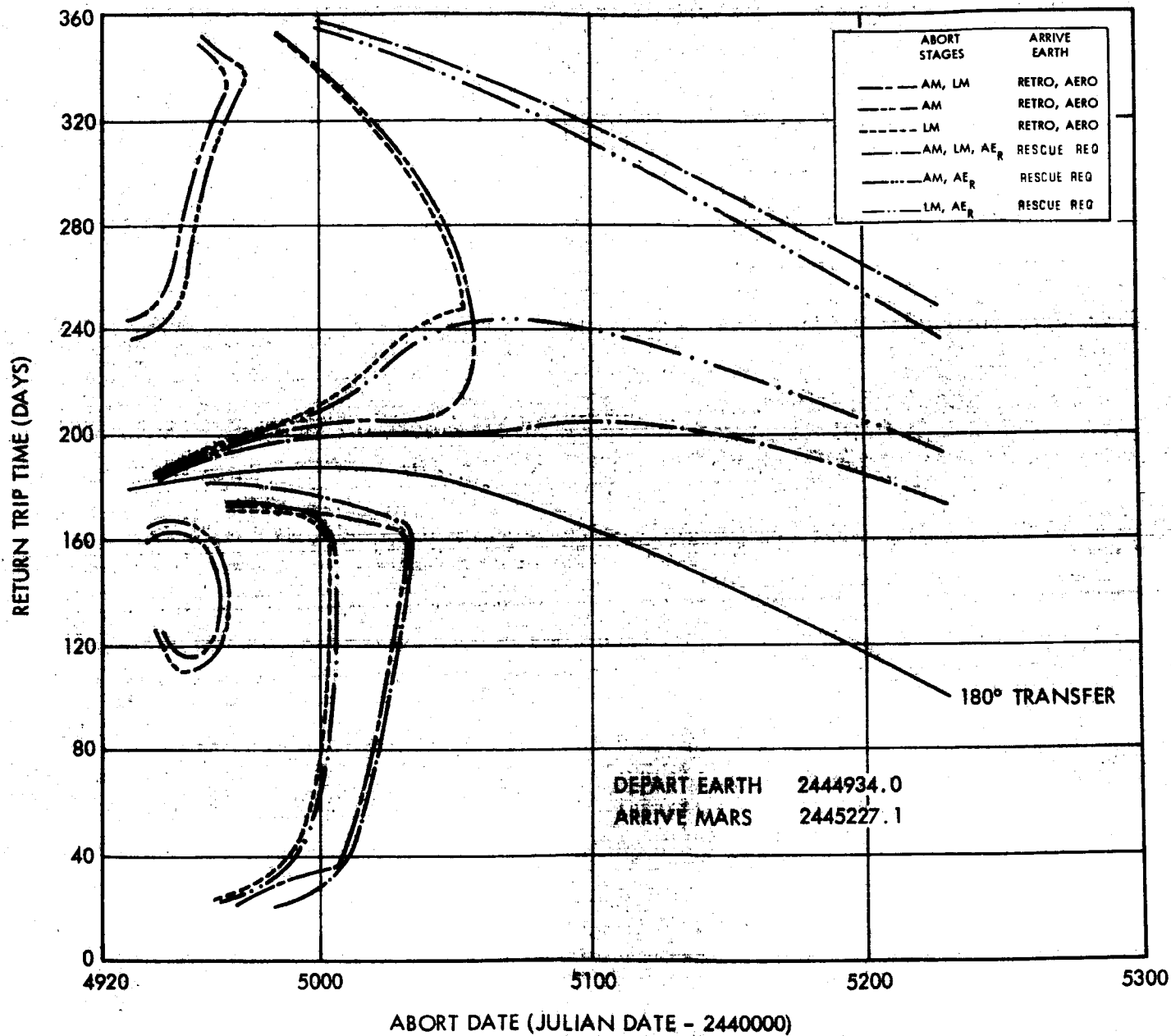
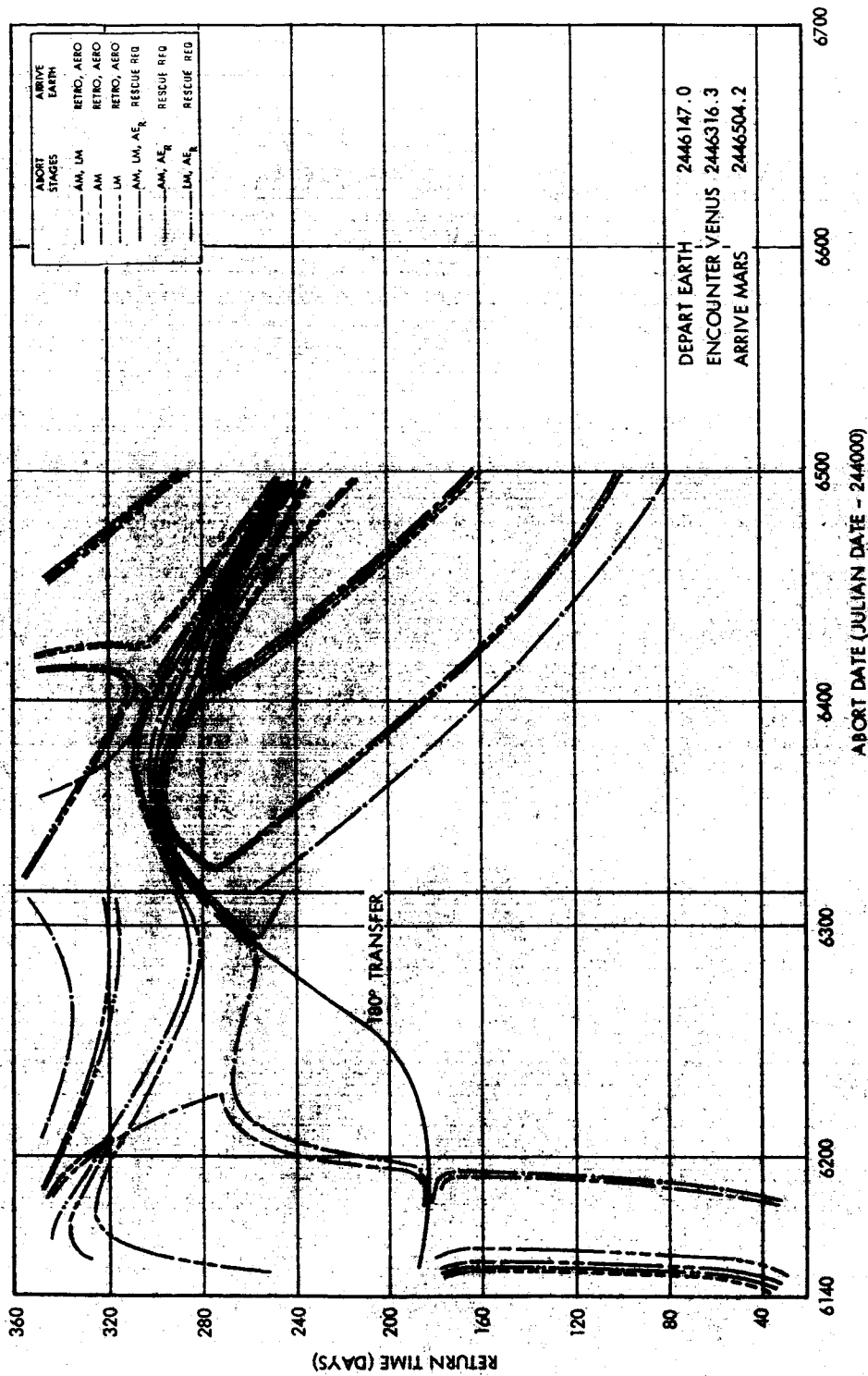


Figure IV-4a. 1982 Inbound Swingby Mission Vehicle Abort Capability

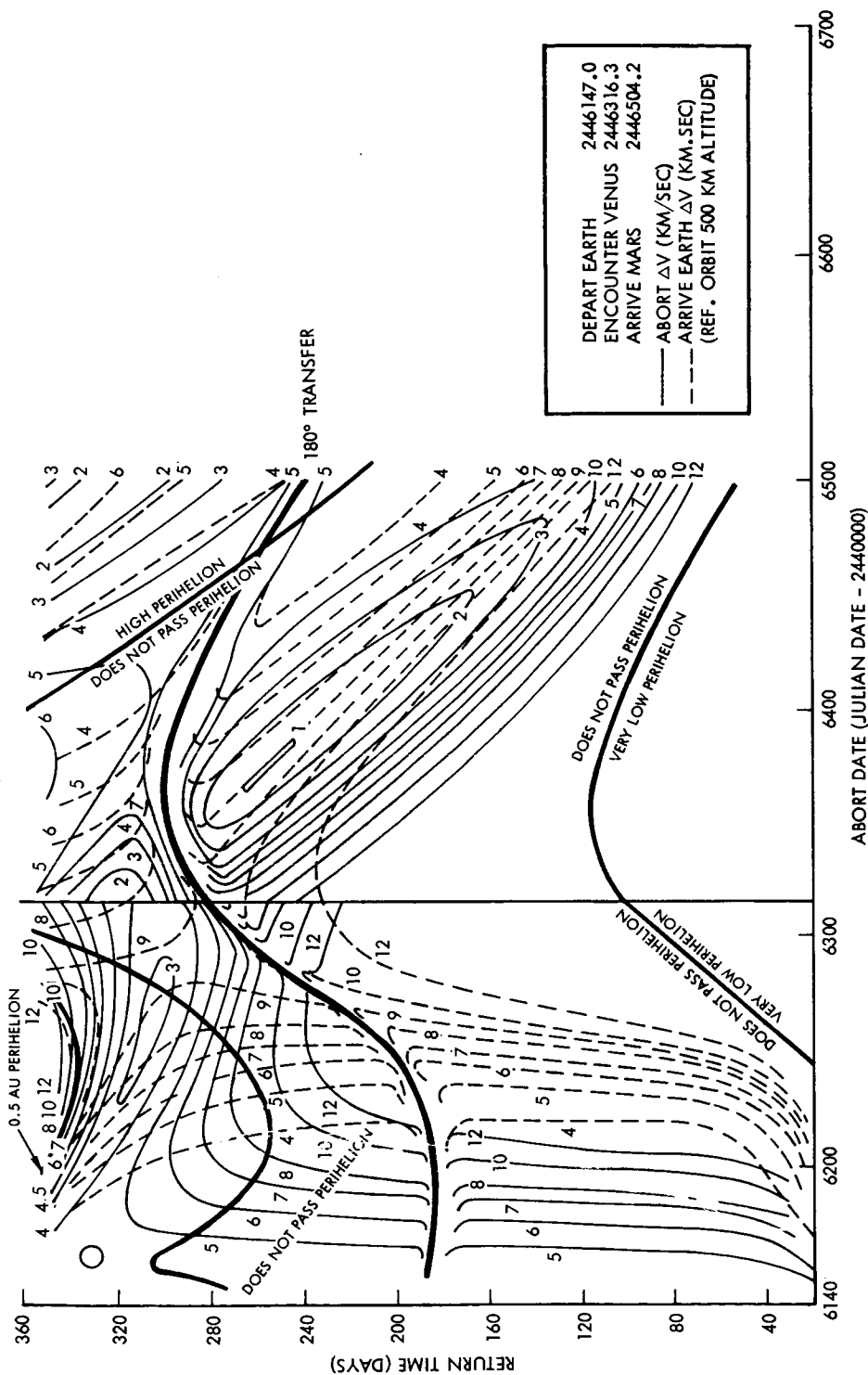
1986 OUTBOUND SWINGBY MISSION - TYPE 3A
NNNS(P) CONNECTING MODE



IV-11a

Figure IV-5a. 1986 Outbound Swingby Mission Vehicle Abort Capability

1986 OUTBOUND SWINGBY MISSION - TYPE 3A
NNNS(P) CONNECTING MODE



IV-11b

Figure IV-5b. 1986 Outbound Swingby Mission Abort Velocity Contour Map

or has been utilized for the abort ΔV , no successful abort is possible since the vehicle is left without the necessary means for performing its arrival maneuver at Earth. This condition exists because the vehicle will arrive at Earth at a relative speed greater than parabolic velocity. Since for this vehicle, it has been assumed that its aerodynamic braking capability extends only to parabolic entry velocity, a successful abort would require either a rescue mode by an Earth-based vehicle or a redundant propulsive retro. Therefore, although abort regions are shown on the graphs for three such cases, it must be noted that rescue at Earth or added propulsive or aerodynamic braking capability must be provided to the vehicle.

The results of the abort analysis for the inbound swingby are given in Figure IV-4. These results are essentially similar to those of the preceding conjunction class mission. That is, a successful abort at best can be accomplished only during the first third of the outbound leg if rescue at Earth or an increased arrive Earth braking capability is not available to the spacecraft.

The contour map of aborts from an outbound Venus swingby shown in Figure IV-5, is actually a composite of two contour maps. For J.D. 2446147 to J.D. 2446316.3 it is a contour map of aborts from the Earth-to-Venus transfer trajectory, and from J.D. 2446316.3 to J.D. 2446504.2 it is a map of aborts from the Venus-to-Mars transfer trajectory. The abort ΔV contours are discontinuous across the boundary between the two maps, but the Earth arrival ΔV contours are continuous. As for the previous figures, the regions of possible aborts, on each side of the ridge line (180° transfer line), lie within the area partially enclosed by the capability curves.

Without resorting to an Earth rescue mode or an increased arrive Earth braking capability, aborts for the outbound swingby as shown in Figure IV-5, are possible at best during approximately the first half of the Earth-Venus leg and during the last 75 percent of the Venus-Mars leg.

A vehicle Earth braking capability consisting of a retro maneuver to parabolic entry velocity followed by aerodynamic entry is a reasonable assumption for the conjunction class and swingby missions considering their nominal mission arrival velocities. However, as these abort analysis results indicate, the abort capability of the vehicle is severely limited if the retro stage is not available at Earth arrival. Furthermore, it becomes apparent that by increasing the aerobraking

capability for all of the missions analyzed, a greater abort flexibility is achieved and the regions in which aborts are possible are increased. The same effect is obtained if the arrive Earth retro stage is sized to be greater than that required for the nominal mission. It should be noted that the effects are additive if both the retro and aerodynamic braking capabilities are increased.

V. LAUNCH AZIMUTH CONSTRAINT ANALYSIS

TASK DESCRIPTION

An analysis was conducted to determine the effects on Mars stopover mission launches due to the constraints imposed on allowable launch azimuths by range safety restrictions and the physical limits on the departure declination achievable for launches from the ETR. The regions in which the interplanetary departure declinations exceed the allowable limits were superimposed on energy contour maps together with points representing the optimum trips for several types of missions, interplanetary trajectories, and vehicle configurations. Mission opportunities from 1975 to 1990 were investigated. Opposition class, conjunction class, and outbound and inbound swingby missions were considered.

For those missions and opportunities for which the optimum (minimum weight) trajectories require Earth departure declinations that exceed the allowable limits, weight penalties were determined for three methods of circumventing the launch azimuth limitations. These included the use of plane changes, the use of non-optimum trips which have permissible declinations, and the use of the optimum, opposite type of outbound trip, i.e., the type I in lieu of the type II.

ASSUMPTIONS AND CONSTRAINTS

Mission Matrix

The matrix of mission types and launch opportunities that were analyzed in this task is shown in Table V-1.

Vehicle Configuration and System Weights

The scaling laws and system weights used in this task for the propellant tanks and propulsion systems are those given in Section II for the connecting mode. In addition, the scaling laws and system weights used for defining the mission payloads, secondary spacecraft systems, and operational modes are those also given in Section II.

Table V-1. Launch Azimuth Constraint Mission Matrix

1975	Opposition	IB, IIB, IIB w/plane change, IIB nonopt.
1978	Opposition	IB, IIB, IIB w/plane change, IIB nonopt.
1980	Opposition	IIB
	Outbound Swingby	3A, 3B
1982	Opposition	IIB
	Inbound Swingby	I3, II3
1983	Conjunction	IA
1984	Opposition	IIB
	Inbound Swingby	I5, II5, II5 w/plane change, II5 nonopt.
1986	Opposition	IB, IIB, IIB w/plane change, IIB nonopt.
	Outbound Swingby	3A, 3B
1988	Opposition	IIB
1990	Opposition	IB, IIB, IIB w/plane change, IIB nonopt.

Vehicle Mode

The vehicle mode used for all missions analyzed in this task is the NNNA connecting mode configuration. The specific impulse of the nuclear propulsion system was 850 sec.

Launch Azimuth and Declination Constraints

Due to safety restrictions imposed on any given launch site, allowable firing sectors are set up and all vehicle launches must be restricted to pass over only these sectors. These sectors are primarily established from the ground rule that during suborbital flight the vehicle must not pass over any inhabited land mass.

For any launch site, the allowable firing sector sets the launch azimuth limits which in turn sets the maximum achievable parking orbit inclination.*

*The functional relationship between inclination and launch azimuth is $\cos(\text{inclination}) = \cos(\text{launch site latitude}) \times \sin(\text{launch azimuth})$. This relationship is precisely true only for a non-rotating Earth. However, the error for a rotating Earth is negligible for the purposes of this study.

In order to achieve the declination of any departure hyperbolic asymptote for launches out of a parking orbit without resorting to plane change maneuvers, the inclination of the parking orbit must be equal to or greater than the declination of the departure hyperbolic asymptote.* Therefore, for the launch azimuth limits set by the ETR allowable firing sector there will be some maximum achievable parking orbit inclination (or declination of the departure hyperbolic excess velocity). The nominal allowable firing sector for ETR is restricted to a region of the Atlantic bounded by the Caribbean Islands and North America as shown in Figure V-1. The approximate launch azimuth range associated with this sector is 44° to 114° . However, for most recent launches, it has been required that the vehicle not pass over Europe during the launch or first orbit. This restriction reduces the launch azimuth range to approximately 72° to 114° .

Together with the latitude of ETR (approximately 28.4°), the azimuth range defines the range of ascent trajectory and parking orbit inclinations that are achievable. The departure declinations which can be achieved from a given parking orbit without plane change maneuvers range from zero up to the maximum achievable orbit inclination. Figure V-2 illustrates the limiting declination as a function of launch azimuth for ETR. The azimuth limits based on the allowable firing sectors are also shown. From these constraint envelopes, the maximum achievable declination can be determined. For the nominal azimuth constraints, the maximum achievable declination is 52.4° (at 44° launch azimuth). For the reduced azimuth range which misses Europe, the maximum achievable declination is 36.6° (at 114° launch azimuth).

ANALYSIS APPROACH

For each of the optimum (minimum weight) interplanetary missions considered in this task it was necessary to determine if the necessary departure declination could be achieved with nominal launches out of ETR. For those missions requiring a departure declination greater than the maximum achievable, several methods were investigated for circumventing the declination restrictions.

For all of the launch opportunities considered, Earth to Mars and Earth to Venus trajectory data were used to construct basic contour maps showing the contours of hyperbolic excess speed leaving Earth and arriving at Mars or Venus.

*This conclusion is true for direct ascent Earth departures as well as parking orbits.

DASH LINES SHOW TYPICAL GROUND TRACKS FOR EASTWARD LAUNCH FROM ETR

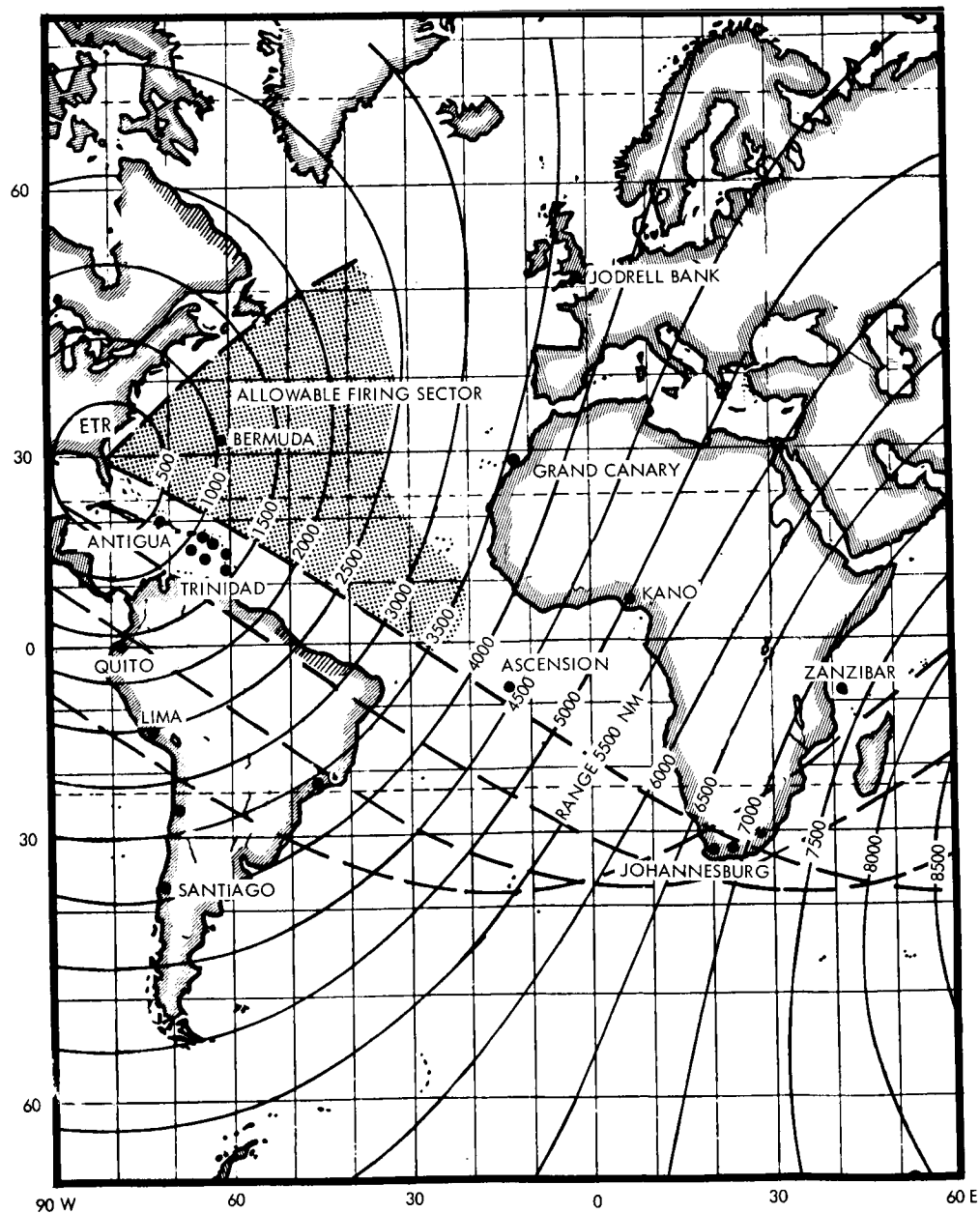


Figure V-1. Allowable Firing Sector for ETR

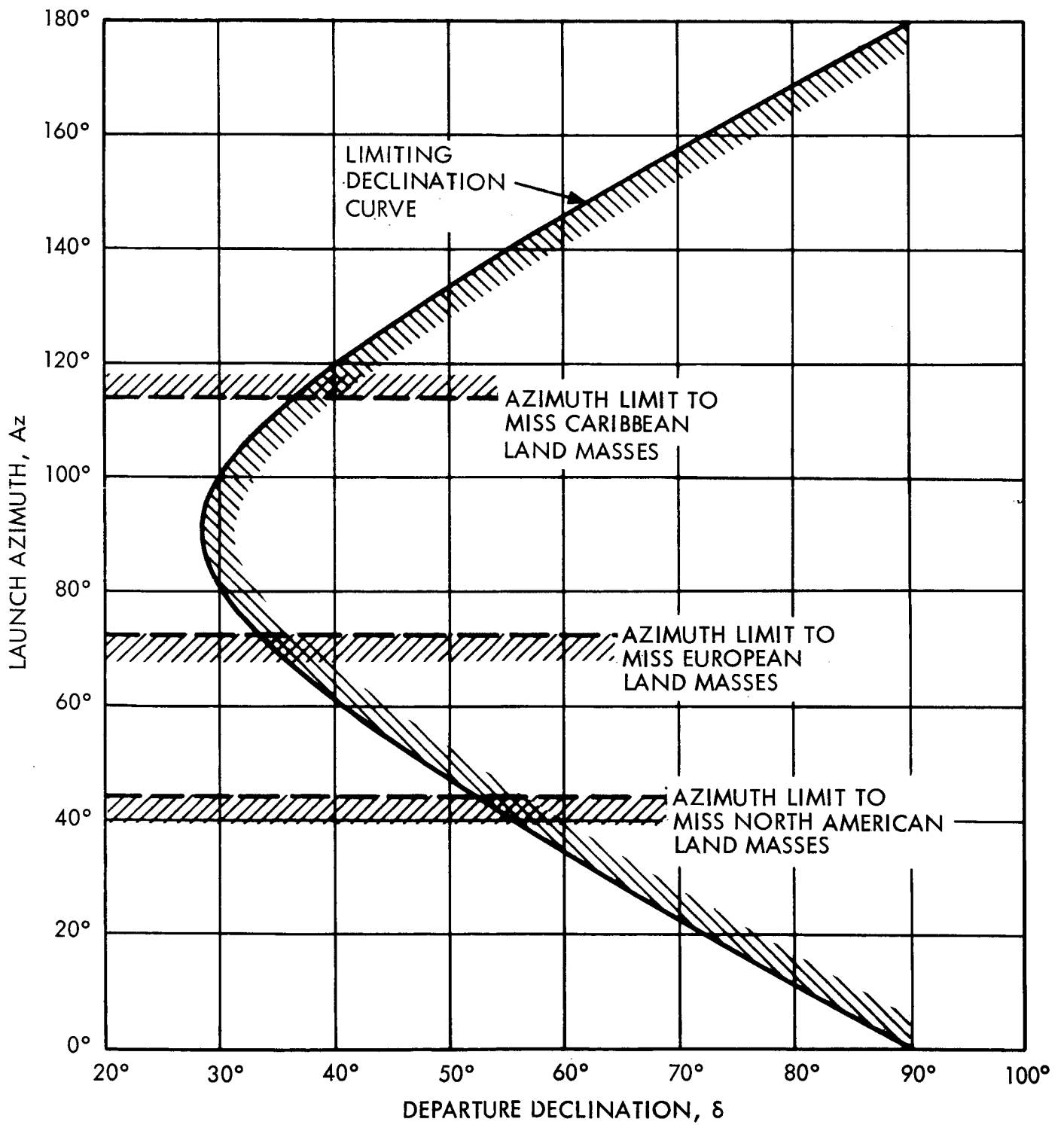


Figure V-2. Launch Azimuth and Declination Limits for ETR

The regions where the Earth departure declinations exceed the limits of 36.6° and 52.4° were superimposed on the contour maps. Points were plotted on these maps representing all of the optimum missions. From these graphs it was easily ascertained which missions require Earth departure declinations that exceed the achievable limits.

Next, three alternative modes of carrying out the mission were evaluated for those missions exceeding the declination limits. This evaluation was made by determining the weight penalty associated with each of the three mission alternatives. The three alternative modes were:

- o Make a plane change during the parking orbit escape maneuver to reach the necessary declination for the "optimum" trip.
- o Use a non-optimum outbound trip for which the departure declination does not exceed the achievable limit.
- o Use the opposite type outbound trajectory (which in all cases required declinations less than the achievable limit).

Two additional alternative modes could also be employed. These are:

- o Make a plane change maneuver during the ascent to the parking orbit to achieve the required higher orbit inclination.
- o Use two maneuvers during Earth departure (either restarting the engine or staging the propulsion system) using the second maneuver for a plane change when the vehicle is far from Earth.

Although these two additional alternative modes were not investigated in this analysis task since they were outside the scope of the study, they are worthy of note for consideration in future launch azimuth constraint analyses.

It is important to point out that this analysis should be considered preliminary in nature because of several factors. First, an approximate definition was used to determine the allowable ETR firing sector, viz, that during suborbital flight the vehicle must not pass over any inhabited land mass. Actually, the locus of predicted instantaneous impact points of any jettisoned stage or of the vehicle in case of failure, including consideration of possible wind effects and all tolerances affecting the flight path, must not cross an inhabited land mass. A range safety analysis

based on this definition of the allowable firing sectors is vehicle dependent and would require a detailed launch trajectory analysis.

Second, it is important to note that the effects of providing an Earth launch window, which would require higher inclinations for the parking orbit than those for just the optimum mission, were not considered. Finally, variation of the Saturn launch vehicle payload capability with variations in launch azimuth was not included; the actual launch vehicle payload capability is a strong function of the launch azimuths. However, it is felt that the qualitative conclusions obtained in this analysis task would still be applicable even if the above factors were considered in a more rigorous analysis.

RESULTS AND DISCUSSIONS

The results of the launch azimuth constraint analysis, i.e., the energy contour plots with superimposed regions of Earth departure declinations exceeding 36.6° and 52.4° , are given in Figures V-3 to V-12 together with the points that represent the trips leaving Earth for the various mission types. Table VI-2 contains the detailed trajectory data for these missions including the weight penalties associated with the three alternative modes used for circumventing the declination limits for those optimum missions that exceed the limits.

It is apparent from Figures V-3 to V-12 that if the nominal azimuth range of 44° to 114° is allowed for the manned Mars missions from 1975 to 1990, no declination constraint problems will be encountered. However, if range safety restrictions require using the launch azimuth range of 72° to 114° , then five of the optimum missions analyzed will require adjustments to compensate for the declination constraints. The results obtained by using the alternative launching modes for these five missions are shown on Table V-2.

Of the three alternative modes considered, the use of a nonoptimum outbound trajectory, in general, required the lowest vehicle weight increase to compensate for the declination constraints. The opposite type outbound trajectories, i.e., a type I in lieu of a type II, gave the next lowest weight increase for all except those missions only slightly out of the declination limits. The plane change maneuver during departure generally required greater weight increases than the other two methods of compensating for the declination constraints.

Table V-2. Effects of Earth Departure Declination Limits

Alternative Modes for Missions Exceeding Declination Limit of 36.6° (4)

Planet	Mission Class	Year and Type	Earth Departure Date (J.D. - 2440000)	Mars Arrival Date (J.D. - 2440000)	Venus Arrival Date (J.D. - 2440000)	Earth Departure Declination (Degrees)	Initial Weight for Optimum Mission (10 ⁶ lbs.)	Opposite Type Trajectory			Plane Change Out of Parking Orbit			Non optimum Outbound Trajectory		
								Vehicle Weight for Opposite Type Trajectory (10 ⁶ lbs.)	Weight Penalty for Opposite Type Trajectory (1)	ΔV for Plane Change if out of Azimuth Range (km/sec) (2)	Vehicle Weight with Plane Change to Achieve Declination (10 ⁶ lbs.)	Weight Penalty Due to Plane Change (1)	Earth Departure Date for Non optimum Trajectory (3)	Vehicle Weight for Non optimum Trajectory (10 ⁶ lbs.)	Weight Penalty Due to Non optimum Trajectory (2)	
Mars	Opposition	1975 11B 1B	2667.6 2594.8	2864.1 2857.1		45.7	2.558	2.688	5.1	0.524	2.854	11.6	2684.0	2.655	3.8	
Mars	Opposition	1978 11B 1B	3433.9 3375.1	3648.4 3655.2		48.0	2.725	2.923	7.3	0.791	3.271	20.0	3454.8	2.926	7.4	
Mars	Opposition	1980 11B	4192.5	4425.8		33.4										
Mars	Opposition	1982 11B	4963.7	5180.6		-6.5										
Mars	Opposition	1984 11B	5747.9	5943.5		-35.0										
Mars	Opposition	1986 11B 1B	6540.5 6454.8	6719.5 6706.0		-51.2	1.724	2.064	19.7	1.484	2.408	39.7	6571.0	1.979	14.8	
Mars	Opposition	1988 11B	7337.3	7516.7		8.1										
Mars	Opposition	1990 11B 1B	8128.5 8050.0	8317.9 8299.2		40.7	2.532	2.697	6.5	0.126	2.598	2.6	8136.4	2.554	0.9	
Mars	Conjunction	1983 1A	4937.5	5239.3		27.3										
Mars	Out. Sw.	1980 3A 3B	3838.3 3840.4		3998.4 4000.8	2.3 3.6										
Mars	In. Sw.	1982 13 113	4933.7 4981.1	5226.5 5221.3		26.4 -7.5										
Mars	In. Sw.	1984 115 15	5735.0 5656.7	5916.9 5912.2		-37.2 0.2	2.283	2.344	2.4	.005	2.289	0.07	5735.8	2.290	0.09	
Mars	Out. Sw.	1986 3A 3B	6148.2 6146.5		6317.2 6317.4	20.1 20.1										
Venus		1980 11B	4343.0		4452.3	-9.7										

- Notes: (1) Weight penalty based on increase in weight for type I trajectory over optimum type II trajectory.
(2) ΔV penalty for doing a plane change during the single burn escape maneuver; two possible azimuth ranges were considered: 72° to 114° giving a maximum achievable declination of 36.6° (at azimuth = 114°); 44° to 114° giving a maximum achievable declination of 52.4° (at azimuth = 44°); the declination does not exceed 52.4° for any of these missions.
(3) Mars arrival date is held fixed and the nearest depart Earth date outside the declination limits is found.
(4) Vehicle configuration for all missions: MNNA, 850 sec, connecting mode.

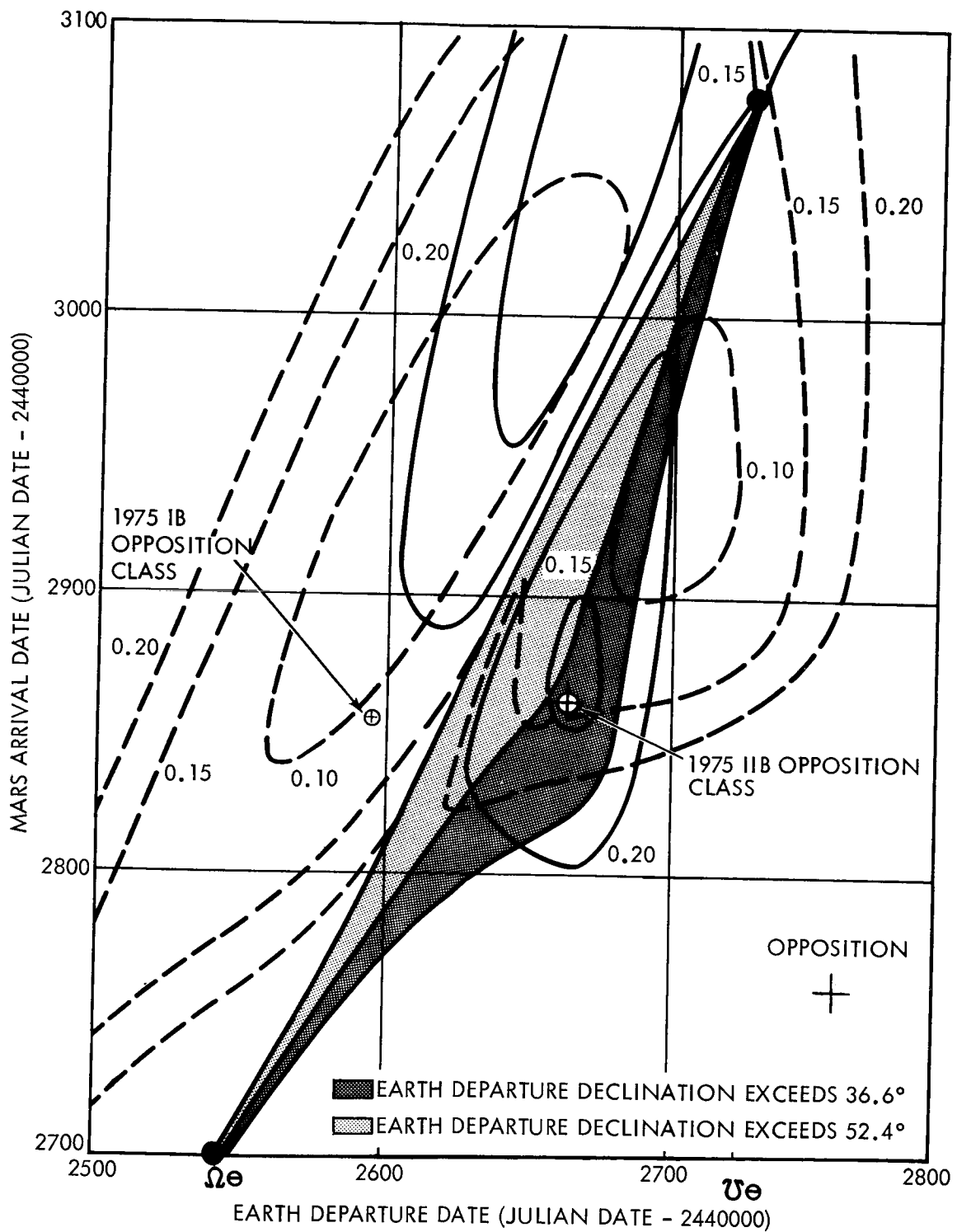


Figure V-3. 1975 Earth Departure Declination Limits

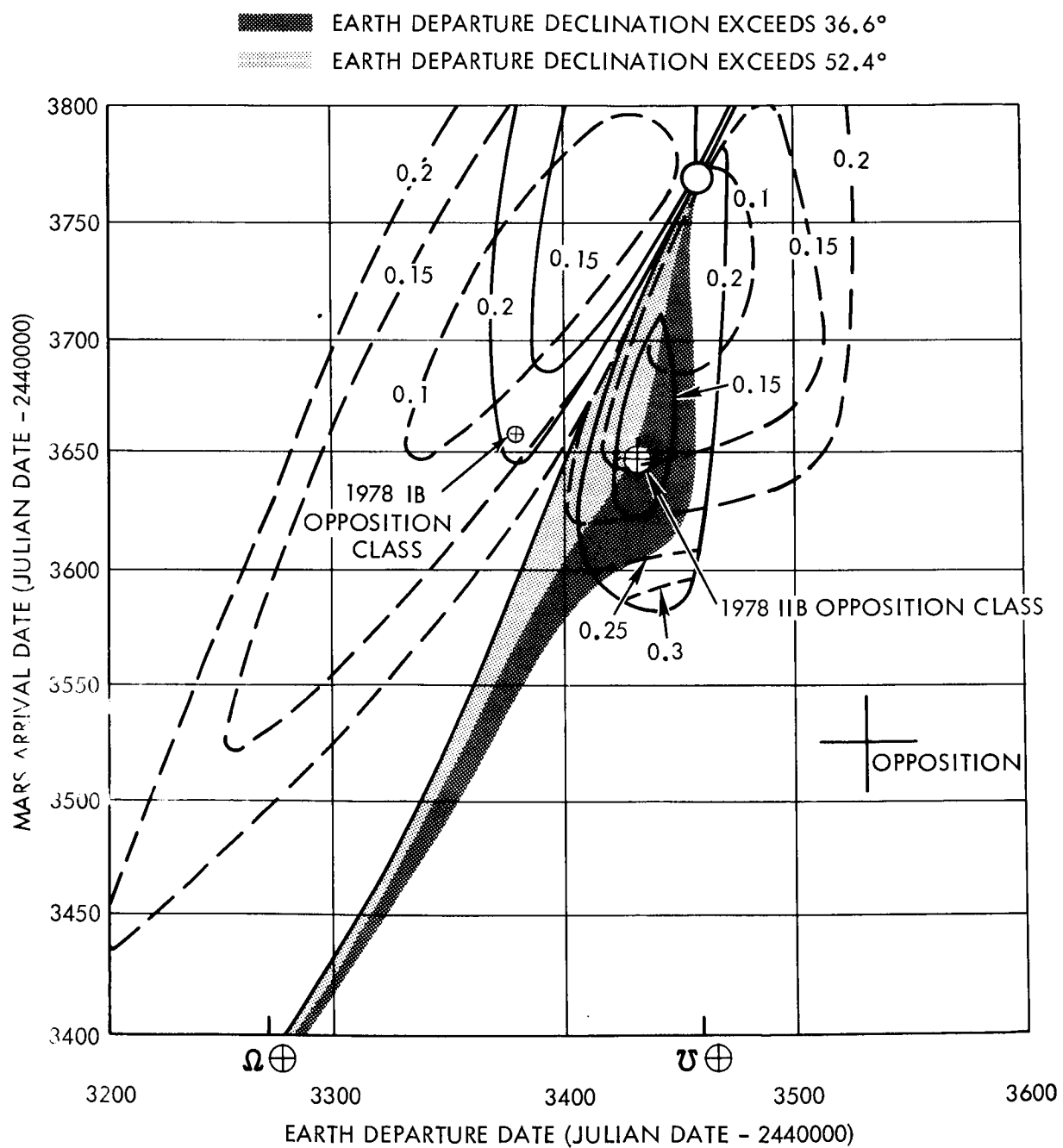


Figure V-4. 1978 Earth Departure Declination Limits

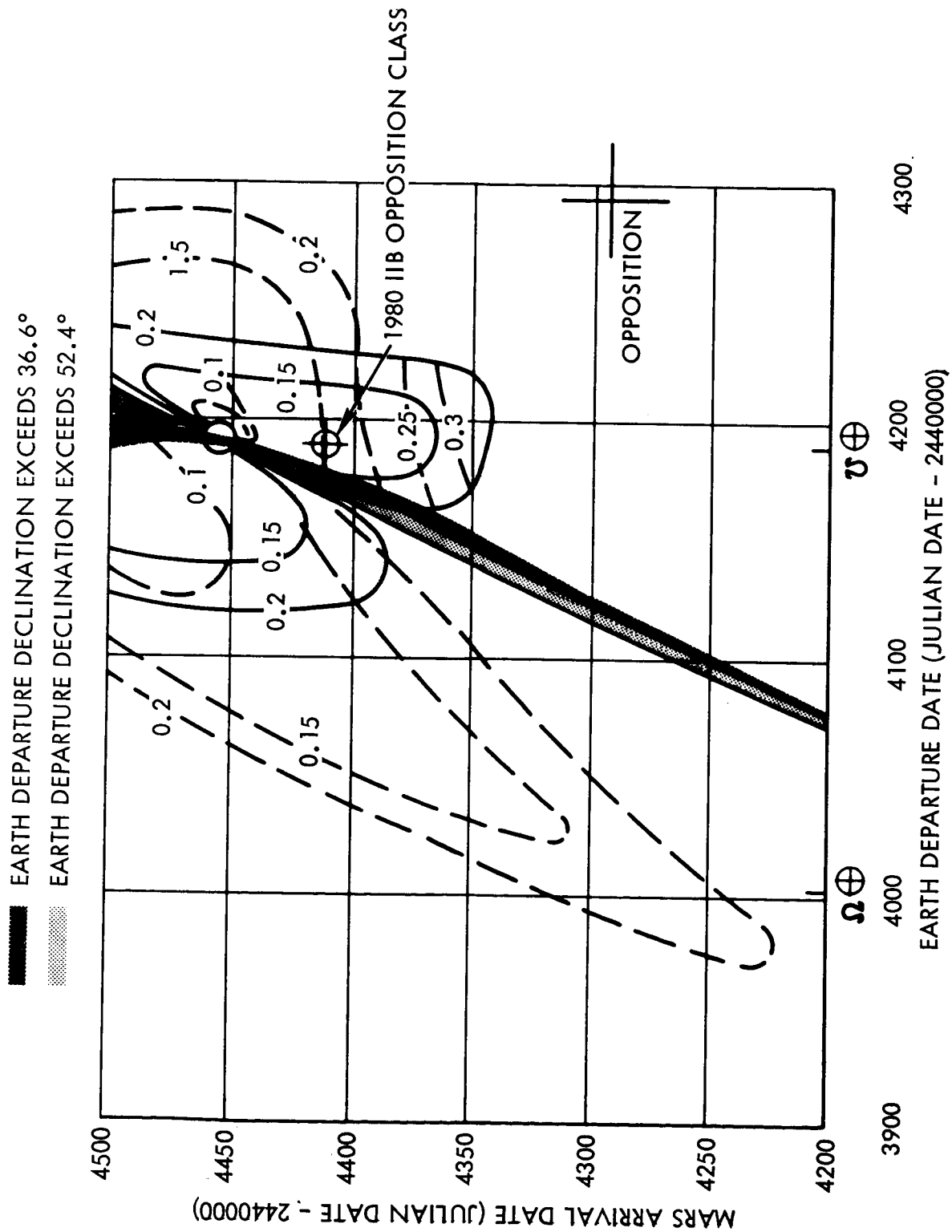


Figure V-5. 1980 Earth Departure Declination Limits

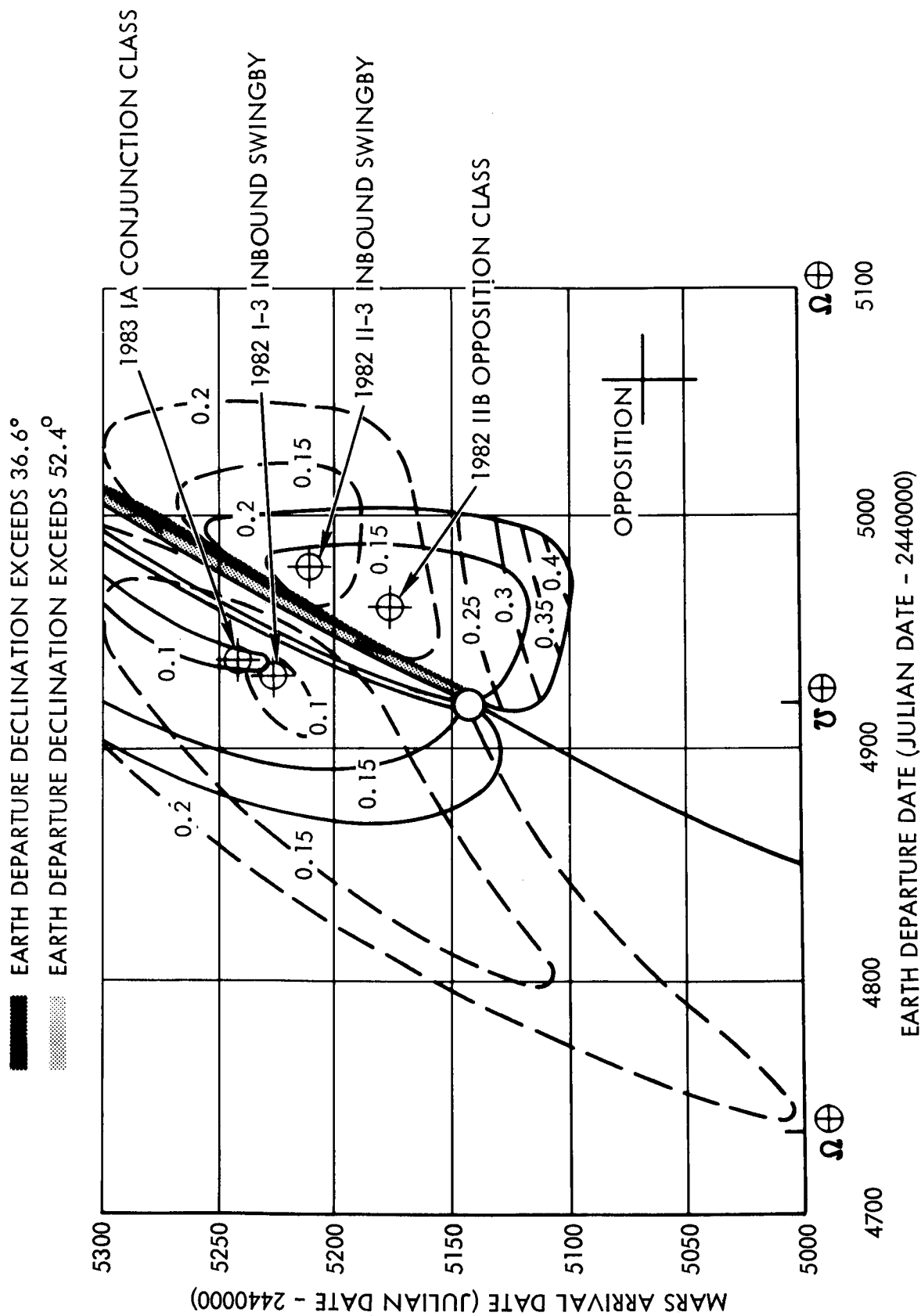


Figure V-6. 1982 Earth Departure Declination Limits

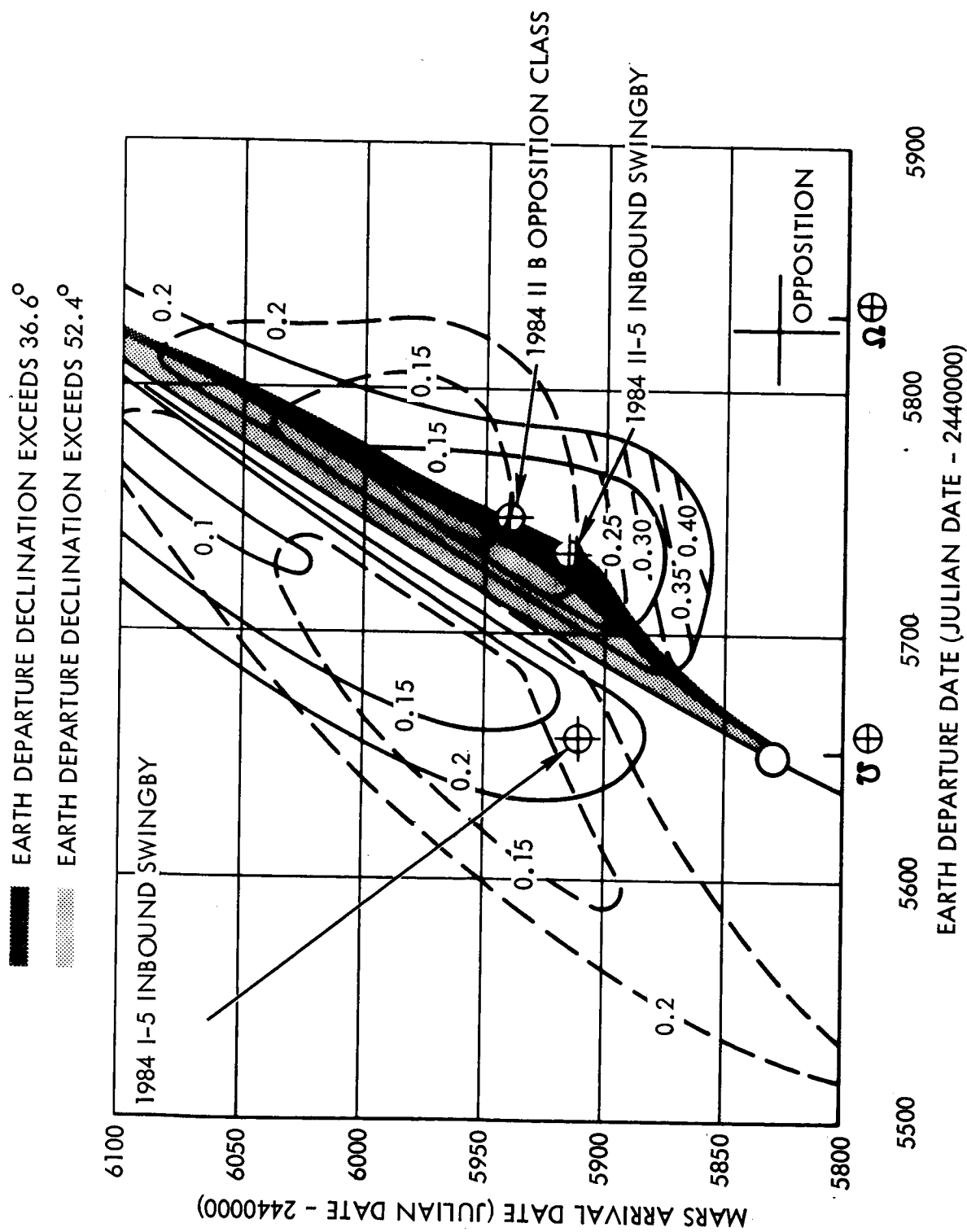


Figure V-7. 1984 Earth Departure Declination Limits

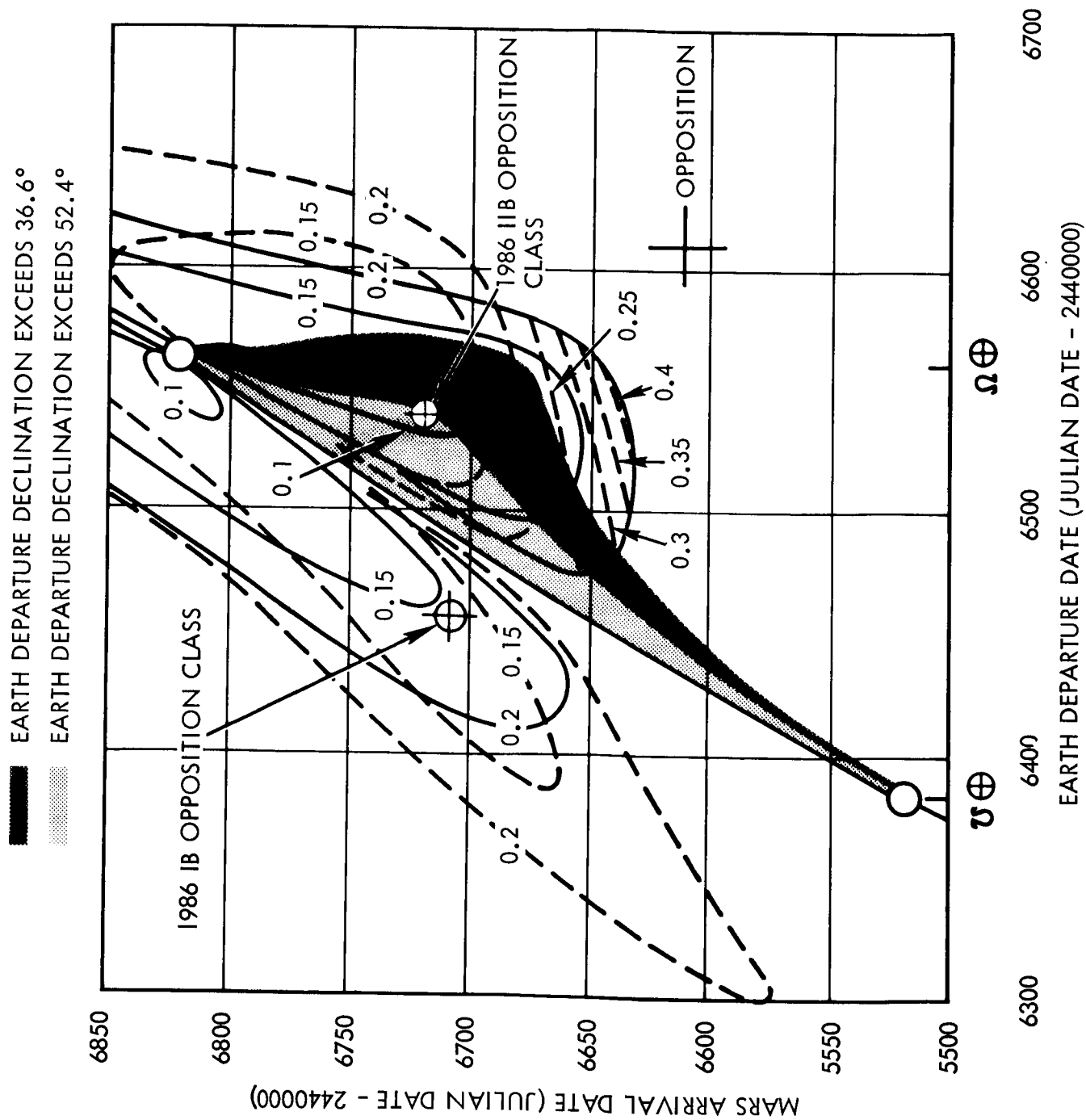


Figure V-8. 1986 Earth Departure Declination Limits

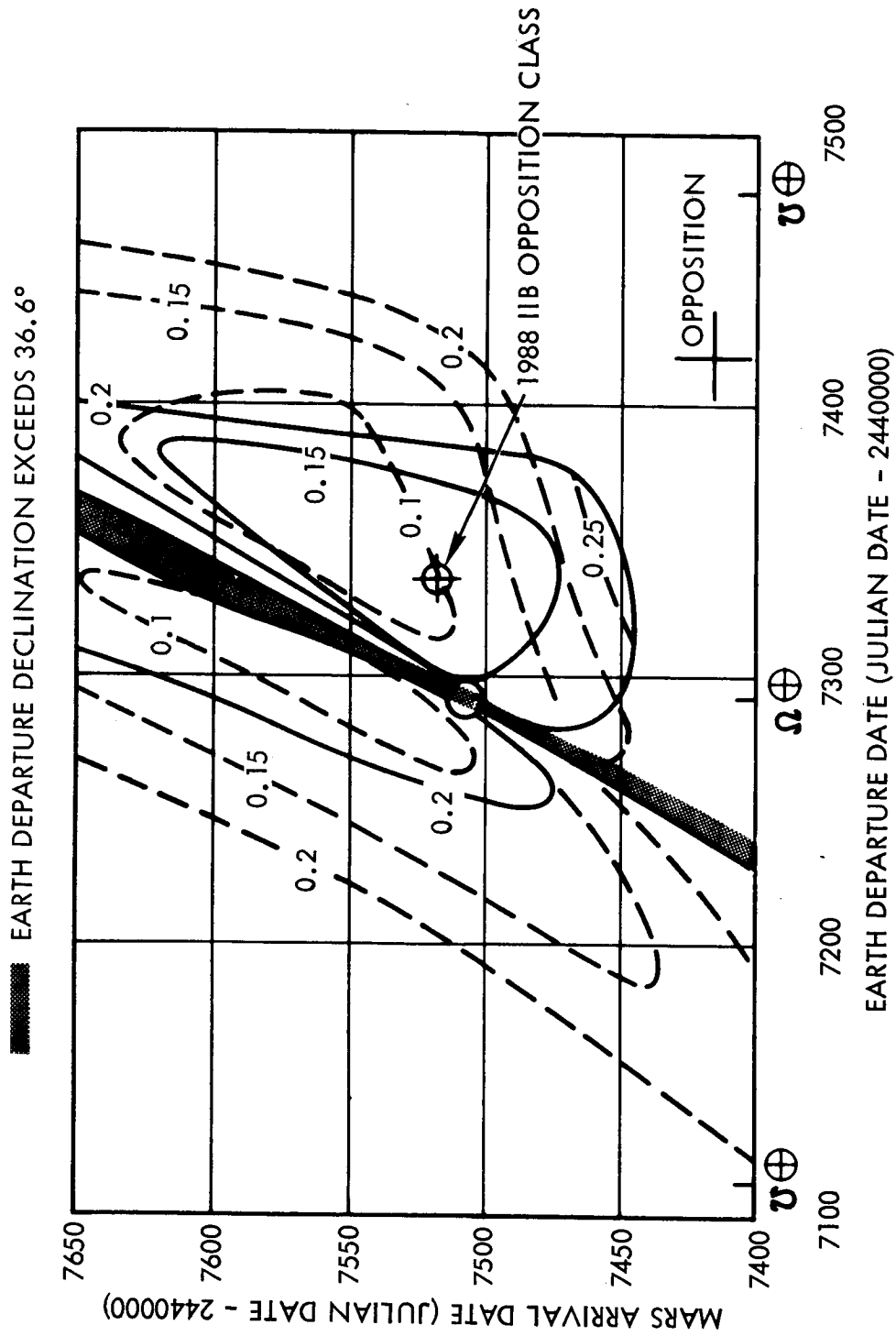


Figure V-9. 1988 Earth Departure Declination Limits

- EARTH DEPARTURE DECLINATION EXCEEDS 36.6°
- EARTH DEPARTURE DECLINATION EXCEEDS 52.4°

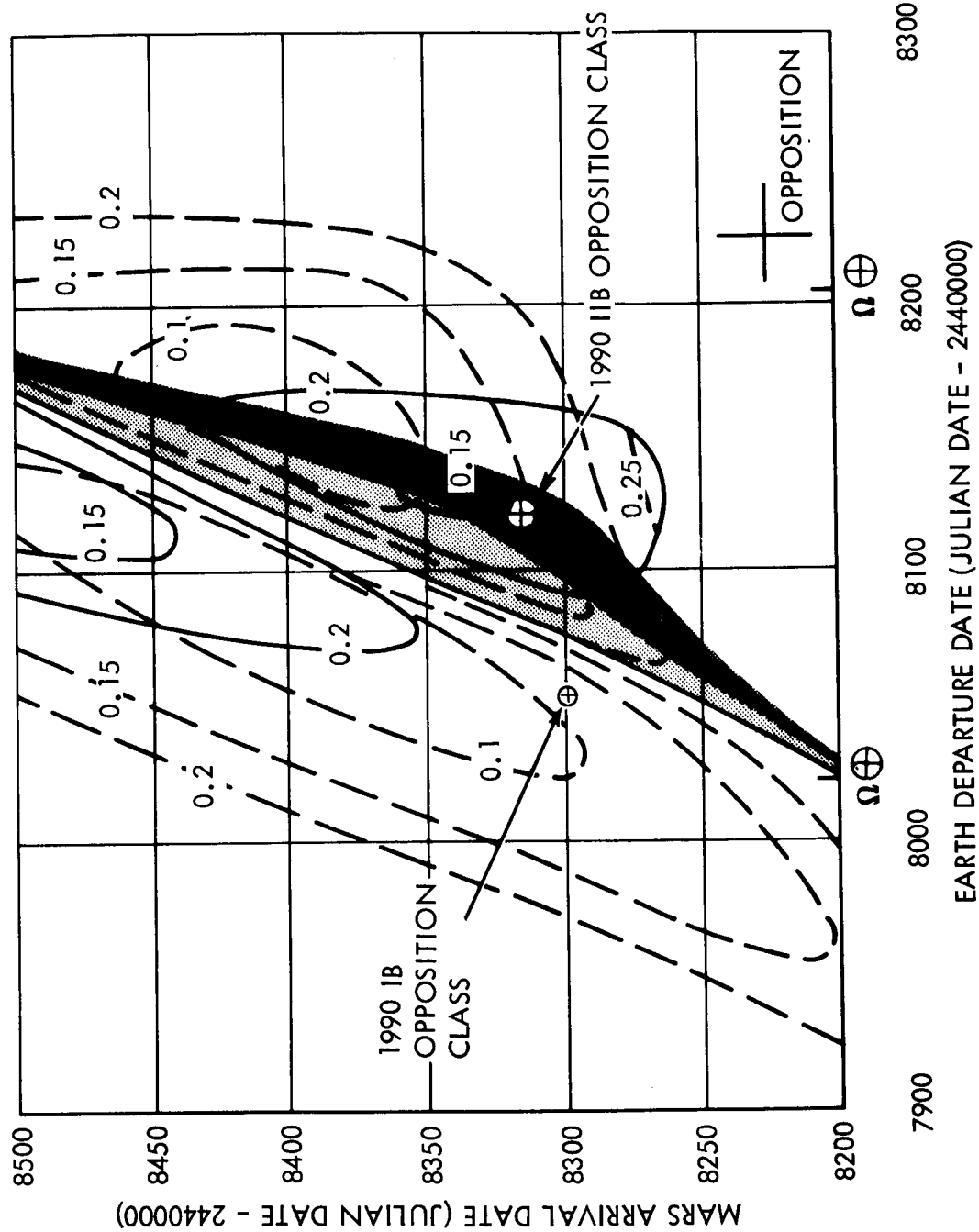


Figure V-10. 1990 Earth Departure Declination Limits

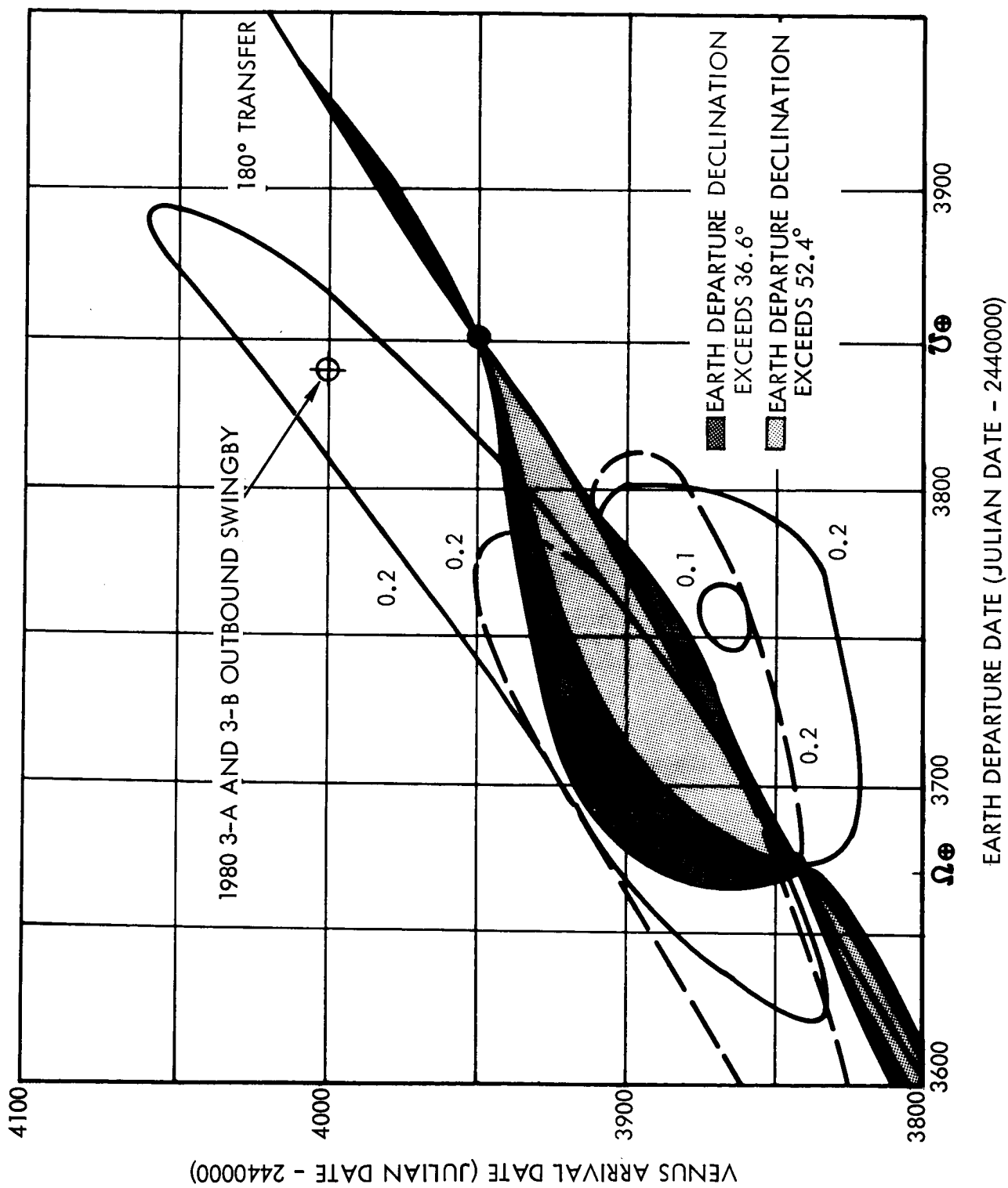


Figure V-11. 1980 Earth Departure Declination Limits

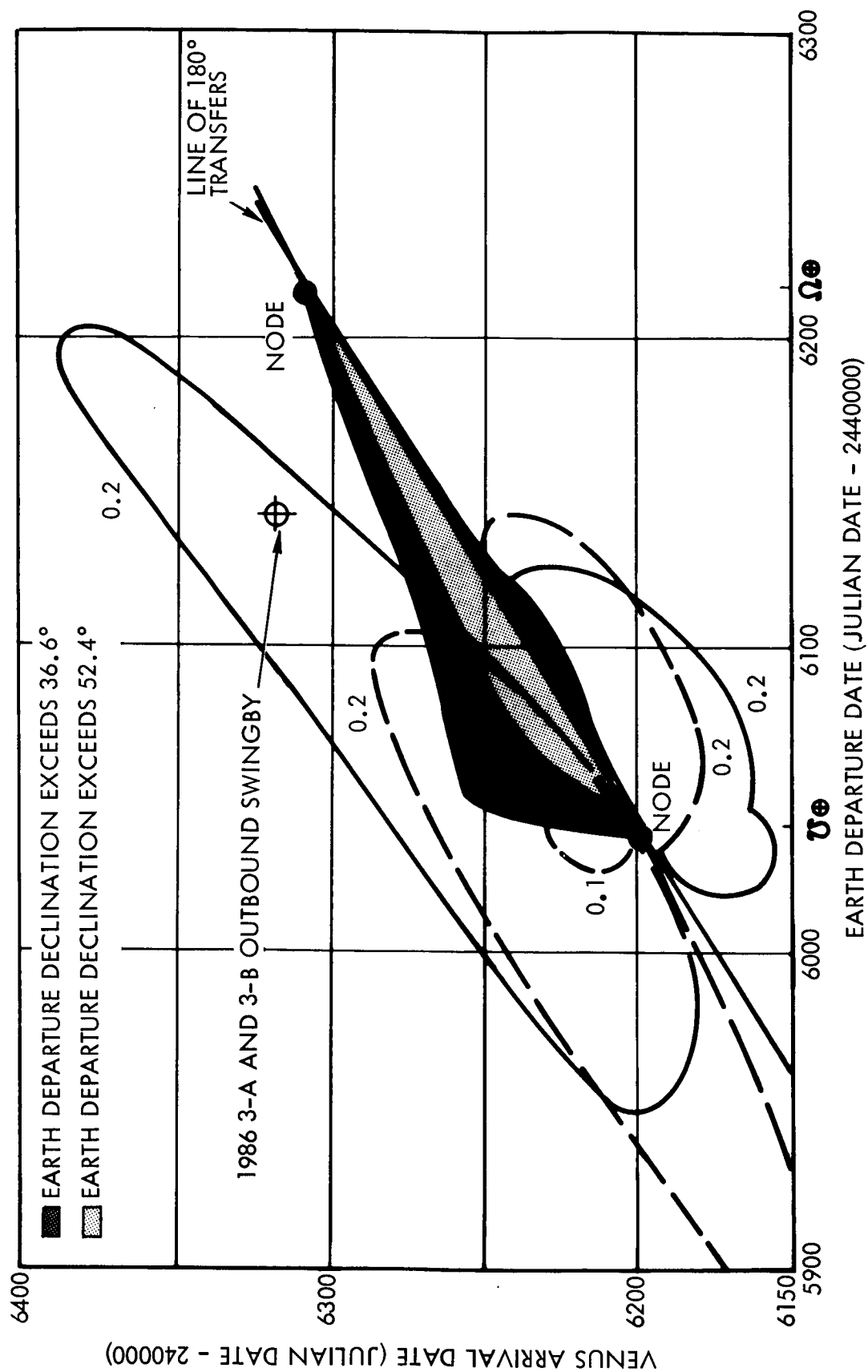


Figure V-12. 1986 Earth Departure Declination Limits

The mission most affected by the declination constraints is the 1986 opposition class mission, Figure V-8. The optimum IIB mission requires a very low vehicle weight, but the departure declination associated with the optimum trip is -51.2° . The weight penalties to compensate for the declination constraint if the nonoptimum or the opposite type outbound trajectories are used are 14.8 percent and 19.7 percent, respectively. However, even with these severe penalties, the 1986 opposition class mission requires lower vehicle weight than most of the other missions.

The other four optimum missions that exceeded the declination limits, viz, the 1975, 1978, and 1990 opposition class and the 1984 swingby missions, incur weight penalties that are less than four percent when the nonoptimum outbound trip is employed.

As was pointed out previously, this analysis did not consider any launch window effects for departing Earth. It is likely that the nonoptimum trips used to avoid the region of declination constraints would be undesirable when launch window requirements are taken into account. The launch window effects would place a constraint on the start of the launch window as well requiring the nominal date or center of the window to shift to a later depart date. It appears likely that if declination constraints and launch window requirements were considered simultaneously, the opposite type outbound trajectory would yield the lowest vehicle weight.

VI. SUMMARY

Due to the diverse and detailed nature of each of the tasks in this study, an overall summary of the results in depth is neither warranted nor possible in this section without rendering a repetition of the discussion included at the end of each section. Therefore, this summary is limited to a recapitulation of only the more salient results for each task.

SWINGBY MISSION ANALYSIS

The results of the swingby mission analysis task showed that for manned stopover missions, the type 3 swingby leg coupled with the long direct leg (type 1 or B) yielded the lowest weight vehicle in the years 1980 and 1982. However, in 1986, the type 3 swingby with the short, type A direct leg (3A round trip trajectory) leads to both a lower weight vehicle and shorter trip time. In 1984, an inbound type 5 swingby is best for the all propulsive modes (NNN or CCC modes) while the outbound type 5 swingby is preferable for the Mars aerodynamic braking modes (NAS or CAS modes); the long direct leg is best for both of the latter mission types. The vehicle weights for swingby missions for the NNNA mode increase in the following order: 1982 (minimum), 1986, 1980 and 1984 (maximum). For the NASA mode, the weight is a minimum in 1986, and increases in 1980, 1984, and 1982 (maximum). A comparison of the three different mission types shows that for the NNN mode, the opposition class mission yields the minimum vehicle weight in 1984 and 1986; the swingby mission is minimum in 1982; and a conjunction class mission yields the minimum vehicle weight in 1980. The powered swingby analysis revealed that the powered swingby produces no weight savings over the unpowered swingby for either the type 1 or type 3 trajectories.

CONJUNCTION CLASS MISSION ANALYSIS

The conjunction mission analysis showed that the type IA trajectory (long outbound, short inbound) yielded the minimum weight vehicle. The vehicle weight was eleven percent less than for the shortest trip time trajectory (type IIA) but had a four percent increase in total trip time, 920 to 956 days.

LAUNCH WINDOW ANALYSIS

As mentioned previously, the launch window analysis is in the process of being revised and the results of this task will be presented in a supplemental report at a later date.

MISSION ABORT ANALYSIS

It was shown for all missions analyzed that aborts were generally possible during the first third to first half of the outbound leg duration. These possible abort regions can be extended to cover essentially the entire outbound leg durations by providing the vehicle with sufficient retro and aerodynamic braking capability. The combined retro and aerodynamic braking capability would have to be increased to permit braking at Earth for Earth arrival velocities from 15 to 18 km per sec (approximately 50,000 to 60,000 ft per sec).

LAUNCH AZIMUTH CONSTRAINT ANALYSIS

It was shown in the launch azimuth constraint analysis that for all mission types and launch opportunities considered, launches are possible if the nominal allowable firing sector (departure declination limit of 52.4°) can be used. If the departure declination limit of 36.6° is imposed, the optimum 1975, 1978, 1986 and 1990 opposition class missions, and the 1984 inbound swingby mission are not possible. By resorting to the long (type I) direct leg for these missions, the launches are possible but the vehicle weights are increased by 2 to 7 percent for all missions except the 1986 opposition class; the vehicle weight for this latter mission is increased by approximately 20 percent.

VII. REFERENCES

1. Mission Oriented Advanced Nuclear System Parameters Study, Volume II, Detailed Technical Report, Mission and Vehicle Analysis, TRW/STL, 8423-6006-RU000, March 1965.
2. Mission Oriented Advanced Nuclear System Parameters Study, Volume III, Parametric Mission Performance Data, TRW/STL, 8423-6007-RU000, March 1965.
3. The Venus Swingby Mission Mode and Its Role in the Manned Exploration of Mars, Rollin W. Gillespie and Stanley Ross, AIAA paper, No. 66-37, January 1966.
4. Optimum Transfer to Mars via Venus, Walter M. Hollister and John E. Prussing, AIAA paper, No. 65-700, September 1965.
5. Analytic Interplanetary Program, Volume III, Engineering Manual, TRW Systems, 05952-6006-R000, December 1966.
6. Optimum Transfers Between Hyperbolic Asymptotes, Frank W. Gobetz, AIAA Journal, Vol 1, No. 9, September 1963.